SAPIENZA
Università di Roma
Facoltà di Scienze Matematiche Fisiche e Naturali

DOTTORATO DI RICERCA
IN GENETICA E BIOLOGIA MOLECOLARE

XXV Ciclo
(A.A. 2011/2012)

Genetic dissection of meiotic cytokinesis in *Drosophila melanogaster* males

Dottorando
Stefano Sechi

Docente guida
Dott.ssa Maria Grazia Giansanti

Tutore
Prof. Rodolfo Negri

Coordinatore
Prof. Irene Bozzoni

INDEX

GLOSSARY.

Cytokinesis: the process by which the genomic material and the cytoplasm of the mother cell is partitioned into two daughters at the end of cell division.

Central spindle: central spindle (CS), an array of antiparallel, interdigitating microtubule (MT) bundles that lies between the two sets of chromosomes during anaphase and telophase.

Contractile ring: in animal cells, a contractile ring composed of F-actin filaments and active Myosin II assembled just beneath the plasma membrane around the cell equator generates the constricting force that separates the cell into two.

Rab proteins: they represent the largest branch of the Ras GTPase superfamily. Rabs use the guanine nucleotide-dependent switch mechanism common to the superfamily to regulate each of the four majors steps in membrane traffic: vesicle budding, vesicle delivery, vesicle tethering, and fusion of the vesicle membrane with that of the target compartment.

ABSTRACT.

Studies in a variety of organisms indicate that membrane traffic to the cleavage furrow is an essential facet of cytokinesis involving components of the secretory and endocytic/recycling trafficking pathways, as well as the membrane fusion machinery.
My PhD project focused around the characterization of two genes required for cleavage furrow formation and ingression in male meiotic cells namely *sauron* and *Cog7* which encode the *Drosophila* orthologues of two known players of membrane trafficking pathways.
Sauron is the *Drosophila* orthologue of Golgi phosphoprotein 3 (GOLPH3) which has recently been recognized as a potent oncogene amplified in many human cancers. Studies in both yeast and mammalian cells have implicated this protein in several vesicle trafficking events.
I show that Sau/dGOLPH3 is required during the early steps of spermatocyte cytokinesis playing an essential role in both contractile ring assembly and vesicle trafficking during furrow ingression. Consistently my work suggests that Sau/dGOLPH3 might interact with components of both the contractile apparatus and the membrane trafficking machinery in male germ cells.
The conserved oligomeric Golgi (COG) Complex plays essential roles for Golgi function, vesicle trafficking and glycosylation. Mutations in the genes encoding human *COG1, COG4-COG8* have been associated with congenital disorders of glycosylation (CDG). Deletions of human *COG7* are associated with a rare multisystemic congenital disorder of glycosylation causing mortality within the first year of life. I show that, similar to *Drosophila* Cog5, Cog7 controls furrow ingression during cytokinesis. Importantly, *Cog7* is required to localize the small GTPase Rab11 and the phosphatidylinositol transfer protein (PITP) Giotto (Gio) to the cleavage site of spermatocytes. In addition Gio coimmunoprecipitates with both Cog7 and Rab11 in *Drosophila*

testes suggesting that these proteins may interact in male germ cells.

INTRODUCTION

1.1 Cytokinesis in animal cells

Cytokinesis partitions the genomic material and the cytoplasm of the mother cell into two daughters at the end of cell division (reviewed in Green et al., 2012). Besides being fundamental for normal development this process is also required for maintaining ploidy in adult tissues. Failures in cytokinesis lead to the formation of genetically unstable tetraploid cells with multiple centrosomes, whose mitotic division results in aneuploid cells that promote carcinogenesis (Boveri, 1929; Nigg, 2002, Fujiwara et al., 2005, Caldwell et al., 2007 Barr and Gruneberg, 2007). Thus, the identification of novel cytokinesis genes and an elucidation of the molecular mechanisms of the process can contribute to both cancer diagnosis and therapy.

In animal cells, a contractile ring composed of F-actin filaments and active Myosin II assembled just beneath the plasma membrane around the cell equator (Miller, 2011) generates the constricting force that separates the cell into two (**Figure 1**). Constriction of the actomyosin ring draws in the plasma membrane and leads to the formation of a cleavage furrow that invaginates until the two daughter cells remain connected by a thin cytoplasmic bridge. During the last step of cytokinesis, the intercellular bridge is ultimately severed during abscission, resulting in the complete separation of daughter cells (Schweitzer, 2004; Glotzer, 2005).

The pioneering studies of Ray Rappaport (1961) indicated for the first time the key role of anaphase spindle microtubules in establishing the cleavage site in animal cells. Anaphase mitotic spindles are largely comprised of astral microtubules, which emanate radially from the two separated centrosomes toward the poles of the cell, and the central spindle (CS), an array of antiparallel, interdigitating microtubule (MT) bundles that lies

between the two sets of chromosomes (Glotzer, 2009). Central spindle assembly is regulated by the coordinated action of kinesin motor proteins, microtubule associated proteins (MAPs) and protein kinases (Glotzer, 2009). The cleavage furrow forms in a position that bisects the axis of chromosome segregation, thus ensuring that each daughter cell receives a single copy of the genome (Glotzer; 2009). While CS microtubules send stimulatory signals to the cell equator for contractile ring assembly, astral microtubules are thought to send inhibitory signal(s) that prevent the localization of contractile ring proteins at the poles of the cell (Bringman and Hyman, 2005; Dechant and Glotzer, 2003; Lewellyn et al., 2010).

A crucial signaling event that sets up the site of cleavage furrow formation for cytokinesis is the accumulation of active Rho GTPase at an equatorial position at the cortex. This localized active Rho GTPase controls both profilin-mediated nucleation of F-actin assembly at the plasma membrane and Myosin II activation (**Figure 2**; reviewed D'Avino et al., 2005; Piekny et al., 2005). The central spindle transmits the spatial information required for cleavage furrow formation by delivering regulators of Rho to the equatorial cortex (reviewed in D'Avino et al., 2005; Glotzer, 2009). During cytokinesis, the balance between the active state (GTP-bound) and inactive state (GDP-bound) of Rho is regulated by the GEF ECT2/Pebble and the GAP MgcRacGAP/RacGAP50C (Piekny et al, 2005). MgcRacGAP/RacGAP50C interacts with the kinesin MKLP1/Pavarotti to form the centralspindlin complex, an evolutionary conserved heterotetramer required for central spindle assembly. Compelling data have led to the proposal that Rho GEF ECT2/ Pebble in turn associates with the MgcRacGAP/RacGAP50C component of centralspindlin to form a ternary complex that transduces spatial localization of centralspindlin to the plus ends of CS microtubules to local activation of Rho at the overlying cell cortex (Somers and Saint,

2003; Kamijo et al., 2006; Nishimura and Yonemura, 2006; Yuce et al., 2005; Zhao and Fang, 2005; Piekny et al., 2005).

Successful cytokinesis also requires a network of cytoskeletal scaffolding proteins that serve to anchor the actomyosin ring to the plasma membrane. Key among these are the Septins, GTP-binding proteins that polymerize into hetero-oligomeric complexes to form a membrane-associated filament system (Mostowy and Cossart, 2012). Recruitment of the Septins to the contractile ring is mediated by another scaffolding protein, Anillin, which was shown to bind F-Actin, Myosin II, Rho, and MgcRacGAP/RacGAP50C (reviewed in D'Avino et al., 2009). Anillin may thus provide an essential bridge function that helps stabilize attachment of the plasma membrane to the contractile apparatus under the forces of cleavage furrow constriction.

In addition to the force generated by constriction of the actomyosin contractile ring at the cell equator, successful cleavage furrow ingression may also require an increase in surface area of the plasma membrane to encapsulate each daughter cell into a separate membrane compartment. Indeed, recent studies have demonstrated that targeted vesicle transport plays an important role during cleavage furrow ingression, as well as in the later events of abscission (McKay and Burgess, 2011; Neto et al., 2011). Also, several studies point to the importance of plasma membrane lipid composition in cytokinesis. Indeed, special lipid composition at the cleavage site can facilitate cell shape changes during furrow ingression, regulate new membrane addition, and provide a platform for signaling pathways controlling cytokinesis (reviewed in Neto et al., 2011).

Cytokinesis is an intricate process that requires the activity of not less than one hundred proteins (Eggert et al., 2006; Barr and Gruneberg, 2007; Pollard, 2010). Progress in the identification of cytokinesis proteins has been hampered by difficulties in applying biochemical strategies that have been particularly successful in other studies. A major limitation in proteomic analysis of cytokinesis has been the isolation of the transient structures

involved in this process that assemble and disassemble during a limited cell cycle window. Skop and co-workers isolated mid-bodies from Chinese hamster ovary cells (CHO) and analyzed the proteins enriched in these structures by tandem liquid chromatography and mass spectrometry (Skop, 2004). However mid-bodies characterize only very late stages of cytokinesis. A fruitful approach, that allowed to identify several molecular players, consists of the genetic dissection of this process in suitable model organisms such as *Drosophila melanogaster* (Giansanti et al., 2012; Giansanti and Fuller, 2012).

1.2 *Drosophila* spermatocytes as a system for study of cytokinesis.

Drosophila male meiosis offers a well-suited cell system for investigating cytokinesis. Spermatocytes are large cells particularly suitable for immunocytological and *in vivo* analysis of the cytokinetic structures. In addition mutants that affect male meiotic cytokinesis can be easily identified by a simple screen of unfixed tissue (see below).

In *D. melanogaster*, spermatogenesis starts with the asymmetric mitotic division of a germ-line stem cell that generates another stem cell and a spermatogonial cell. The primary spermatogonium undergoes four gonial mitotic divisions giving rise to 16 primary spermatocytes (**Figure 3A**). Before entering meiosis, each spermatocyte undergoes an impressive growth phase, lasting approximately 90 hours, leading to in a 25-fold increase in volume. As a result, by the onset of the first meiotic division, spermatocytes are considerably larger than most somatic cells. The 16 spermatocytes in the cyst then synchronously embark in quick succession of two meiotic divisions, producing a cyst of 64 haploid round spermatids (**Figure 3B**). During both the gonial mitoses and the spermatocyte meiotic divisions, cytokinesis is incomplete. Cleavage furrows constrict but abscission does not take place and daughter cells remain interconnected by cytoplasmic intercellular bridges called ring canals (Lindsley, 1980; Fuller, 1993; Skop, 2004). Other than this developmentally

programmed lack of abscission, the molecular mechanisms of cleavage furrow formation and ingression are largely conserved in spermatocytes compared with other animal cells (Giansanti et al. 2012).

During male meiotic divisions, the nuclear envelope does not disassemble by metaphase, but becomes fenestrated near the spindle poles. A small number of microtubules penetrate these fenestrations to contact the kinetochores, while the bulk of the metaphase spindle remains outside the nuclear envelope (Tates, 1971; Church and Lin, 1982). At metaphase I, spermatocyte nuclei become spindle shaped and maintain a double-membrane that encircles the meiotic chromosomes during meiosis in addition 5 to 7 double membranes named parafusorial membranes (Tates, 1971; Church and Lin, 1982). During each meiotic division mitochondria line up along the parafusorial membranes; this arrangement ensures the equal partitioning of mitochondria between the two daughter cells at the end of cytokinesis. The nuclear envelopes eventually break down in anaphase and new nuclear envelopes form around the separated daughter nuclei in telophase. After the second meiotic division, the mitochondria in each early round spermatid fuse to form a complex interlaced structure named the nebenkern (Fuller, 1993; **Figure 4**). When viewed by phase-contrast optics, wild type early round spermatids contain a phase-dark nebenkern and a single phase-light haploid nucleus (**Figure 4A**), and all the 64 interconnected spermatids within a cyst have the same size nebenkern and the same sized nucleus. This characteristic arrangement of nuclei and nebenkerne in spermatid cysts allows easy scoring of mutants defective in meiotic cytokinesis. Cytokinesis failures during one or both meiotic divisions disrupt partitioning of mitochondria between daughter cells resulting in spermatids containing respectively 2 or 4 nuclei associated with an enlarged nebenkern (**Figure 4B**). Thus, the presence of multinucleate spermatids is diagnostic of defects in cytokinesis in the meiotic divisions (Fuller, 1993). In addition, since the volume of each nucleus in the onion-stage

spermatids is proportional to its chromatin content, variations in nuclear size reflect defects in chromosome segregation during meiosis (Fuller, 1993). Mutants affecting both chromosome segregation and cytokinesis exhibit onion-stage spermatids containing large nebenkern associated with multiple nuclei of different size.

In this context, one peculiarity of male meiotic cells that is particularly advantageous when studying cytokinesis, is the lack of a robust spindle assembly checkpoint (Rebollo and Gonzalez, 2000). The spindle assembly checkpoint (SAC) signaling pathway normally monitors kinetochore attachment to spindle microtubules (Musacchio and Salmon, 2007). In somatic cells, SAC blocks cells in metaphase in the presence of unattached chromosomes or malformed spindles. In spermatocytes, in contrast such abnormalities only cause a small delay in both anaphase onset and meiotic progression (Rebollo, 2000; Wakefield, 2001; Riparbelli, 2002). This particular characteristic of spermatocytes offers the advantage to investigate whether gene products required for chromosome segregation play also functions during later stages of cell divisions that are masked in somatic cells by the strong SAC of these cells (Wakefield et al., 2000; Giansanti and Fuller, 2012).

1.3 Central spindle assembly and cleavage furrow formation in *Drosophila* spermatocytes

Since the studies of Ray Rappaport (Rappaport, 1961) it was clear the importance of mitotic spindle for signaling cleavage furrow formation. Mutational analysis in *Drosophila* was useful to dissect the role of different spindle components in signaling cytokinesis (**Table 1**; reviewed in Giansanti et al., 2012). Mutant spermatocytes devoid of astral microtubules assemble regular contractile rings and successfully complete cytokinesis (Bonaccorsi et al., 1998; Giansanti et al., 2008; Bucciarelli et al., 2003). Similarly secondary spermatocytes devoid of chromosomes as a consequence of mutations that perturb chromosome segregation during the first meiotic division, assemble regular

central spindles and contractile rings and undergo cytokinesis even in the absence of chromosomes. However mutations that perturb central spindle assembly invariably result in defects in F-actin ring assembly and cause early cytokinesis failure indicating that central spindle microtubules are the only spindle components that are strictly required for signaling cytokinesis. (Giansanti et al, 1999; Giansanti et al., 2004).
Major central spindle components include MAPs, plus-end directed kinesins, and the chromosomal passenger complex. Among the MAPs, the ortholog of the highly conserved Protein Regulating Cytokinesis I (PRC1) Fascetto (Feo) is one of the first markers that localizes to the overlap central region of the anaphase central spindle in spermatocytes (**Figure 5**; Vernì et al, 2004; Szafer-Glusman et al., 2011). The effects of *feo* mutations in spermatocyte cytokinesis have not been studied. However, loss of Feo leads to cytokinesis defects and affects central spindle organization in both larval neuroblasts and S2 cells (Vernì et al., 2004)

As revealed by time lapse video microscopy, two different populations of MTs comprise central spindles of *Drosophila* spermatocytes (**Figure 5**; Inoue et al., 2004). The so called "peripheral" astral microtubules contact the cortex at the future cleavage site and bundle together to promote furrow ingression. A distinct set of microtubule bundles named "interior" MTs, confined inside the nuclear envelope, merges with peripheral astral microtubules to complete furrow ingression and cytokinesis (**Figure 5**). The microtubule plus-end binding protein Orbit localizes to the central spindle midzone but, in contrast to Feo, it associates with the subset of microtubule bundles that comprise the "interior central spindle" (Inoue et al., 2004). Mutations in the gene encoding the microtubule-associated protein Orbit specifically disrupt the interior central spindle bundles but do not affect the peripheral astral microtubules that can promote initial furrow ingression. The interior central spindle microtubules are

essential for cytokinesis progression, as cleavage furrows are unstable and rapidly regress in *orbit* mutant spermatocytes.

Plus-end directed microtubule motor proteins of the kinesin family are also structural components of the spermatocyte central spindle. Two conserved plus-end directed, microtubule kinesins play essential roles in central spindle assembly, the kinesin 6 family member MKLP1/Pavarotti (Pav) and the chromokinesin KIF4/ KLP3A (for reviews see D'Avino, 2005; Douglas, 2010). The plus-end directed motor of MKLP1 can cross-link microtubules and promote sliding of one microtubule over another (Nislow, 1992). Thus, the activity of this kinesin is essential to mediate interactions between overlapping microbule bundles during central spindle formation. Consistent with this function, the ortholog of MKLP1, Pavarotti (Pav), accumulates at the central spindle midzone where the microtubule plus-ends overlap during anaphase of *Drosophila* spermatocytes (**Figure 5**; Carmena, 1998). The *Drosophila* ortholog of KIF4, KLP3A is also concentrated at central spindle mid-zone and is required for central spindle assembly in spermatocytes (Williams, 1995). The involvement of KIF4 and KLP3A in central spindle formation could be due to their ability to form a complex with the microtubule bundling protein PRC1/Feo (Kurasawa, 2004; D'Avino, 2007). Centralspindlin, composed of two molecules of the kinesin family member Pav and two molecules of the Rho family GAP RacGAP50C plays a key role in activation of RhoA (named Rho1 in *Drosophila*).

In *Drosophila,* as in all animal cells, contractile ring assembly and furrowing are orchestrated by the small GTPase Rho1 (the *Drosophila* homolog of RhoA) at the cortex. Cycling between the GDP-bound inactive form and the GTP-bound active form of Rho1 depends on the activity of guanine nucleotide exchange factors (GEFs) and GTPase activating proteins (GAPs) (**Figure 5**). Centralspindlin translocates to the plus ends of equatorial and central spindle microtubules through the activity of its motor component. Based on studies in *Drosophila* and

mammalian cells, it has been proposed that the association between the centralspindlin component RacGAP and RhoGEF/Pebble leads to local activation of RhoA/Rho1 at the cleavage site (Somers, 2003; Piekny, 2005; Chalamalasetty, 2006; Nishimura, 2006).

Regulation of centralspindlin activity and recruitment of ECT2/Pebble involve the activities of multifunctional serine/threonine kinases Aurora B kinase and Polo-like kinase 1 (Plk1). Aurora B mediated phosphorylation of MKLP1/Pavarotti is critical for central spindlin formation (Guse et al., 2005; Neef et al., 2006; Douglas et al., 2010), while targeting of the RhoGEF ECT2/Pebble to the cortex depends at least in part on phosphorylation of MgRacGAP/RacGAP50 by Polo kinase (**Figure 5**; Brennan et al., 2007; Santamaria et al, 2007; Burkard et al., 2009; Wolfe et al., 2009).

Polo and Aurora B serine/threonine kinases also regulate early events of cell division such as chromosome condensation, spindle formation and chromosome segregation (for reviews see Barr et al., 2004; Van der Waal et al., 2012). Thus, in most cell types loss of Polo or Aurora B is associated with an early mitotic arrest caused by activation of the spindle checkpoint. The lax checkpoint control of *Drosophila* male meiosis, has enabled analysis of the functional roles of the Polo and Aurora B kinases during cytokinesis. In *Drosophila* spermatocytes at anaphase, Polo kinase, just like Aurora B, is enriched at the spindle midzone and enables Pav localization, central spindle formation and F actin ring assembly (D'Avino, 2005). *Drosophila* male mutants carrying a hypomorphic *polo* allele are viable and progress though male meiosis, allowing investigation of the function of Polo in cytokinesis (Carmena et al., 1998). During anaphase, Polo accumulates at the spindle midzone and is required for proper localization of Pav and for formation of both the CS and F-actin ring (Carmena et al., 1998; Herrmann et al., 1998).

Aurora B is the enzymatic subunit of the Chromosomal passenger Complex (CPC) that contains three additional CPC

subunits, Inner Centromere Protein, Survivin, and Borealin, localize and activate the kinase (Ruchaud et al., 2007; van der Waal et al., 2012). The CPC plays several essential roles during mitosis and meiosis showing a dynamic, cell cycle dependent localization. During interphase, it associates with chromatin and regulates chromosome condensation, then it concentrates at the inner centromeres from prometaphase until anaphase onset and monitors the kinetochore attachment to spindle microtubules. In anaphase, the CPC transfers to the spindle midzone and equatorial cortex (Adams et al., 2000; Vagnarelli and Earnshaw, 2004; Vader et al., 2006; Szafer-Glusman et al., 2011; Van der Waal et al., 2012). The *D. melanogaster* genome encodes two Borealin paralogs, Borealin-related (Borr) and Australin (Aust; Gao et al., 2008): the latter replaces Borr in male meiosis. Dividing spermatocytes from males carrying either an hypomorphic allele of *dmINCENP* or a null allele of *australin (aust)* display a similar phenotype: early cytokinesis arrest with defective central spindles and failure to recruit Pav to the cell equator (Resnick et al., 2006; Gao et al.., 2008; Szafer-Glusman et al., 2011), suggesting a role for the CPC in activation and/or localization of the centralspindlin complex.

The strict interdependence of the four CPC subunits (Ruchaud et al., 2007) has complicated the analysis of the function of each single component; indeed, in human cells knockdown of each CPC protein impaired the localization and function of the whole complex (Adams et al., 2001; Carvalho et al., 2003; Honda et al., 2003; Lens et al., 2006; Gassmann et al., 2004). A recent study has elucidated the role of both *Drosophila* Survivin/Deterin and the CPC specifically during anaphase and cytokinesis (Szafer-Glusman et al, 2011). *scapolo* (*scpo*), is a *Dsurvivin*/*deterin* allele, containing a missense mutation that substitutes a Serine for the wild type Proline at position 86 in the dSurvivin BIR domain. Cytological analysis has revealed that *scpo* is a “separation-of-function” allele: it allows the recruitment and function of the CPC until anaphase onset but impairs its activity in later stages. Just

like Survivin is essential for central spindle formation and to target the CPC and Pav to the central spindle and equatorial cortex. In spermatocytes, Survivin is also essential to localize Polo and Rho1 at the equatorial cortex. Based on these results, it has been suggested that failure to localize Polo to the cell equator of *scpo* spermatocytes would prevent localization of RhoGEF by the centralspindlin complex and impair Rho1 activation and actomyosin ring assembly.

1.4 Scaffolding proteins in the cleavage furrow of *Drosophila* spermatocytes.

Rho•GTP activates downstream effectors that lead to actin polymerization and Myosin II activation at the equatorial cortex (**Figure 2**; Piekny et al., 2005; Goode and Eck, 2007) Non-muscle Myosin II hexamers assemble into filaments in the contractile ring. Each Myosin II hexamer consists of a dimer of heavy chains, two essential light chains and two regulatory light chains. Phosphorylation of the regulatory light chains (rMLC), required for activation of Myosin II motor activity and bipolar filament assembly provides a key step during cytokinesis as demonstrated by the opposite effects of phosphomimetic and non phosphorylatable alleles of the *Drosophila* rMLC Spaghetti Squash (Sqh) on cytokinesis (Jordan and Karess, 1997).

The traditional cytokinesis model proposes that furrow ingression is driven by a ring-shaped structure composed of F-actin and nonmuscle Myosin II. According to this model bipolar filaments of Myosin II would use their motor activity to walk along antiparallel actin filaments, drawing the F actin strands together in a purse-string like fashion like fashion (Schroeder et al., 1990; Satterwhite and Pollard, 1992). Because the cortex/plasma membrane is attached to the F-actin filaments, constriction of the actomyosin ring draws inward the membrane in a cleavage furrow just under the cell cortex. However alternative models for contractile ring organization and constriction have been proposed (Carvalho et al., 2009; Kee et al. 2012; Ma et al., 2012; reviewed in Green et al., 2012) and recent studies in

Dictyostelium and vertebrate cells have led to suggest that Myosin II does not translocate actin but is required to cross-link actin filaments and to exert tension on actin during cytokinesis (Kee et al., 2012; Ma et al., 2012).

In addition to Myosin II and F-actin, the contractile ring contains a network of cytoskeletal proteins that act as a scaffold at the at the cleavage furrow. Scaffolding proteins (for a review see D'Avino, 2009) include the GTP-binding Septins and Anillin (**Table 1**). In *Drosophila melanogaster* five septins have been identified so far named Sep1, Sep2, Sep3, Sep4 and Sep5 (Adam et al., 2000). In *Drosophila* spermatocytes Peanut (Sep3), Sep1 and Sep2 have been localized to contractile rings and in the ring canals that remain to connect sister cells after the incomplete cytokinesis typical of mitotic spermatogonia and the meiotic divisions of spermatocytes (Hime et al., 1996; Giansanti et al., 2001).

Originally identified as an actin-binding protein in *Drosophila* embryo extracts (Miller et al., 1989), Anillin is an evolutionarily conserved protein. Studies in several systems showed that Anillin also binds activated Myosin II and Septins which are also filament-forming proteins making it a suitable candidate for the proper organization of the actomyosin contractile structures (Kinoshita et al., 2002; Straight et al., 2005; D'Avino et al., 2008; reviewed in D'Avino et al., 2009). Recent data have also indicated that *Drosophila* Anillin interacts with RacGAP50C (D'Avino et al., 2008; Gregory et al., 2008). It has been suggested that Anillin might mediate interactions between central spindle microtubules and the equatorial cortex during furrowing In *Drosophila* spermatocytes Anillin is one of the first markers of cleavage furrows starting to concentrate at the cell equator during anaphase, before appearance of the F-actin (**Figure 5**). Consistent with this temporal order, analysis of spermatocytes from mutants defective in F-actin ring assembly indicated that the initial formation of the Anillin cortical band does not depend on the presence of an F-actin (Giansanti et al., 1999). The role of Anillin

in *Drosophila* male germ cell development has been recently addressed by Goldbach and coauthors (2010). This study demonstrated that Anillin is required for the recruitment of Septins to the cleavage furrow and for the maintenance of Rho, F-actin and Myosin II in the contractile ring during later stages of cytokinesis. Based on these data it has been hypothesized that Anillin might stabilize the cleavage furrow by linking the actomyosin ring to Septin filaments on the furrow membrane (Goldbach et al., 2010).

1.5 Membrane remodeling and membrane traffic in male meiotic cytokinesis.

During cytokinesis both cleavage furrow ingression and abscission depend on targeted membrane addition from internal membrane stores involving components two vesicle-trafficking pathways: the recycling endosome pathway and the secretory pathway (Prekeris and Gould, 2008; McKay and Burgess, 2011; Neto et al., 2011).

The secretory pathway involves vesicle transport from the endoplasmic reticulum (ER) to the Golgi and then to the plasma membrane. In the endocytic pathway, plasma membrane-derived vesicles proceed through the early endosome and the recycling endosome (RE), which directs them back to the plasma membrane (**Figure 7;** Albertson *et al.*, 2005; Prekeris and Gould, 2008; McKay and Burgess, 2011; Neto et al., 2011).

Drosophila male meiosis provides a well suited model system to dissect membrane trafficking during cytokinesis. *Drosophila* spermatocytes are quite large cells (more than 20 μm in diameter), that complete two meiotic divisions in less than two hours with a very short intervening interphase (Fuller, 1993; Giansanti et al., 2001). In addition these cells lack plasma mebrane protrusions and microvilli (Tates, 1971) that might be used as plasma membrane reservoir during cytokinesis. These could be the reasons because male meiotic cytokinesis is especially dependent on membrane trafficking from internal membrane compartments (Giansanti and Fuller, 2012). Indeed forward genetic screens have revealed that spermatocyte cytokinesis is particularly sensitive to mutations

affecting vesicle traffic components (Brill et al., 2000; Farkas et al., 2003; Dyer et al., 2007; Gatt and Glover; 2006; Giansanti et al., 2006; Giansanti et al., 2007; Polevoy et al., 2009; Robinett et al., 2009; Xu et al., 2002a; Zhou et al., 2011).

Several data have implicated secretory trafficking in spermatocyte cytokinesis. Cytokinesis of these cells is sensitive to Brefeldin A, a fungal metabolite that interferes with anterograde transport from the ER to the Golgi (Robinett et al., 2009; Kitazawa et al., 2012). In addition mutational analysis has involved in this process the intra-Golgi trafficking components Cog5 (Farkas et al, 2003), Cog7 (Belloni et al., 2012), the ER-to-Golgi vesicle docking protein Syntaxin 5 (Xu et al., 2002), the *Drosophila* ortholog of the yeast TRAPP II TRS120p subunit Brunelleschi (Bru) (Robinett et al., 2009). A recent study has also demonstrated the requirement during cytokinesis for proteins that function in the retrograde transport from Golgi to ER such as subunits of the coatomer protein I (COPI) and the small GTPase Arf1 **(**Kitazawa et al., 2012**)**.

Endocytic traffic also contributes to male meiotic cytokinesis. The small GTPase Rab11, involved in both the secretory and the endocytic traffic, is also essential for cytokinesis in *Drosophila* male meiotic cells (Giansanti et al., 2007). In dividing spermatocytes, the endosomal GTPase ARF6 colocalizes with Rab11 on recycling endosomes and with Rab4 on the early endosomes. ARF6 is not required to recruit Rab11 and Rab4 to the spindle midzone. However ARF6 is required to boost the recycling rate required for fast cleavage furrow ingression. ARF6 physically interacts with the centralspindlin component Pav suggesting that this protein might contribute to ARF6 recruitment to central spindle endosomes (Dyer et al., 2007).

Remarkably cytological analysis of several mutants affecting vesicle trafficking components such as *Cog5*, *Cog7*, *bru*, *Rab11*, and *Arf6* revealed a common cytokinetic phenotype: mutant spermatocytes assemble regular central spindles and contractile rings during early telophase but the rings fail to complete

constriction, resulting in cytokinesis failure (Farkas et al., 2003; Giansanti et al., 2007; Dyer et al., 2007; Robinett et al., 2009; Wainman et al., 2012). In addition, time-lapse analysis of *arf6* and *rab11* mutant spermatocytes undergoing cytokinesis indicated similar defects in furrow ingression (Dyer et al., 2007; Giansanti et al., 2007). In spermatocytes expressing b-tubulin-EGFP, central spindles transiently formed and furrows initially ingressed at rates similar to wild type cells for almost 15 minutes during the early stages of cytokinesis in the mutants. However, in most cells from *arf6* and *rab11* central spindle microtubule bundles disassembled and cleavage furrows slowly regressed.

Successful cytokinesis also depends on a special lipid composition at the cleavage furrow. Special membrane domains are emerging as key factors in regulating both the dynamics of cytokinetic structures and membrane addition (reviewed in Neto et al. 2011). The *Drosophila* gene *bond* (named after James Bond because of the lack of a ring) encodes a member of the Elovl family involved in the biosynthesis of VLCFAs (Szafer-Glusman et al., 2008. In *bond* mutant spermatocytes, central spindles fail to assemble and the contractile ring, visualized by Sqh-GFP, detaches from the membrane and collapses to one side of the cell (Szafer-Glusman et al., 2008). These findings suggest that VLCFAs are required to allow the plasma membrane to undergo cleavage furrow invagination and indicate an intimate relationship between membrane lipids and the dynamics of cytoskeletal structures during cytokinesis.

Phosphatidylinositol phosphates are also important signaling molecules during cytokinesis (for a review see Brill et al., 2011). The *Drosophila* phosphatidylinositol (PI) transfer protein Giotto/Vibrator (Gio) concentrates in both the ER membranes and the cleavage furrow in dividing spermatocytes. Spermatocytes and neuroblasts from *gio* mutants are defective in contractile ring constriction and exhibit an accumulation of Golgi-derived vesicles at the cleavage site, suggesting a defect in

membrane addition (Gatt and Glover, 2006; Giansanti et al., 2006; Giansanti et al., 2007).

The phosphoinositide Phosphatidylinositol 4,5-biphosphate (PIP2), enriched in the plasma membrane of the cleavage furrow of *Drosophila* spermatocytes, is crucial for cleavage furrow stability (Wong et al., 2005). Compelling data indicate that PIP2 promotes actin polymerization (reviewed in Yin and Janmey, 2003). In addition, the polybasic domain of Septins and the the pleckstrin homology domain of Anillin can mediate interactions with PIP2 (Bertin et al., 2010; Liu et al., 2012). Thus, disruption of PIP2 at the furrow might affect the recruitment and/or the stability of contractile ring proteins. PIP2 turnover is also important during cytokinesis; drugs that interfere with PIP2 hydrolysis mediated by phospholipase C affected the completion of furrow ingression in spermatocytes (Wong et al., 2005).

Genetic analysis in *Drosophila* also indicates that phosphatidylinositol 4-phosphate (PI4P) may have a key role in cytokinesis of male meiotic cells. *fwd* encodes a *Drosophila* PI4KIIIb (Brill et al., 2002). Dividing spermatocytes from *fwd* mutant males exhibit a cytokinetic phenotype similar to that of *gio* and *Rab11* mutants (Giansanti et al., 2006; Giansanti et al., 2007; Polevoy et al., 2009). Fwd binds the GTPase Rab11 and colocalizes with both Rab11 and PI4P markers on Golgi membranes. Loss of *fwd* disrupts the localization of Rab11 and PI4P at the cell equator. Moreover phenotypic analysis of single and double mutants in *fwd, rab11,* and *gio* indicated that Rab11, Gio and Fwd might function in the same pathway during cytokinesis, with Gio and Fwd required upstream of Rab11 (Giansanti et al., 2006).

Fig. 1, Schematic representation of the Cleavage furrow ingression.

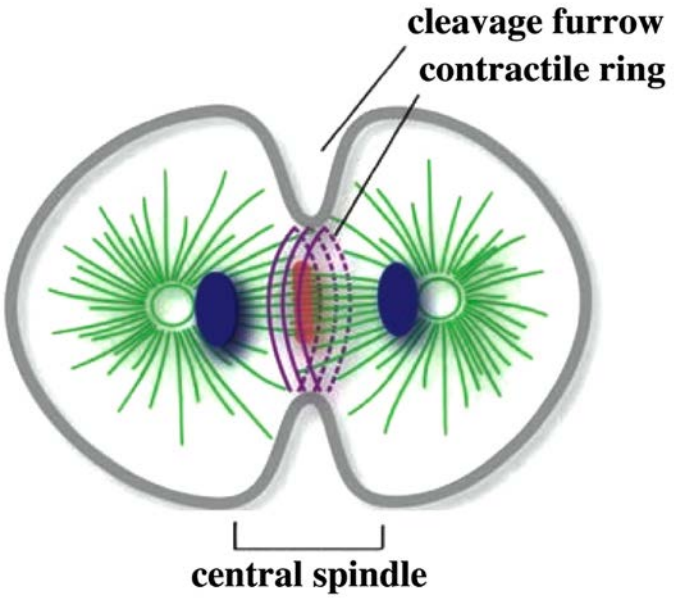

In animal cells, a contractile ring composed of F-actin filaments and non-muscle Myosin II, assembled just beneath the plasma membrane around the cell equator, generates the constricting force that separates the cell into two. Constriction of the actomyosin ring draws in the plasma membrane and leads to the formation of a cleavage furrow.

Fig. 2, Schematic representation of the Rho pathway.

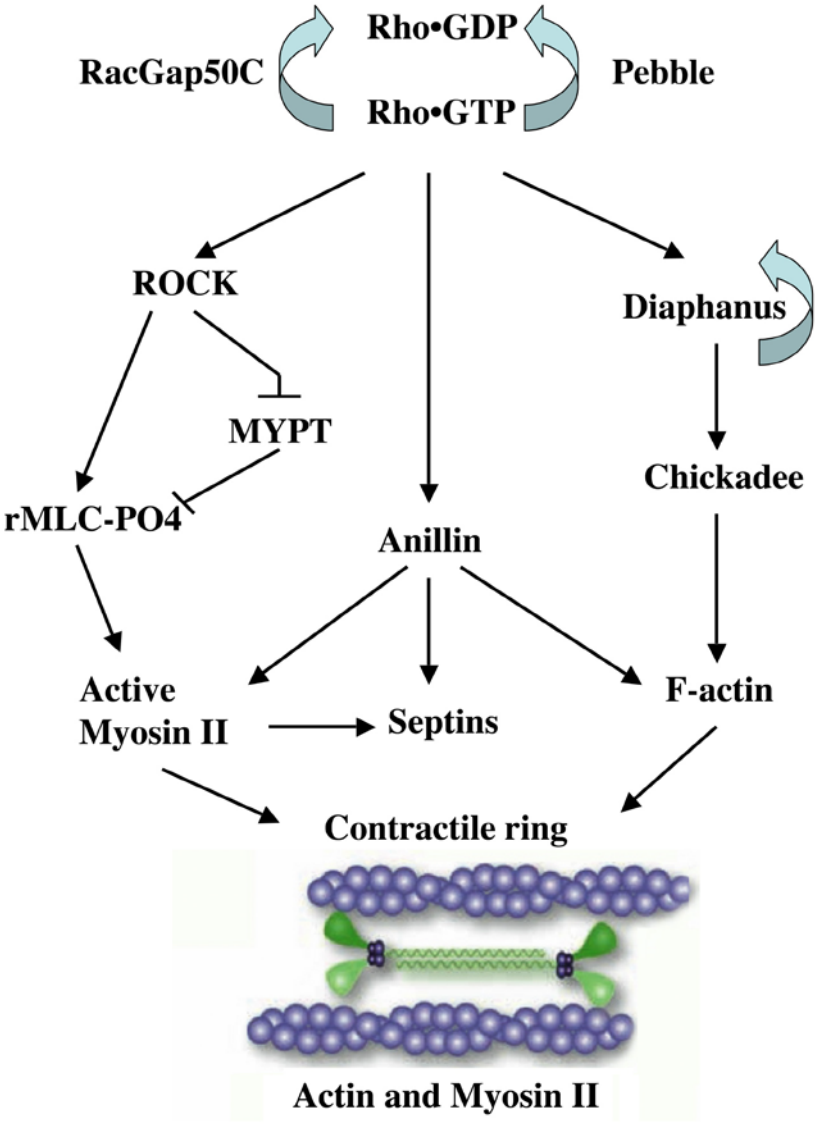

Contractile ring assembly is directed by the RhoA GTPase which induces Actin nucleation and activates Myosin II.

Fig. 3, Schematic representation of spermatogenesis in *Drosophila melanogaster*.

3A, Gonial mitotic divisions.

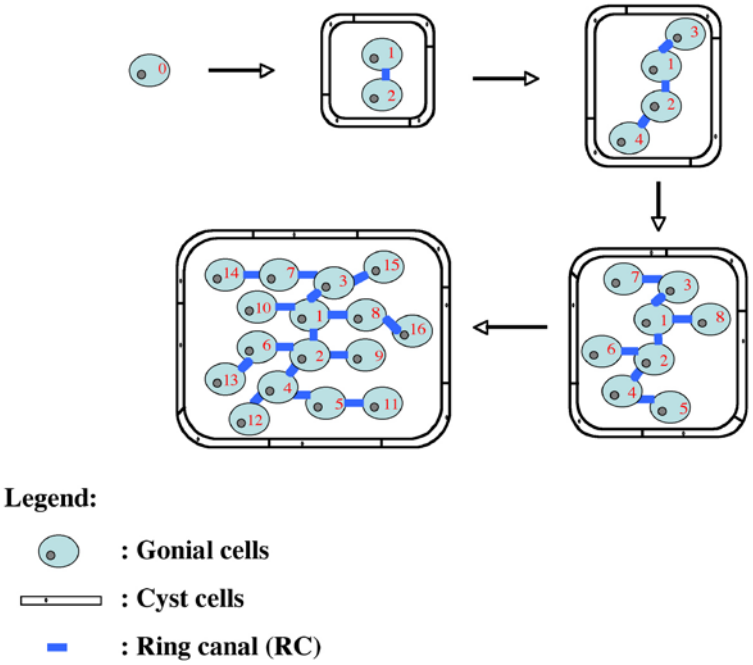

A single primary spermatogonium undergoes four mitotic divisions. Numbers indicate gonial cells.

3B, Spermatocyte growth and meiosis.

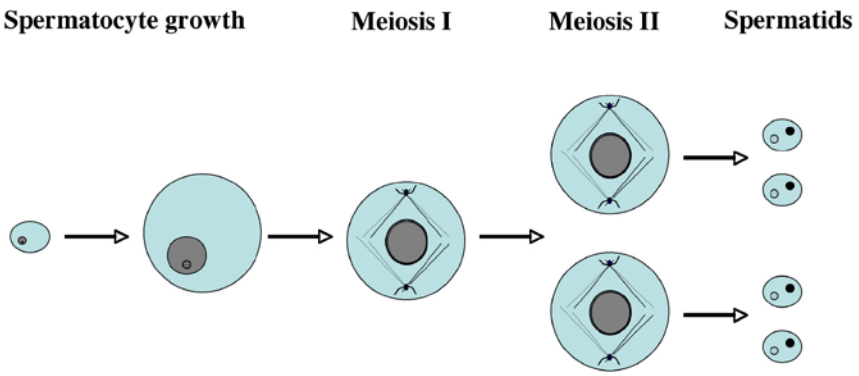

Each primary spermatocyte undergoes a growth phase, which lasts 90 h before undergoing two meiotic divisions. A wild type spermatid cyst at the so-called onion stage contains 64 spermatids connected by 63 ring canals (not shown). Each spermatid contains a single nucleus (white) associated with a nebenkern (black) of similar size. Only four spermatids are represented.

Fig. 4, spermatids at the onion-stage viewed by phase-contrast microscopy.

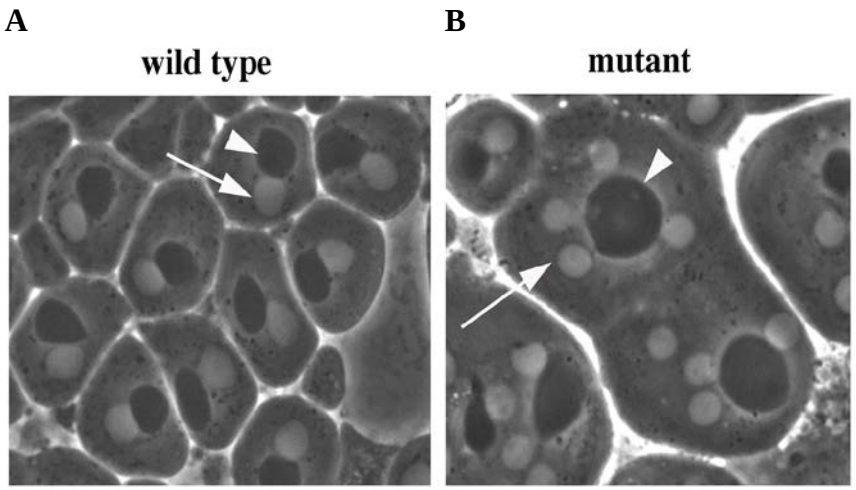

Each wild type spermatid contains a single light nucleus (arrow) associated with a dark nebenkern (arrowhead). Spermatids from a mutant defective in male meiotic cytokinesis, contain large nebenkern (arrowhead) associated 4 nuclei of similar size (arrows).

Fig. 5, Schematic representation of different stages of male meiotic cytokinesis.

Late Anaphase

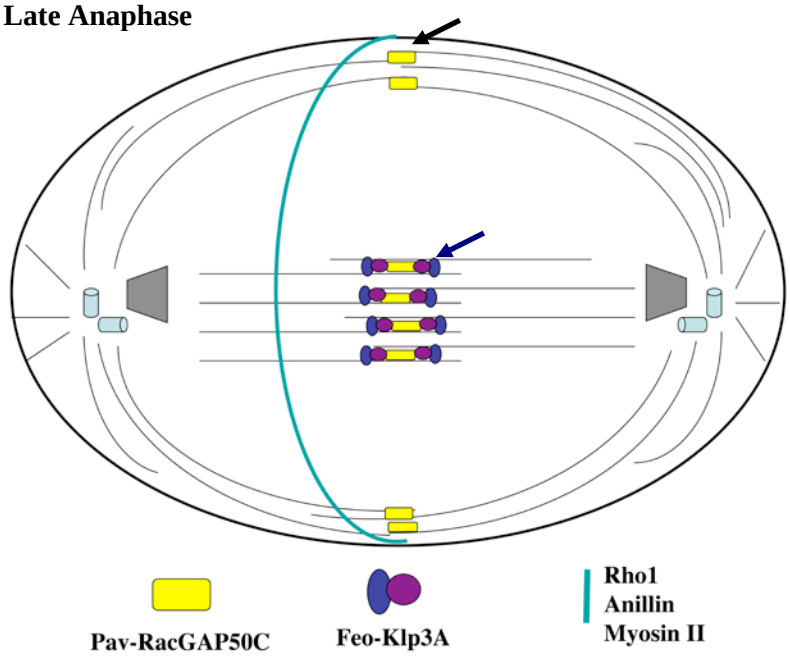

Early Telophase

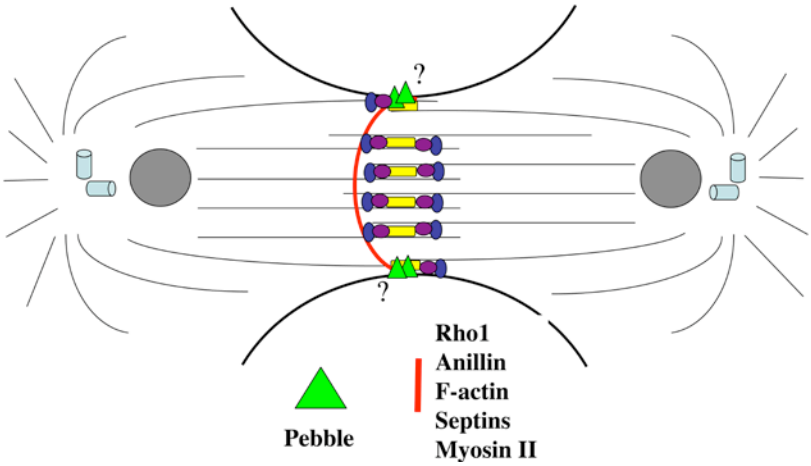

During late anaphase the central spindle is made up of two distinct populations of microtubule bundles, the “peripheral” astral microtubules (black arrow) and the “interior” central spindle microtubules (blue arrow). The centralspindlin complex (Pavarotti and RacGAP50C) is enriched at the central spindle midzone and associates with both populations of microtubule bundles.
Other microtubule associated proteins, required for central spindle formation, such as the CPC complex are not depicted.
Rho1, Myo II and Anillin concentrate in a narrow cortical ring during late anaphase, before the recruitment of F-actin.
During early- and mid-telophase, peripheral astral microtubule bundles merge with interior microtubule bundles completing central spindle structure.

Fig. 6, Schematic representation depicting membrane trafficking routes involved in membrane addition during cytokinesis. Subcellular localization of different species of phosphoinositides that regulate this process are also shown.

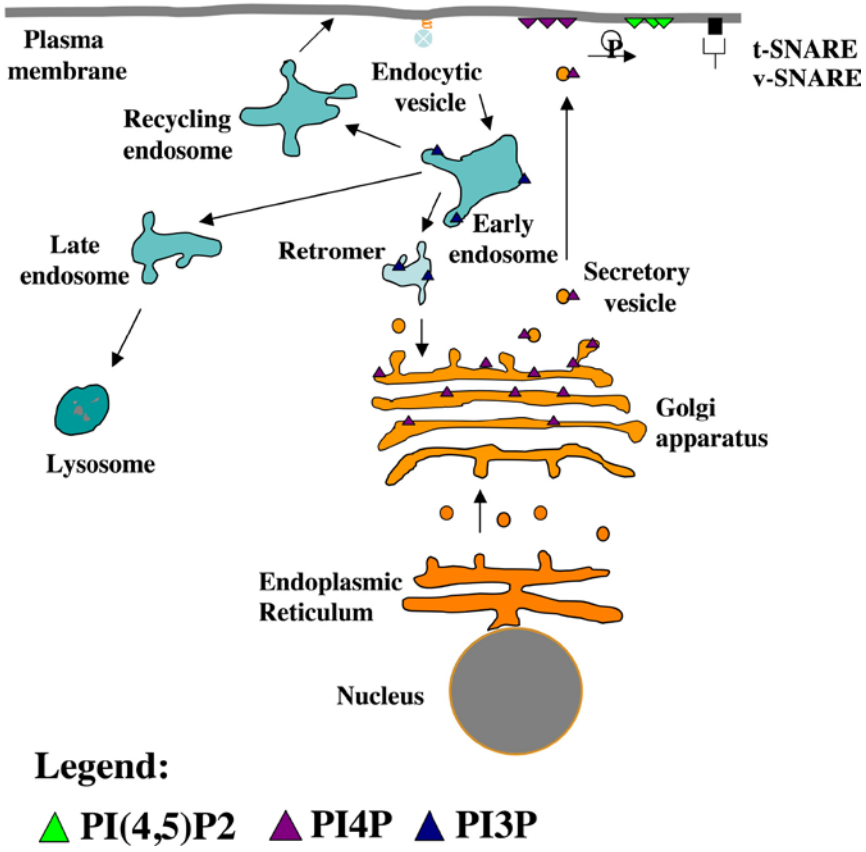

Tab. 1, Proteins/genes involved in cytokinesis of *Drosophila* spermatocytes, localizations in dividing spermatocytes.

Protein/ *gene*	**Protein family**	**Predicted protein function**	**Localization***	**Refs**
Rho GTPase module				
Rho1	RhoA	Rho GTPase Cleavage site determination	Cleavage furrow Cortical ring	1, 2
Pebble	ECT2	Cleavage ring assembly RhoGEF	Cleavage furrow, Cortical ring	3
Contractile ring components				
Actin 5C	Actin	F-Actin	Contractile ring	4
Zipper	Myosin II	Myosin II heavy chains	Contractile ring	5, 6
Spaghetti squash	MRLC	Myosin II regulatory light chains	Contractile ring	1, 2, 6
Anillin	Anillin	Anillin, actin binding Scaffolding Protein	Contractile ring	1, 5, 7
Peanut, Sep1, Sep2	Septin	Septins, Scaffolding Protein	Contractile ring	5, 6
Actin filaments formation				
Diaphanus	Formin	Actin nucleator	ND	3, 8, 9
Chickadee	Profillin	Actin-binding protein	Equatorial cortex	7, 8

Tab. 1, Proteins/genes involved in cytokinesis of Drosophila spermatocytes, localizations in dividing spermatocytes.

Protein/ *gene*	**Protein family**	**Predicted protein function**	**Localization***	**Refs**
Associated with central spinale microtubules				
Pavarotti	MKLP1	Kinesin motor 6, microtubule motor, centralspindlin component	CS midzone	2, 10
Fascetto	PRC1	Microtuble bundling	CS midzone	2, 11, 12
Klp3A	Kif4A/B	Kinesin motor 4, microtuble motor	CS midzone	7, 8, 13
Klp67A	Kif18	Kinesin motor 8, microtuble motor	Cell equator	14, 15
Abnormal spindle	ASPM	Microtuble binding protein	Minus end of CS	16, 17
Cytokinesis regulation				
Aurora B	Aurora B	CPC subunit	CS midzone	2, 12, 18
INCENP	Incenp	CPC subunit	CS midzone	2, 12, 19
Deterin/Scapolo	Survivin	CPC subunit	CS midzone	2

Tab. 1, Proteins/genes involved in cytokinesis of Drosophila spermatocytes, localizations in dividing spermatocytes.

Protein/ *gene*	**Protein family**	**Predicted protein function**	**Localization***	**Refs**
Cytokinesis regulation				
Australin	Borealin	CPC subunit	CS midzone	12
Polo	Polo	Polo kinase	CS midzone	10, 20, 21
Cdc37	Cdc37	Required for the activity andstability of protein kinases, it forms a complex with Aurora B and Hsp90	ND	22
Membrane remodeling and vesciche traffic				
Syntaxin 5	Syntaxin 5	Golgi traffic, vesicle fusion	Golgi	23
Four way stop (Cog5), Cog7	COG complex	Golgi integrity, vesicle trafficking and glycosilation Golgi traffic	Golgi	24, 25
Brunel-leschi	TRAPPII subunit PITP	Phosphatidylinositol transfer vesicle traffic endocytic traffic	Golgi	26
Giotto/vib	PITP	Phosphatidylino-sitol transfer vesicle traffic	ER, CF	27, 28, 29

Tab. 1, Proteins/genes involved in cytokinesis of Drosophila spermatocytes, localizations in dividing spermatocytes.

Protein/ *gene*	**Protein family**	**Predicted protein function**	**Localizzation***	**Refs**
Membrane remodeling and vesciche traffic				
Arf6	Arf6	endocytic traffic	Recycling endosome	30
Four wheel drive	PI4Kβ	phosphatidylinositol 4-Kinase	Golgi	28, 31, 32
Rab11	Rab11	Rab11GTPase, Golgi and endocytic traffic	Golgi, vesicle, CF	26, 28, 30, 32
Rho GTPase module				
Twistar	Cofillin	Actin severing	ND	4
Sticky/ Dck	citron kinase	Serine-Threonine kinase	CF	33
Nessun Dorma	Nessun Dorma	Centralspindlin Partener, hight affinità for b-galactoside	CF and ring canal	34

***** Localization of some proteins has not ben studied in dividing spermatocytes.

ND, not determined; CS, central spindle; CR, contractile ring; CF, cleavage furrow; CPC, chromosomal passenger complex; ER, endoplasmic reticulum; PI4Kβ, phosphatidylinositol 4-Kinase β.

References:

1) Goldbach, 2010; **2)** Szafer-Glusman, 2011; **3)** Giansanti, 2004; **4)** Gunsalus, 1995; **5)** Hime, 1996; **6)** Giansanti, 2001; **7)** Giansanti, 1999; **8)** Giansanti, 1998; **9)** Castrillon, 1994; **10)** Carmena, 1998; **11)** Vernì,

2004; **12)** Gao, 2008; **13)** Williams, 1995; **14)** Gandhi, 2003; **15)** Gatt, 2005; **16)** Wakefield, 2001; **17)** Riparbelli, 2002; **18)** Bucciarelli, 2003; **19)** Resnick, 2006; **20)** Herrmann, 1998; **21)** Sampaio, 2001; **22)** Lange, 2002; **23)** Xu, 2002; **24)** Farkas, 2003; **25)** Belloni, 2012; **26)** Robinett, 2009; **27)** Giansanti, 2006; **28)** Giansanti, 2007; **29)** Gatt, 2006; **30)** Dyer, 2007; **31)** Brill, 2000; **32)** Polevoy, 2009; **33)** Naim, 2004; **34)** Montembault, 2010.

The roles of the *Drosophila* orthologue of human GOLPH3 during cytokinesis.

Introduction.

I have isolated a male sterile mutation in the gene encoding the *Drosophila* othologue of human Golgi phosphoprotein 3 (GOLPH3) which has recently been recognized as a potent oncogene amplified in many human cancers (Scott et al, 2009, Scott and Chin, 2010; Hu et al, 2012; Hua et al, 2012; kunigou et al, 2012; Li et al, 2012; Wang et al, 2012; Zeng et al, 2012; Zhou et al, 2012). GOLPH3, a highly conserved 34-kDa protein, was initially identified through a proteomic analysis of the Golgi apparatus and was described as a Golgi-localized coatlike protein (Bell et al., 2001; Snyder et al., 2006). Recruitment of Vps74/GOLPH3 to the Golgi apparatus depends on the specific recognition of the lipid PtdIns(4)P in a conserved putative binding pocket on the surface of the protein (Dippold et al., 2009; Wood et al., 2009). Human GOLPH3 also interacts with the unconventional myosin MYO18A, mediating a linkage with the F-actin cytoskeleton that was proposed to facilitate the flattening of the Golgi as well as vesicle formation (Dippold et al., 2009). In the context of cancer pathogenesis, GOLPH3 was implicated in cellular transformation via changes in the activity of mTOR (Scott et al, 2009, Scott and Chin, 2010). The mammalian TOR kinase is the catalytic subunit of two distinct signaling complexes within cells referred to as mTORC1 and mTORC2, which differ in subunit composition and sensitivity to the bacterial macrolide rapamycin (Guertin and Sabatini, 2007). mTORC1 is a key regulator of growth factor and nutrient signaling; S6 kinase is the best characterized downstream effector of this complex. mTORC2 plays roles in regulating the actin cytoskeleton and in activating AKT/protein kinase B through Ser473 phosphorylation (Guertin and Sabatini, 2007). GOLPH3 physically interacts with Vps35, a component of the retromer protein trafficking complex known to

activate both mTOR complexes in budding yeast (Scott et al, 2009, Scott and Chin, 2010).

My work provides the first information to date implicating GOLPH3/Vps74p in cytokinesis.

2 RESULTS

2.1 Sauron encodes the *Drosophila* ortholog of *GOLPH3*.

The *sau*^{Z2217} mutant allele was isolated in the course of a screen for mutants defective in spermatocyte cytokinesis (Giansanti et al., 2004). Deficiency mapping showed that *sau*^{Z2217} was uncovered by both *Df(2L)Exel6007* and *Df(2L)Exel7010* defining a small polytene chromosome region containing 22 genes (**Figure 1**). DNA sequencing of *sau*^{Z2217} revealed a single point mutation in the annotated gene *CG7085* resulting in a substitution of Lysine in place of a conserved Glutamic-acid at position 273 of the C-terminus of the predicted protein (**Figure 2**). A P element lethal insertion in the *CG7085* gene, namely *l(2)s5379*, failed to complement *sau*^{Z2217} mutation for both male sterility and meiotic cytokinesis (Figure 1). In addition testes from males expressing dsRNA against *CG7085* contained frequent aberrant multi-nucleate spermatids and a cytokinetic phenotype that was fully comparable to *sau*^{Z2217}, *sau*^{Z2217}/*l(2)s5379* and *sau*^{Z2217}/*Df(2L)Exel7010* males (**Figure 3**). We generated transgenic flies that express GFP-Sau under the control of a tubulin promoter. The GFP-Sau protein rescued the defects of *sau*^{Z2217} and *sau*^{Z2217}/*l(2)s5379* mutants confirming that the cytokinesis phenotype is the consequence of alterations in the *Drosophila* GOLPH3 orthologue. Taken together these results indicate that *sau* encodes a polypeptide of 294 amino acids sharing an identity of 70% to human GOLPH3 (**Figure 2**), a Golgi protein that was recognized as a potent oncogene amplified in many human cancers (Dippold et al., 2009; Scott et al., 2009).

2.2 Sau/GOLPH3 concentrated in the cleavage furrow of *Drosophila* dividing spermatocytes.

In order to study the localization of Sau/GOLPH3, I raised polyclonal antibodies directed against the entire protein. The antibodies recognized a band of the predicted molecular weight in western blots from adult testis extracts (**Figure 4**). This band was

substantially reduced in blots from males expressing dsRNA against *CG7085* indicating that the antibodies specifically reacted with Sau/GOLPH3 (**Figure 4**). In prophase I spermatocytes, both the GFP-tagged protein and the endogenous protein were enriched at multiple round structures that also contained the Golgi marker Lava Lamp (Lva, Sisson et al., 2000) indicating that Sau/GOLPH3 localized to the Golgi stacks (**Figure 5**). I also explored the possible association of this protein with endosomes. In prophase spermatocytes from males co-expressing GFP-Sau Vps35-RPF, Sau/GOLPH3 co-localized with the endosomal marker Vps-35 (**Figure 6**). During metaphase and anaphase GOLPH3/Sau was associated with vesicles in the polar regions of the cell (**Figure 5**). During telophase Sau/GOLPH3 accumulated at the cleavage furrow suggesting a role in cytokinesis (**Figure 6**). Anti-Sauron staining was absent from male germ cells depleted of *sauron* confirmining the specificity of our antibodies.

2.3 Dividing spermatocytes from *sauron* mutants were defective in early steps of cytokinesis.

Previous analysis conducted in homozygous sau^{Z2217} mutant males failed to detect central spindles and F-actin rings in most telophase spermatocytes suggesting a role for Sau/GOLPH3 in the assembly and/or stability of these cytokinetic structures (Giansanti et al., 2004). Examination of F-actin using an improved protocol (see Material and Methods) confirmed defects in F-actin ring assembly in hemizygous sau^{Z2217} mutant spermatocytes: most telophase spermatocytes (85% of cells examined, n= 34; n=44 control cells) did not display an F-actin ring although irregular patches of F-actin could be rarely visualised at cell equator (**Figure 7**). I extended the analysis of *sau* phenotype and explored whether the localization of other components of the cytokinetic apparatus was also affected in hemizygous sau^{Z2217} mutant cells. In wild-type spermatocytes, Myosin II started to concentrate into rings at cell equator during late anaphase, (100% of cells, n=48; **Figure 8A**) that constricted in cells at mid-late telophase (100% of cells, n=65; **Figure 8A**). Most spermatocytes from sau^{Z2217} hemizygotes fixed during late

anaphase appeared devoid of clear Myosin rings (50% of cells examined; n=44). In these cells Myosin II appeared associated with patches located at the equatorial cortex (**Figure 8B**). In *sau^{Z2217}/Df(2L)Exel7010* spermatocytes fixed at mid-late telophase, Myosin II was associated with patches in 50% of cells and formed unconstricted large rings in 40% of cells (n=120, **Figure 8B**). I next explored the localization of Septins, cytoskeletal scaffolding proteins that bind to phosphoinositides and form a membrane-associated filament system required to anchor the actomyosin ring to plasma membrane (reviewed by Oh and Bi, 2011; Beise and Trimble, 2011). In wild type dividing spermatocytes Septins started to localize into thin equatorial rings during late anaphase/early telophase (n=45; **Figure 9A**). In spermatocytes fixed during later telophase stages Septin rings appeared thicker as constriction progressed (n=63; **Figure 9A**). In most early telophase spermatocytes from *sau^{Z2217}/Df(2L)Exel7010* hemizygotes Septins failed to concentrate into clear rings (48% of cells, n=42). In mutant spermatocytes fixed at mid-telophase or late telophase Septin rings were either not visible or poorly constricted and substantially thinner than the constricted rings of wild type (81% of cells, n=62; **Figure 9B**).

2.4 Mutations in *sau* affect the organization of the central spindle.

I next focused on the central spindle organization of *sau* mutant spermatocytes. Previous work showed defective central spindles in most fixed telophase spermatocytes from *sau^{Z2217}* homozygous males. Staining for tubulin of *sau^{Z2217}* telophases from hemizygous males confirmed a requirement for Sau/DGolph3 in central spindle assembly and stability. Because central spindle formation is highly dynamic, we analyzed this process in wild type and *sau^{Z2217}* living spermatocytes expressing EGFP-b-tubulin (**Figure 10**). In wild-type (n=10) dividing spermatocytes at anaphase, a set of (MTs) microtubules extending from the poles probed the cell cortex in proximity of the equatorial region (Frame 09 in **Figure 10A**) and started bundling (Frame 16, **Figure 10A**). This initial bundling of

MTs at the equatorial cortex was accompanied by cell elongation and the interdigitation of a second population of MTs (interior MTs) in the center of the cell (Frame 16, **Figure 10A**). Furrow ingression compacted the MTs arrays (Frame 19, **Figure 10A**) giving rise to the characteristic telophase central spindle that was pinched in the middle during cytokinesis (Frames 21, 24, 36, **Figure 10A**).

In most *sau*^{Z2217} mutant spermatocytes (7/10), although peripheral MTs contacted the cortex at cell equator during anaphase (Frame 19; **Figure 10B**), they failed to interdigitate and stabilize (Frames 24, 26, **Figure 10B**). In addition interior MTs failed to bundle at the cell midzone (Frames 24, 26, **Figure 10B**) and cells failed to elongate and to undergo furrow ingression (**Figure 10B**).

This analysis suggested a role for Sau/GOLPH3 in the initial steps of central spindle assembly. I thus asked whether *sauron* mutations affected the localization of proteins required for central spindle formation. Immunofluorescence staining of wild type dividing spermatocytes for the microtubule bundling protein/Fascetto (Feo, Verni et al, 2004), the *Drosophila* orthologue of human Prc1, showed that this protein localized to microtubule bundles at the cell midzone of anaphases (n=44 mutant cells; n= 32 control cells; **Figure 11A and 11B**). However, in *sau*^{Z2217}*/Df(2L)Exel7010* spermatocytes at telophase Feo did not form a tight equatorial band and was either associated with signals scattered between the two nuclei or appeared diffuse (n=50 mutant cells; n= 45 control cells; **Figure 11B**), consistent with the failure of central spindle formation of this mutant. Similar results were obtained by staining for the centralspindlin component Pavarotti (Pav). Telophase spermatocytes from *sau*^{Z2217}*/Df(2L)Exel7010* males exhibited faint Pav accumulations that failed to resemble the tight equatorial bands displayed by wild type males (**Figure 12**).

2.5 GOLPH3/Sau lipid interaction.

Localization of Vps74 and human GOLPH3 to the Golgi apparatus was shown to depend on the lipid PtdIns(4)P (Dippold

et al., 2009) although GOLPH3 was able to interact with also PtdIns(3)P, PtdIns(5)P and PtdIns(4,5)P2 in lipid binding assays (Wood et al., 2009). In order to test whether Sau binding to lipid PtdIns(4)P provided an essential function for cytokinesis I constructed flies carrying *sau*^{Z2217} mutation and expressing a mutant version of GFP-Sau carrying non-conservative substitutions of two positively charged amino acids (K167A/R170L, **Figure 2**) that impair binding of PtdIns4P based on crystal structure of GOLPH3 and Vps74 (Dippold et al., 2009; Wood et al., 2009). GFP-Sau carrying these substitutions failed to localize to the Golgi and to rescue the cytokinetic phenotype of *sau*^{Z2217} mutation (**Figure 13**) demonstrating that recruitment of Sau to Golgi membranes through PtdIns4P was an essential step during cytokinesis.

I next asked whether the Glu-Lys (E273K) mutation in our original *sau*^{Z2217} allele also affected the ability of Sau to bind to phosphoinositides. Wild type Sau and Sau mutant proteins carrying either K167A/R170L or E273K mutations were expressed as GST-tagged proteins and their ability to bind different species of phosphinositides were determined through protein-lipid overlay assays (**Figure 14** see also Material and Methods). My analysis revealed that wild type Sau interacted not only with PtdIns(4)P but also with the two phophoinositides PtdIns(3)P and PtdIns(5)P and the glycerophospholipid phosphatidic acid (**Figure 14**). As expected SauK167A/R170L failed to bind PtdIns(4)P, in addidion the protein carrying this mutation was also unable to bind PtdIns(5)P. Remarkably the pattern of lipid interaction for SauE273K was fully comparable to SauK167A/R170L indicating a defective binding to both PtdIns(4)P and PtdIns(5)P.

2.6 Sau and PtdIns(4)P during cytokinesis.

To validate the dependency of Sau on the PtdIns(4)P lipid in the Golgi stacks, I examined the localization of Sau in spermatocytes from males carrying mutations in the gene *four wheel drive (fwd)* that encodes the phosphatidylinositol-4-kinase (PtdIns-4-kinase)

III β required for PtdIns(4)P synthesis. My analysis revealed that Sau localization was abolished at the Golgi stacks in *fwd* in accordance with the assumption that Sau/GOLPH3 binding to this organelle requires PtdIns(4)P (**Figure 15**). I next asked whether the localization of PtdIns(4)P was affected in *sau* mutants. I analysed the subcellular distribution of PtdIns(4)P in wild type and *sau* spermatocytes expressing an RFP fusion to the PtdIns(4)P marker PH-FAPP (Polevoy et al., 2009). Consistent with data of Polevoy and coauthors (2009), the subcellular distribution of RFP-PH-FAPP signals indicated that PtdIns(4)P was localized on Golgi stacks in prophase spermatocytes (not shown) and enriched on secretory organelles at the midzone during telophase (**Figure 16**). In $sau^{Z2217}/Df(2L)Exel7010$ prophase spermatocytes, RFP-PH-FAPP signals at the Golgi stacks were not affected (not shown). However in telophase spermatocytes from $sau^{Z2217}/Df(2L)Exel7010$ RFP-PH-FAPP signals were completely delocalized and failed to accumulate at the midzone (**Figure 16**). Taken together these results indicate that Sau depends on PtdIns(4)P for its recruitment to the Golgi and that PtdIns(4)P concentration at the cleavage furrow requires the wild type function of Sau. In order to further substantiate the relationship between Fwd and Sau proteins I constructed double mutants carrying both *fwd* and *sau* mutations. Flies that were wild type for *sau* and hemyzygous for *fwd* and flies that were wild type for *fwd* and homozygous for *sau* were viable. However, sau^{Z2217} was fully lethal in combination with $fwd^3/Df(3L)7C$. Individuals of genotypes $sau^{Z2217}/Df(2L)Exel7010$; $fwd^3/Df(3L)7C$ or sau^{Z2217}; $fwd^3/Df(3L)7C$ died in early larval stages indicating a synthetic lethal genetic interaction.

2.7 Sau is required for membrane trafficking to the cleavage site.

The small GTPase Rab11, involved in both the secretory and the endocytic traffic, is essential for cytokinesis in several organisms, including *Drosophila* and mammalian cells (Riggs et al., 2003; Wilson *et al.*, 2005; Giansanti et al., 2007). Recent data showed

that this protein accumulates at the equator of *Drosophila* spermatocyte telophases and is essential for furrow ingression (Giansanti et al., 2007; Polevoy et al., 2009). Rab11 recruitment to the cleavage site was shown to depend on Fwd although this kinase does not localise to cell equator (Giansanti et al., 2012). Data from Polevoy and collaborators (2009) indicated that Fwd is required for synthesis of PI4P on Golgi membranes and for localization of PtdIns(4)P - and Rab11-associated secretory organelles at the cleavage furrow (Polevoy et al., 2009). Because *sau* abolished the localization of PtdIns(4)P - containing organelles to the cleavage furrow, we asked whether this mutation also affected concentration of Rab11 at cell equator. In contrast to wild type, GFP-Rab11 containing signals were completely dispersed during cytokinesis in *sau^{Z2217}/Df(2L)Exel7010* spermatocytes (**Figure 17**).

We next investigated the requirement for Sau in localization of other membrane trafficking markers. In wild type a GFP fusion to clathrin light chain (Clc-GFP, Chang et al., 2002) was enriched in clusters of vesicular structures in early prophase spermatocytes (**Figure 18A**). Clc-GFP puncta started to accumulate at each aster in spermatocytes fixed at late prophase and localized to cell equator of dividing spermatocytes at telophase (**Figure 18A**). In *sau^{Z2217}/Df(2L)Exel7010* mutant spermatocytes during early prophase Clc-GFP was enriched in clusters of vesicles although these structures appeared less numerous than in wild type (**Figure 18B**). In dividing mutant cells Clc-GFP failed to accumulate at the astral regions and to the cleavage furrow and was instead completely delocalized (**Figure 18B**).

2.8 Sau co-precipitates with Myosin II and Septin II in testis extracts.

Because Sau localized to cleavage furrow and was required for proper localization of contractile ring components to the cleavage site we performed co-immunoprecipitation experiments aimed at verifying protein interactions among these proteins. Protein extracts from testes expressing either GFP-Sau were

immunoprecipitated using the GFP-Trap (see material and methods). I found that Myosin II co-immunoprecipitated with Sau in *Drosophila* testes (**Figure 19A**). Similar Co-IP results were obtained in a second experiment from extracts of S2 cells transfected with Sau-GFP and immunoprecipitated for GFP (**Figure 19B**). Moreover GST-Sau pulled down Myosin II from testis extracts suggesting that these proteins might interact in male germ cells (**Figure 19C**). Similar Co-IP and GST pull down experiments suggested that Sau might also interact with Septin 2 in male germ cells (**Figure 20**).

2.9 Co-IP and GST pull down experiments suggest interactions of Sau with several membrane trafficking components.

Because my cytological analysis suggested a requirement for Sau in several vesicle trafficking events we also explored the potential interaction of Sau with membrane trafficking proteins.

The small GTPase proteins Rab5 controls early endocytic events such as clathrin-coated-vesicle-mediated transport from the plasma membrane to the early endosomes and homotypic early endosome fusion (reviewed in Zerial and McBride, 2001). Using a GFP-fusion to Rab5 I could demonstrate that this protein, like Rab11-GFP and Clc-GFP accumulated to the cleavage furrow of dividing spermatocytes during telophase (**Figure 21**). Vps-RFP also concentrated at the midzone of dividing cells although it was only visible during late stages of cyokinesis (**Figure 22A**). Consistent with data from mammalian cells (Scott et al., 2009) our GST and Co-IP experiments suggested that Sau and Vps-35 might form a complex also in *Drosophila* (**Figures 22B and 22C**). In addition when protein extracts from testes expressing either GFP-Rab5 or GFP-Rab11 were immunoprecipitated using the GFP-Trap we found that Sau co-immunoprecipitated with both Rab5 and Rab11 (**Figure 23**). Finally we also explored the potential interaction of Sau with clathrin components (**Figure 24**). We found that Sau co-immunoprecipitated with Clathrin heavy chain (Chc) when extracts from testes expressing Chc-RFP were

immunoprecipitated using the RFP-Trap (**Figure 24A**). In addition GST-Sau pulled down Clc from testis extracts expressing Clc-GFP (**Figure 24B**).

Fig. 1, Schematic representation of genomic deletions used to map *sauron.*

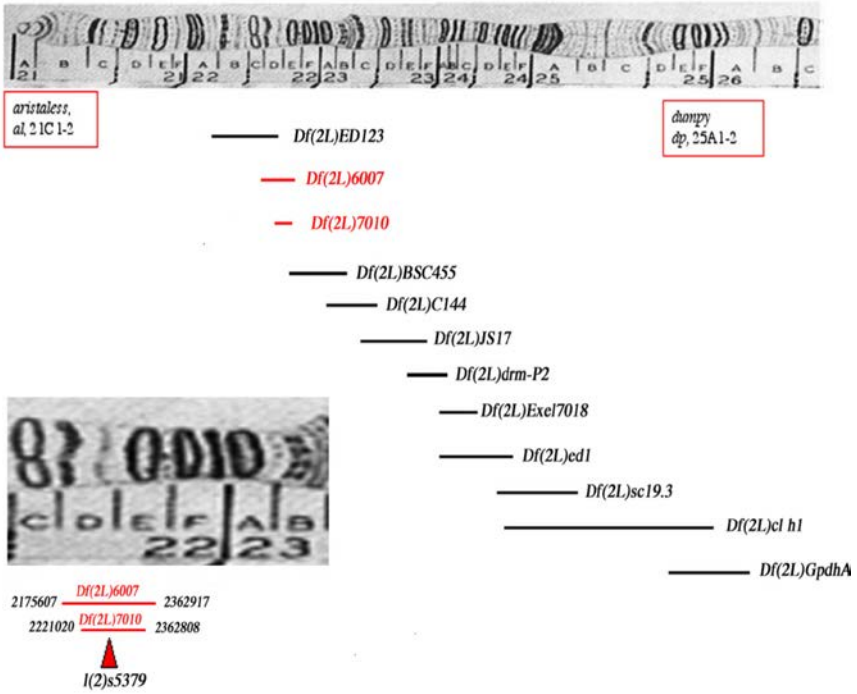

sau ^{Z2217} was uncovered by both *Df(2L)Exel6007* and *Df(2L)Exel7010* defining a small polytene chromosome region containing 22 genes.
The P element lethal insertion *l(2)s5379* in the *CG7085* gene, failed to complement *sau*^{Z2217} mutation for both male sterility and meiotic cytokinesis.

Fig. 2, Alignments between hGOLPH3 and Sauron (Sau) protein sequences.

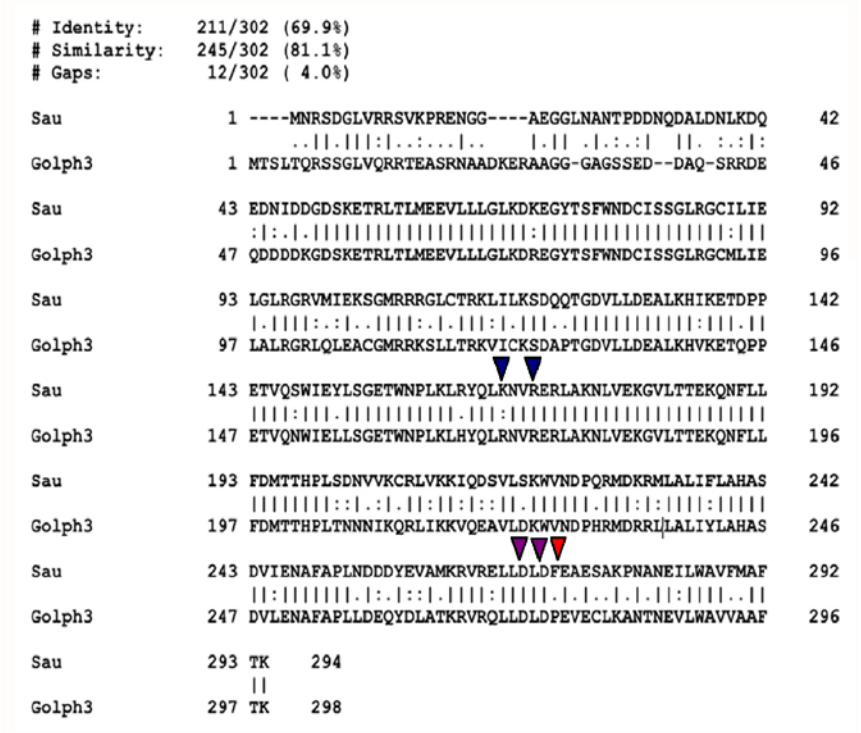

Red triangle indicates the substitution of Lysine in place of Glutamic acid (E273K) at position 273 of Sauron protein sequence.

Blue triangles indicate the two substitution K167A and R170L. This mutant version of Sauron affects the binding to PtdIns4P.

Violet triangles indicate the putative LLDLD consensus sequence for binding to Clathrin heavy chain.

Fig. 3, Spermatids at the onion-stage viewed by phase-contrast microscopy.

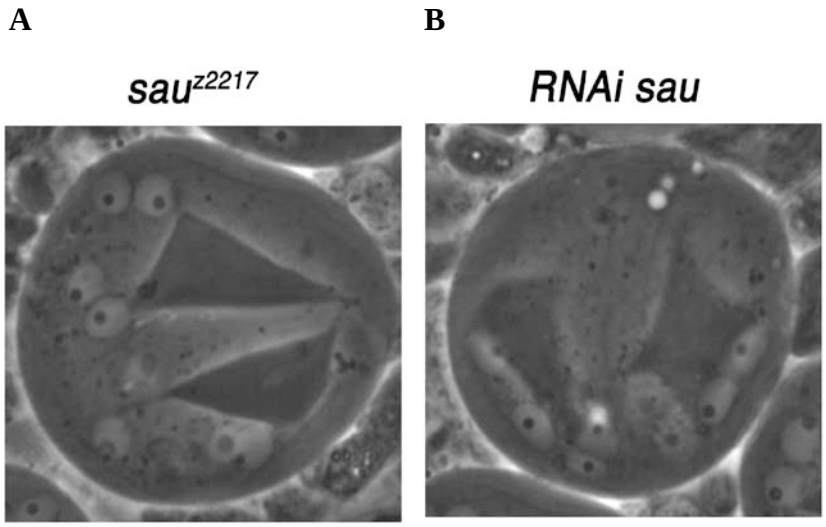

Testes from males expressing dsRNA against *CG7085* contained frequent aberrant multi-nucleate spermatids (**B**) suggeting a phenotype comparable to *sau*^{Z2217} (**A**).

Fig. 4, Western blots from adult testis extracts blotted for Sauron.

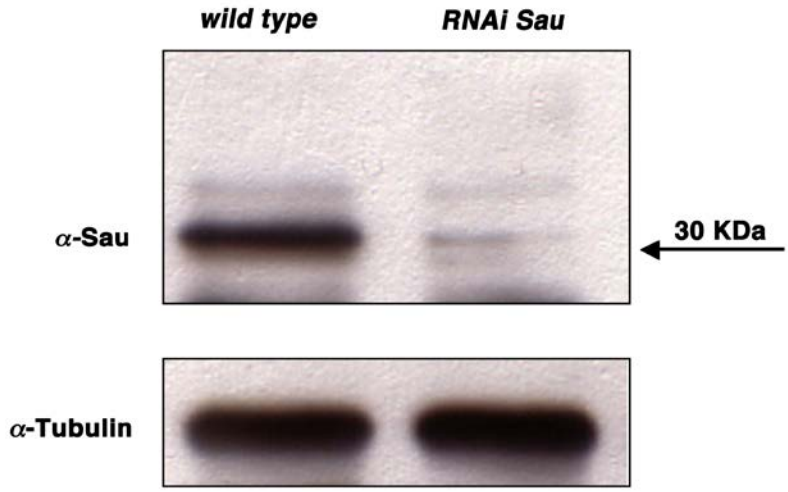

Anti Sauron antibodies recognize a band of the predicted 34 kDa that is strongly reduced in the testes from *sau*::RNAi males.

Fig. 5, Sau localizes to the Golgi stacks during prophase and accumulates at the cleavage furrow at telophase.

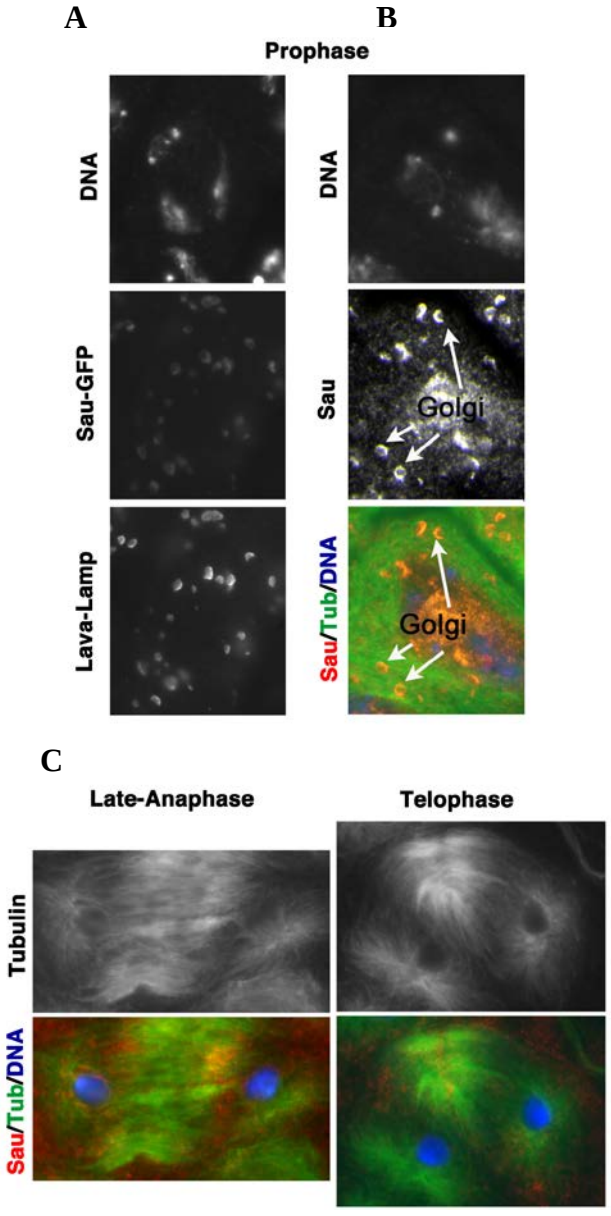

In prophase I spermatocytes, both the GFP-tagged protein (**A**) and the endogenous protein (**B**) were enriched at multiple round structures that also contained the Golgi marker Lava Lamp (Lva) indicating that Sau localized to the Golgi stacks.
During metaphase and anaphase (**C**) Sau was associated with vesicles in the polar regions of the cell.
During telophase Sau accumulated at the cleavage furrow suggesting a role in cytokinesis.

Fig. 6, Sauron colicalises with the retromer subunit Vps35.

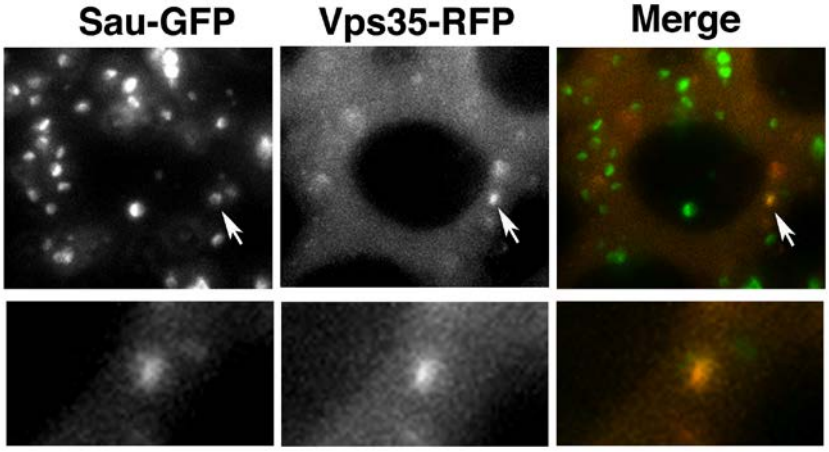

In prophase spermatocytes from males expressing both GFP-Sau and Vps35-RPF, Sau protein co-localized with the endosomal marker Vps35.

Fig. 7, Staining for F-actin in wild type (**A**) and mutant (**B**) dividing spermatocytes.

A

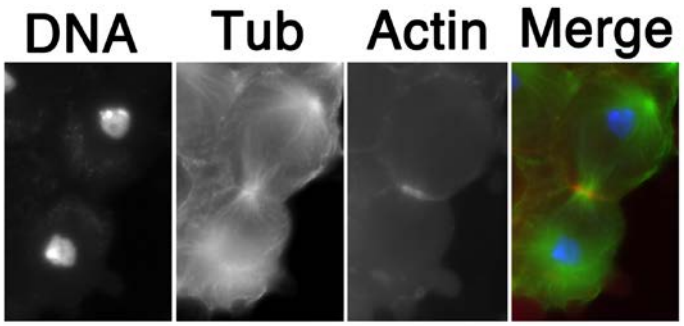

B

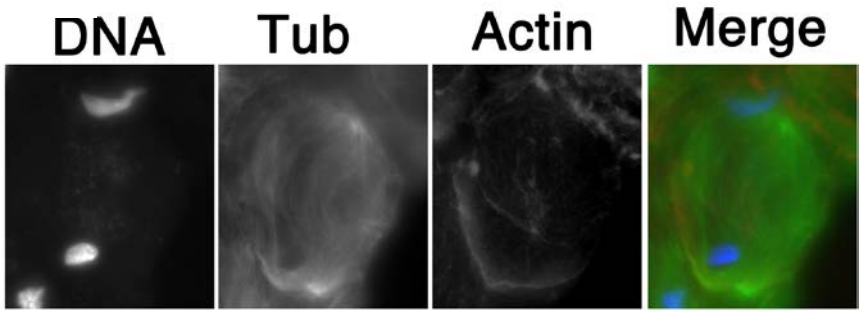

Wild type and hemizygous *sau*^{Z2217} mutant spermatocytes were stained for F-actin (Red), Tubulin (Green) and DNA (Blue).

Fig. 8, Staining for Myosin II in wild type (**A**) and mutant (**B**) dividing spermatocytes.

A

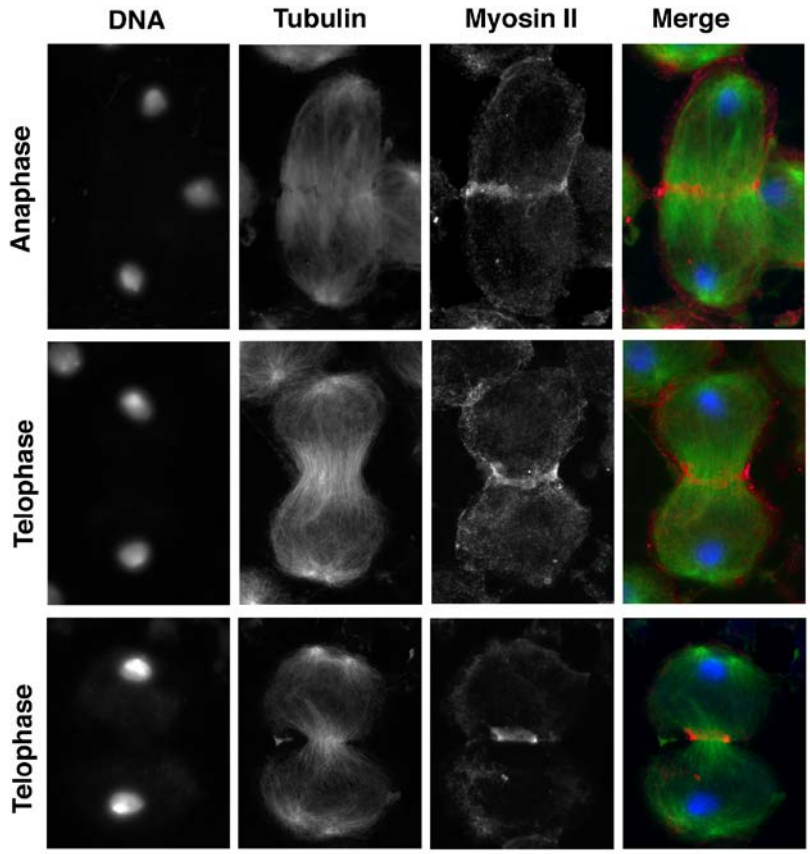

Wild type spermatocytes at anaphase and telophase were stained for non-muscle Myosin II (Red), Tubulin (Green) and DNA (Blue).

B

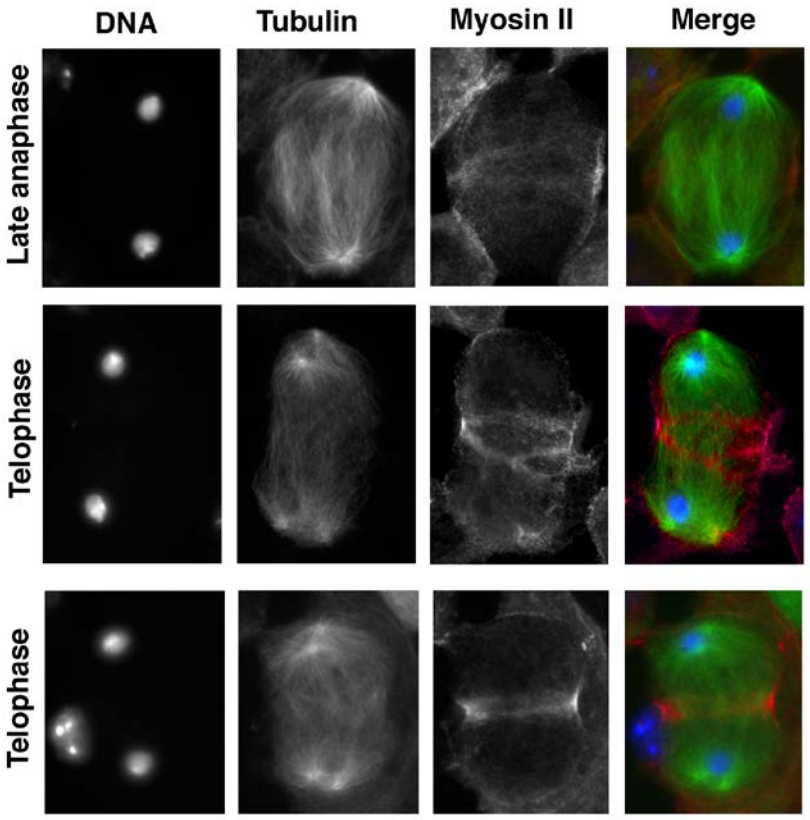

Spermatocytes at anaphase and telophase from *sau*^{Z2217} hemizygotes were stained for Myosin II (*Drosophila* Zipper, Red), Tubulin (Green) and DNA (Blue).

Fig. 9, Staining for Septin 2 in wild type (**A**) and mutant (**B**) dividing spermatocytes.

A

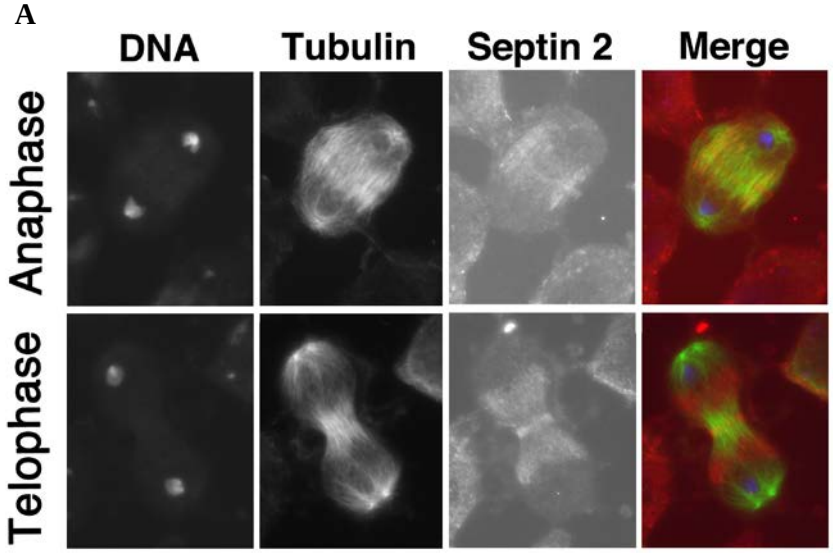

Wild type dividing spermatocytes were fixed and stained for Septin 2 (Red), Tubulin (Green) and DNA (Blue).
Septins start to localize during late anaphase/early telophase into thin equatorial rings that appeared thicker as constriction progressed.

B

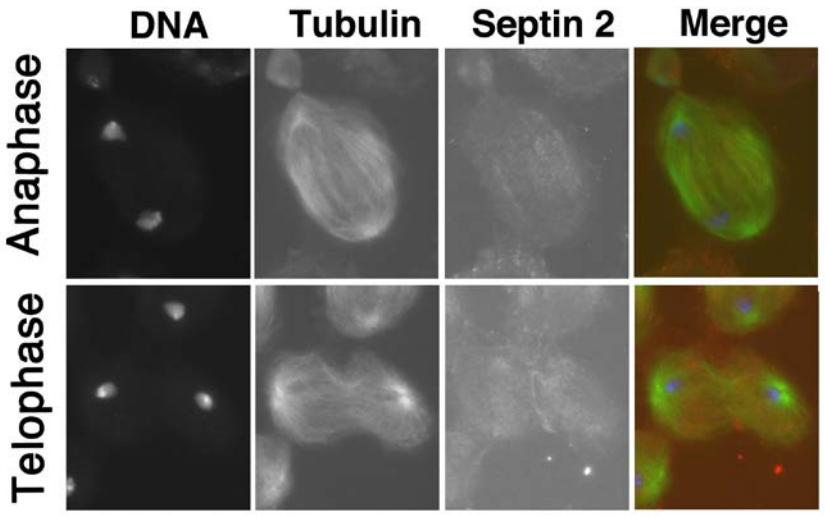

Spermatocytes from *sau* hemizygotes were fixed and stained for Septin 2 (Red), Tubulin (Green) and DNA (Blue).
In most early ana-telophases Septins failed to concentrate into clear rings. In mutant spermatocytes fixed at mid-telophase or late telophase Septin rings were either not visible or poorly constricted and substantially thinner than the constricted rings of wild type.

Fig. 10, Analysis of the dynamics of central spindle formation in wild type (**A**) and *sau*^{Z2217} (**B**) living spermatocytes expressing EGFP-β-tubulin.

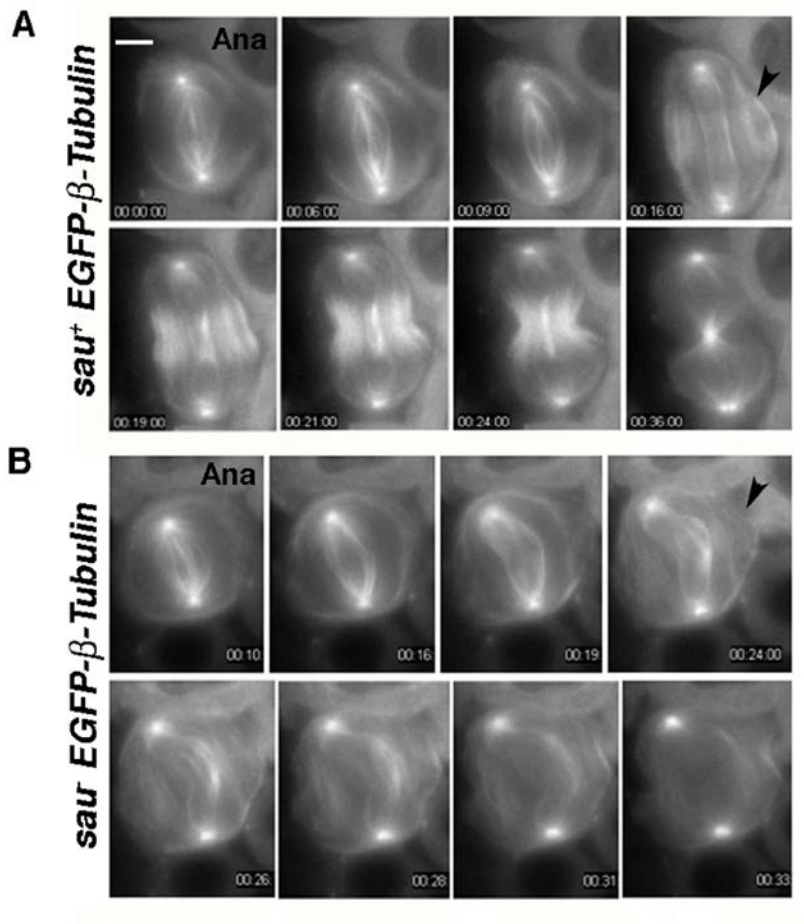

Wild-type (**A**) and *sau* mutant (**B**) dividing spermatocytes that express EGFP-b-tubulin undergoing anaphase and telophase were filmed from anaphase onset (first frame) to telophase. Bar, 10 μm.

Fig. 11, Staining for Feo in wild type (**A**) and mutant (**B**) dividing spermatocytes.

A

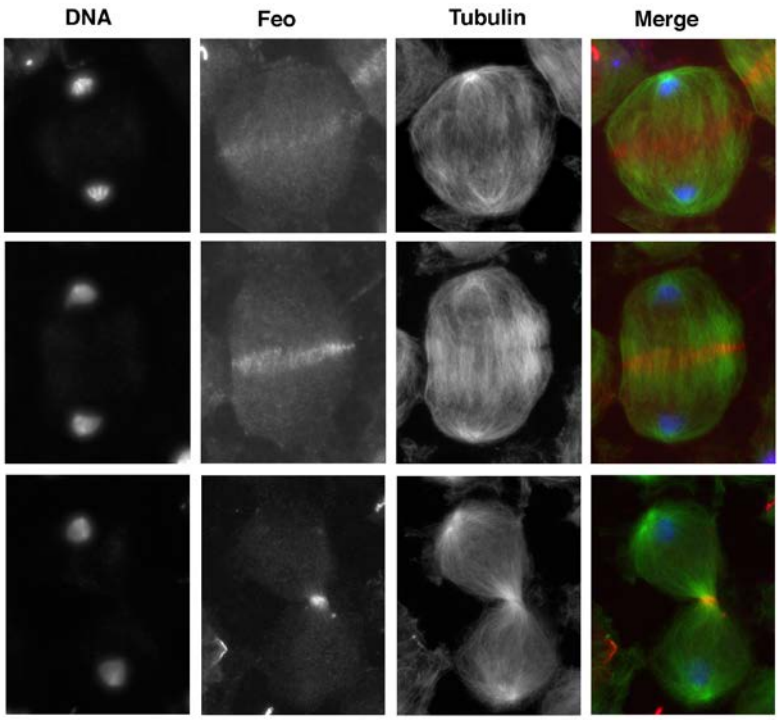

Wild type dividing spermatocytes at late anaphase and telophase were stained for the microtubule bundling protein/Fascetto (Red), Tubulin (Green) and DNA (Blue).

B

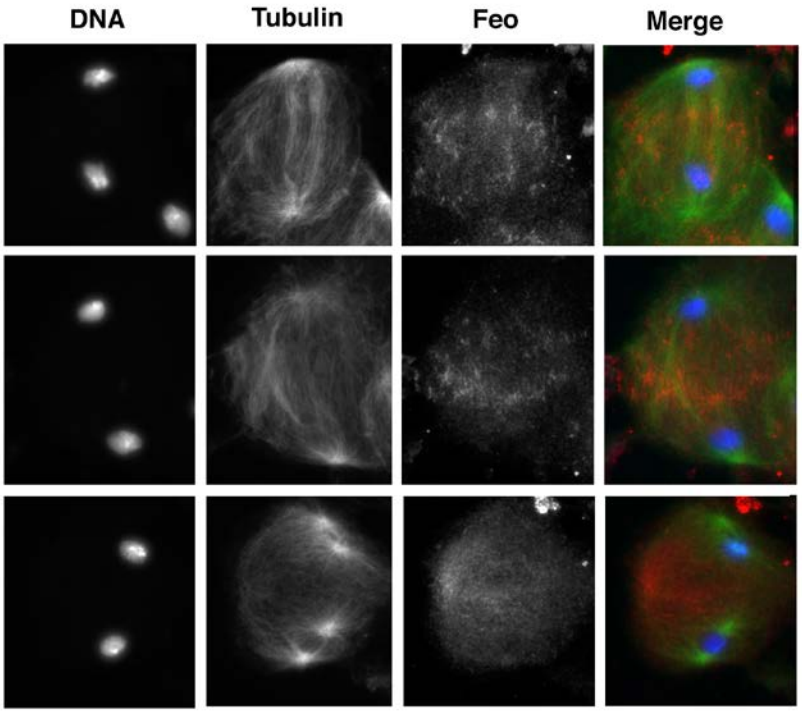

sau hemizygous spermatocytes at anaphase and telophase were fixed Feo (Red), Tubulin (Green) and DNA (Blue).

Fig. 12, Staining for Pav in wild type and mutant dividing spermatocytes.

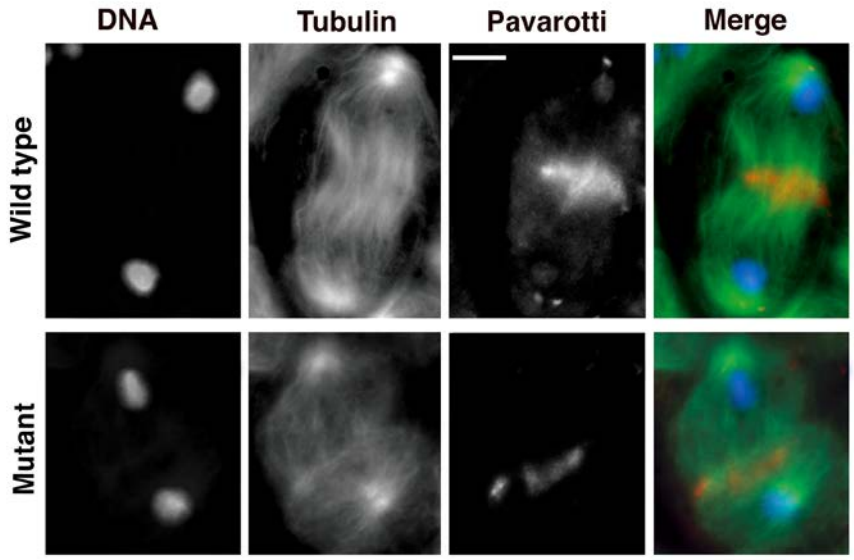

Telophase spermatocytes from wild type and *sau* hemizygous males were fixed and stained for Pav (Red), Tubulin (Green) and DNA (Blue). Telophase spermatocytes from *sau* males exhibited faint Pav accumulations that failed to resemble the tight equatorial bands displayed by wild type.
Bar, 10 μm.

Fig. 13, Analysis of cellular localization of GFP-Sau carrying the K167A/ R170L substitutions.

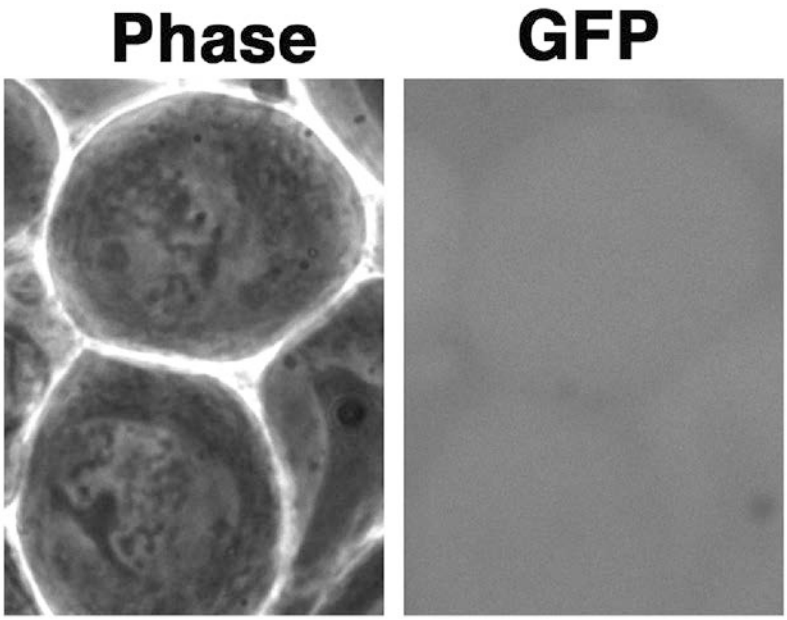

GFP-Sau K167A/R170L fails to rescue *sau* mutants and fails to localize at the Golgi.

Fig. 14, Sau protein-lipid overlay assay.

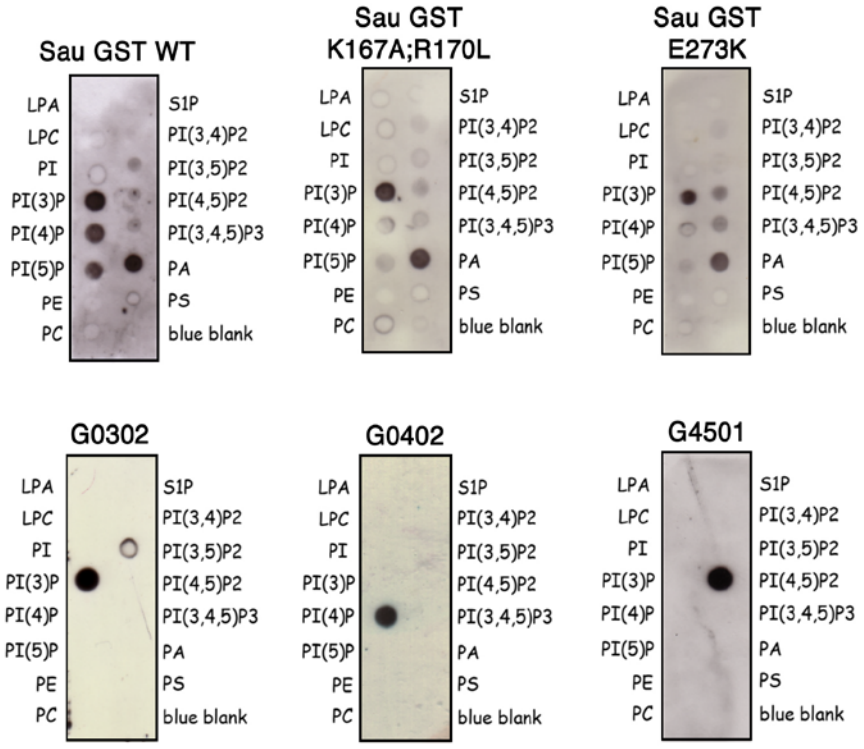

PIP Strips (Echelon) membranes were incubated with:

- Wild type Sau-GST.
- The mutant version of Sau-GST carrying the substitutions K167A/ R170L that affect binding to PtdIns4P.
- Sau-GST carrying the E273K mutation in our *sau*^{z2217} allele.
- Recombinant GST-tagged controls that specifically bind to different lipid spots.

Fig. 15, Analysis of the localization of GFP-Sau in spermatocytes from males carrying mutations in the gene *four wheel drive (fwd)*.

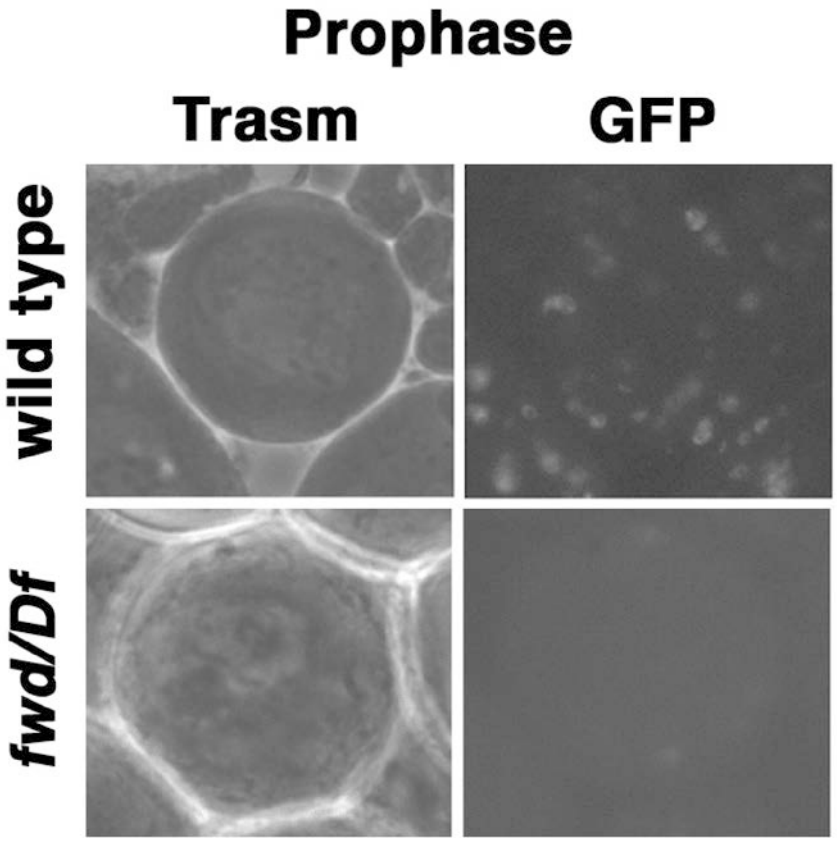

Wild type and *fwd*^{3}*/Df(3L)7C (fwd/Df)* mutant spermatocytes expressing GFP-Sau during prophase were imaged for GFP.

Fig. 16, Subcellular distribution of RFP-PH-FAPP signals in wild type and *sau*^{2217} mutant spermatocytes.

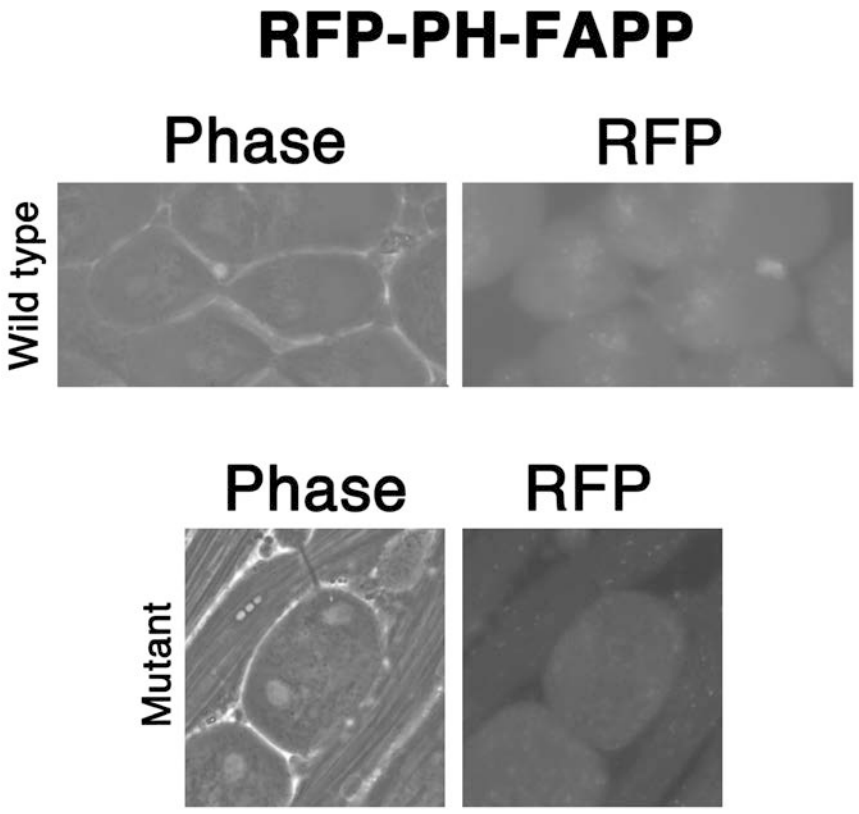

Wild type and *sau* hemizygous spermatocytes expressing RFP-PH-FAPP were imaged during telophase.
Note that RFP-PH-FAPP signals were completely delocalized and failed to accumulate at the midzone of *sau* mutants.

Fig. 17, Subcellular localization of GFP-Rab11 in wild type and *sau*^{z2217} hemizygous mutant spermatocytes.

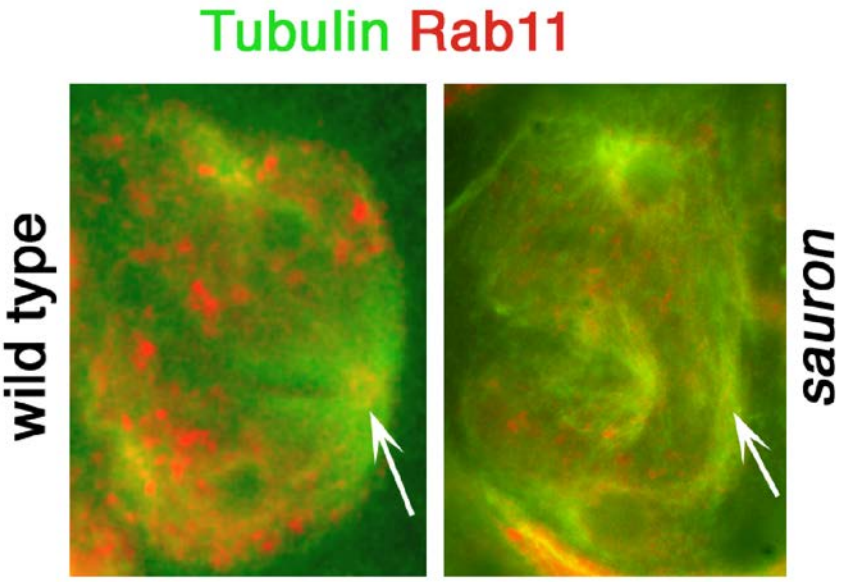

Dividing spermatocytes from wild type and *sau*^{z2217} hemizygous mutant spermatocytes expressing GFP-Rab11 (Red), were stained for tubulin (Green).
In wild type telophases GFP-Rab11 (Red) is associated with secretory organelles that localise at the cleavage furrow.
In contrast GFP-Rab11 containing signals were completely dispersed during cytokinesis of *sau*^{z2217} mutant spermatocytes.

Fig. 18, Subcellular localization of Clathrin light chain (Clc) tagged with GFP in wild type (**A**) and *sau*^{z2217} (**B**) mutants.

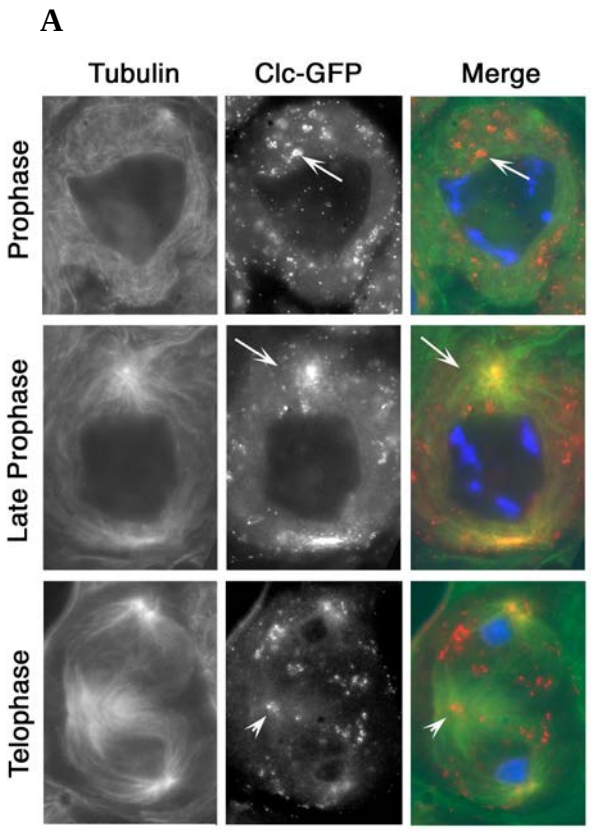

Wild type spermatocytes expressing a GFP fusion to clathrin light chain (Clc-GFP) were fixed and stained for Tubulin (Green) and DNA (Blue). Clc-GFP was enriched in clusters of vesicular structures in early prophase spermatocytes. Clc-GFP puncta started to accumulate around each aster in late prophase and localized to the equator of dividing cells at telophase.

B

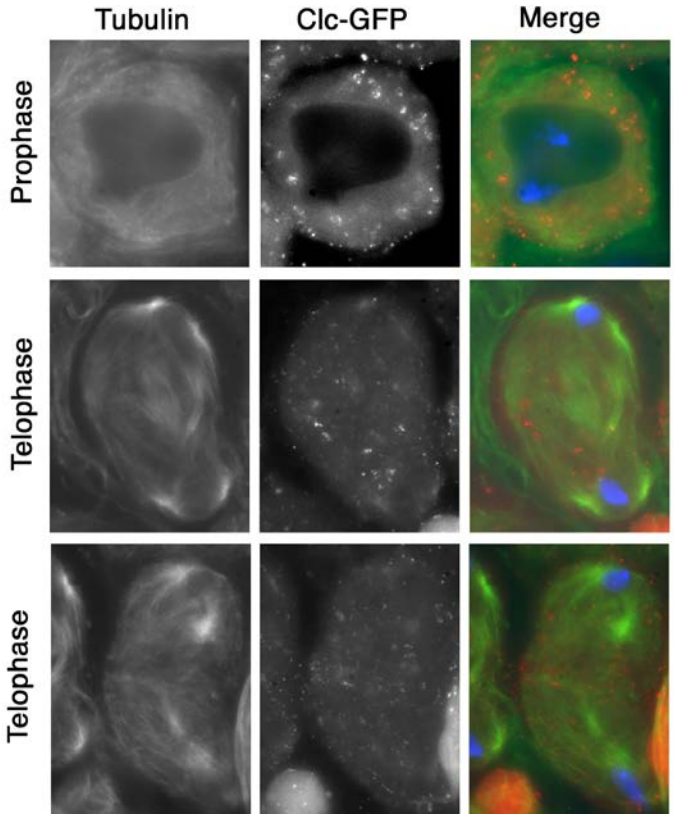

In *sau*^{Z2217} */Df(2L)Exel6007* mutant spermatocytes during early prophase Clc-GFP was enriched in clusters of vesicles although these structures appeared less numerous than in wild type.
In dividing mutant cells Clc-GFP failed to accumulate at the astral regions and to the cleavage furrow and was instead completely delocalized.

Fig. 19, Analysis of interaction between Sauron and Myosin II.

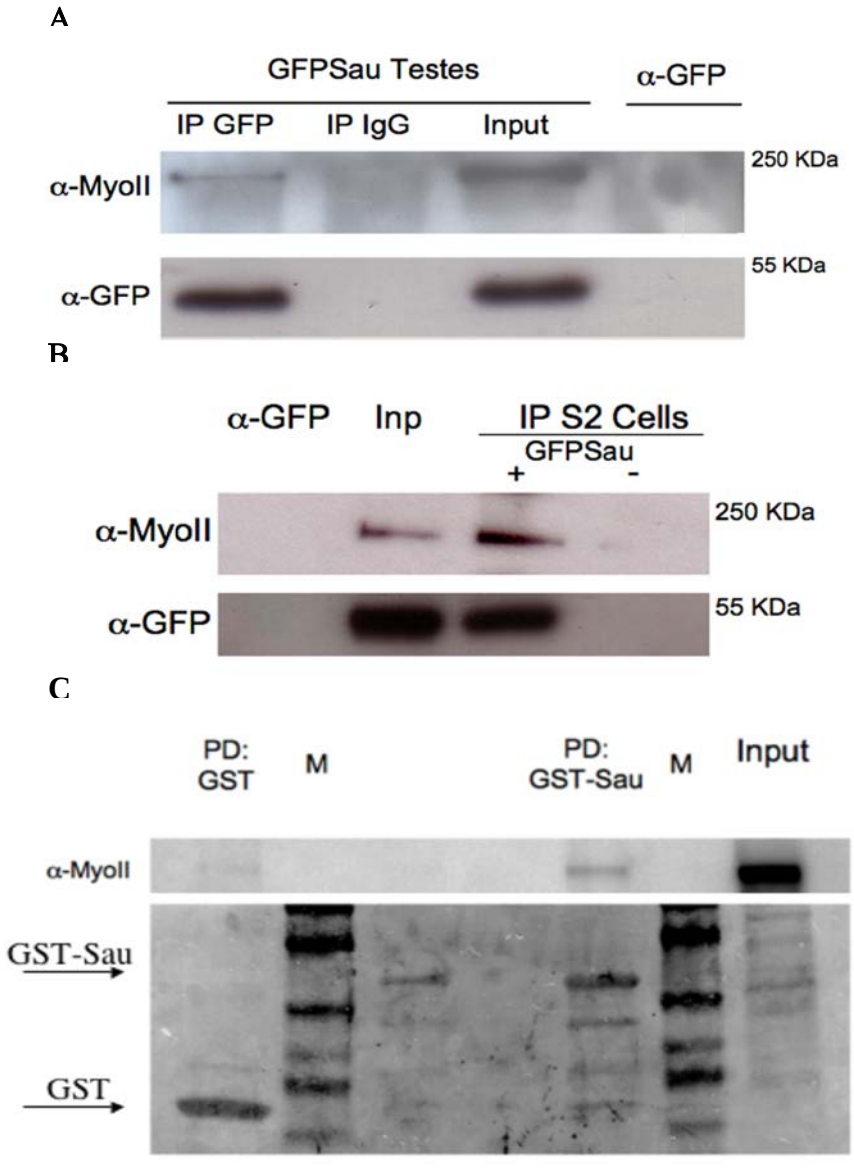

(A) Protein extracts from testes expressing GFP-Sau were immunoprecipitated with either anti-GFP or control IgG. Myosin II co-immunoprecipitated with Sau.
(B) Protein extracts from S2 cells transfected with GFP-Sau and immunoprecipitated with either anti-GFP or control IgG. Myosin II co-immunoprecipitated with Sau.
(C) GST-Sau, but not GST pulled down Myosin II from testis extracts suggesting that Sau and Myosin II might interact in male germ cells.

Fig. 20, Interaction analysis between Sauron and Septin 2.

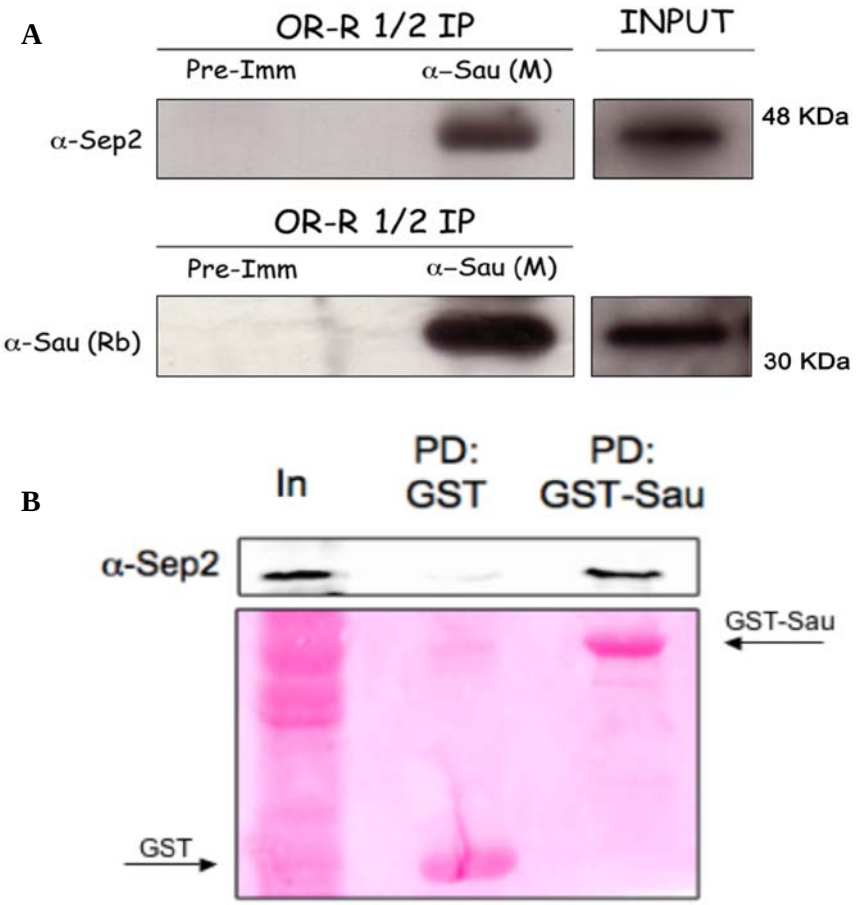

(A) Protein extracts from control Oregon-R testes (OR-R) testes were immunoprecipitated with either mouse anti-Sauron (M) or preimmune serum and blotted for either Sauron (using rabbit anti-Sauron) or Septin 2. Septin 2 co-immunoprecipitated with Sauron in *Drosophila* testes.
(B) GST-Sau pulled down Septin 2 from testis extracts suggesting that Sauron and Septin 2 might interact in *Drosophila* testes.

Fig. 21, Rab5-GFP localization during telophase in *Drosophila* spermatocytes.

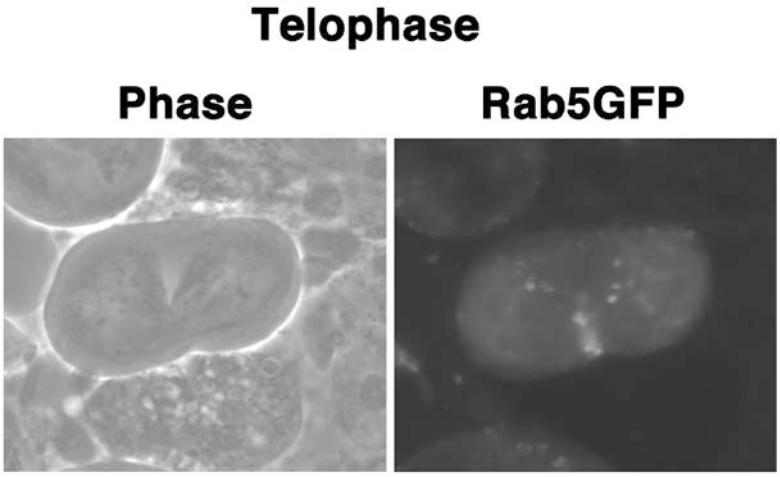

Rab5-GFP accumulated to the cleavage furrow of dividing spermatocytes during telophase.

Fig. 22, Vps35-RFP localization in *Drosophila* spermatocytes and interaction analysis of Vps35 with Sauron.

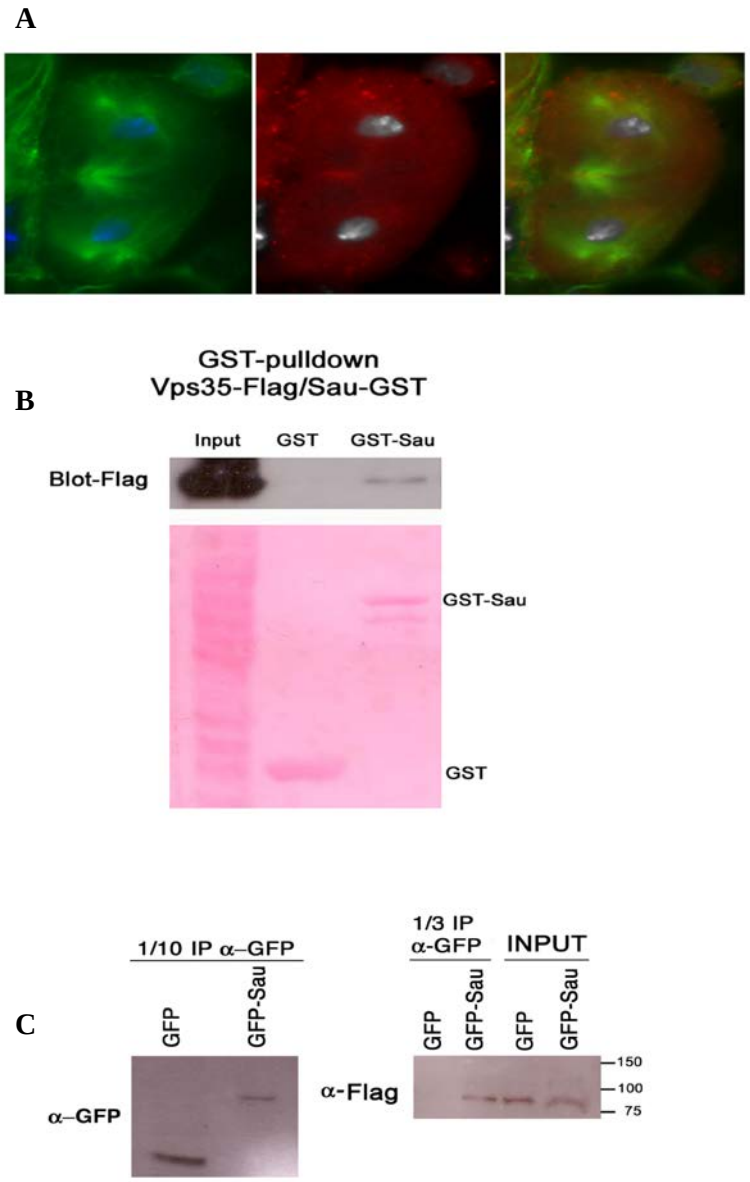

(A) Vps35-RFP accumulates in vesicles at cell poles and concentrates at the cell midzone in dividing spermatocytes at late stages of cyokinesis.
(B) GST-Sau pulls down Vps35-Flag from S2 cells transfected with Vps35-Flag.
(C) S2 cells transfected with Vps35-Flag and either GFP (control) or GFP-Sau were immunoprecitated with anti-GFP and blotted for GFP (left panel) or Flag (right panel).

Fig. 23, Interaction analysis between Sauron and Rab proteins.

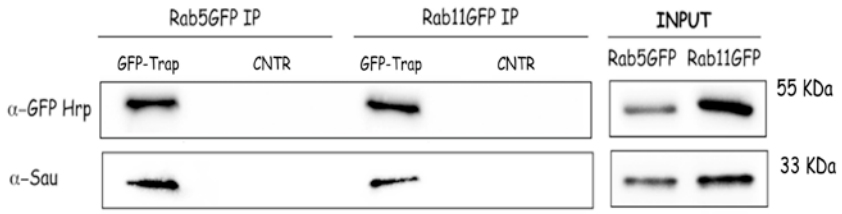

Protein extracts from testes expressing either GFP-Rab5 or GFP-Rab11 were immunoprecipitated with either GFP-Trap or control beads (cntr) and blotted for GFP and Sau.
Note that Sau co-immunoprecipitated with both Rab5 and Rab11.

Fig. 24, Interaction analysis between Sauron and Clathrin.

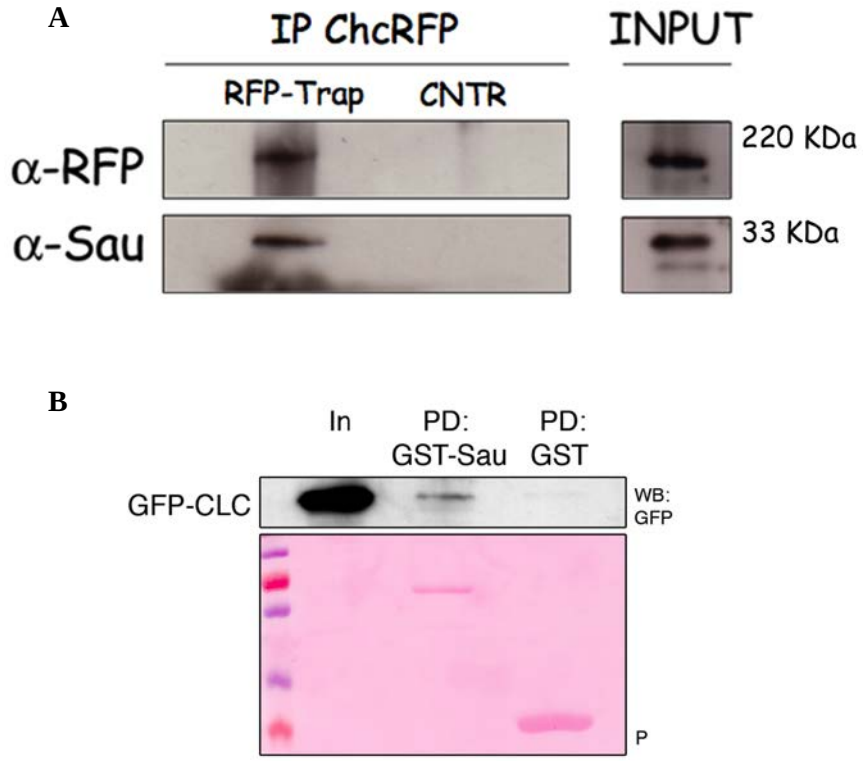

(A) Protein extracts from testes expressing Clathrin heavy chain tagged with RFP (Chc-RFP) were immunoprecipitated with either anti-RFP (RFP-Trap) or control beads (cntr) and blotted for RFP or Sau. Note that Sau co-immunoprecipitated with Chc.
(B) GST-Sau pulled down Clathrin light chain (Clc) from testis extracts expressing Clc-GFP.

3 DISCUSSION.

*GOLPH*3 was recently identified as a new oncogene frequently amplified in many human cancers (Scott et al, 2009, Scott and Chin, 2010; Hu et al, 2012; Hua et al, 2012; kunigou et al, 2012; Li et al, 2012; Wang et al, 2012; Zeng et al, 2012; Zhou et al, 2012). However, the molecular pathways involving this protein in malignant transformation are far from being clarified (Scott and Chin, 2010). Studies in both yeast and mammalian cells have implicated this protein in several vesicle trafficking events (Snyder et al., 2006; Tu et al., 2008; Schmitz et al., 2008; Dippold et al., 2009). Rat GOLPH3/Gmx33 is a dynamic component of the *trans*-Golgi matrix; the GFP tagged protein was visualized on tubulovesicular structures exiting from the Golgi, on endosomal compartments and on the plasma membrane suggesting that GOLPH3 may traffic to these structures and hence provide a function in sorting from the Golgi **(**Snyder et al., 2006). Accordingly siRNA knockdown of human GOLPH3 caused defects in anterograde trafficking from Golgi to PM. Vps74p, the yeast counterpart of GOLPH3, originally identified in a genetic screen for genes that are essential in the absence of the RabGTPase Ypt6p (Tong et al., 2004), was involved in proper docking and localization of glycosyltransferases to the Golgi membranes (Schmitz et al., 2008; Tu et al., 2008). In addition human GOLPH3 was shown to interact with VPS35, a component of the conserved retromer complex, known to regulate trafficking between endosomes and the Trans Golgi Network (TGN) of trasmembrane cargos (Bonaficino et al., 2008; Seaman, 2005). The role of human GOLPH3 in Golgi function and vesicle trafficking is strictly dependent on the interaction with the lipid PtdIns(4)P and unconventional myosin MYO18A that link Golgi to F-actin producing a tensile force that stretches the Golgi and promotes vesicle budding (Dippold et al. 2009).

Drosophila male meiosis, with its unique ease on checkpoint control, offered the exclusive opportunity to determine

how GOLPH3 contributes to cytokinesis. We have shown that the *Drosophila* orthologue of human GOLPH3 is required during the early steps of spermatocyte cytokinesis playing an essential role in both contractile ring assembly and vesicle trafficking during furrow ingression.
In most *sau* mutant telophase spermatocytes F-actin failed to localize at the cleavage furrow and Myosin II and Septins failed to concentrate into regular-shaped rings. A large proportion of mid telophases from *sau* mutants displayed large/unconstricted or broken Myosin II rings indicating that cells that succeeded to assemble a contractile ring were then unable to constrict at later stages of cytokinesis. I have also shown that Sau, as the mammalian and yeast orthologues, bound PtdIns(4)P in lipid binding assays and was required for the accumulation of PtdIns(4)P-containing organelles at the cleavage site. Moreover a mutant version of Sau that is unable to associate with PtdIns(4)P failed to rescue the cytokinesis defects of *sau* mutants. Thus the requirement for Sau in spermatocyte cytokinesis was intimately connected to the ability of this protein to bind PtdIns(4)P. A possible model to illustrate how Sau function could be involved in cytokinesis is depicted in **Figure 25**. Because in the absence of Sau both PtdIns(4)P-and Rab11 are completely delocalized, Sau might have a role in targeting PtdIns(4)P-and Rab11-secretory vesicles that enrich at the cleavage furrow during telophase (Polevoy et al., 2009). PtdIns(4)P is the substrate for PtdIns(4)P 5-kinase for the synthesis of PtdIns(4,5)P2 that is generated in the cleavage furrow and plays crucial roles during cytokinesis (Brill et al., 2011). PtdIns(4,5)P2 is known to promote actin polimerization by modulating the activity and targeting of actin regulatory proteins (reviewed in Yin and Janmey, 2003). Thus failures of *sau* to assemble F-actin rings might be the consequence of a defective PtdIns(4,5)P2 pool at the cleavage site. A defective phosphoinositide concentration might also affects Septin localization. Septins, a family of filamentous GTPases that are thought to anchor the actomyosin ring to the cell membranes, form

a gauze–like mesh tightly associated with plasma membranes (reviewed by Oh and Bi, 2011; Beise and Trimble, 2011). These proteins bind phosphoinositides *in vitro* through a polybasic domain and septin polymerization into filaments is enhanced by the association of these proteins with lipid bilayers (Bertin, 2010; Tanaka-Takiguchi et al., 2009). It has also been suggested that septin filaments interaction with plasma membrane phosphoinositides would not only prevent lateral diffusion of lipids acting as diffusion barriers but also bend the membrane hence helping to stabilize the cleavage furrow (Beise and Trimble, 2011; Brill et al., 2011). Moreover it has also been shown that one of the mammalian septins (SEP2) binds directly Nonmuscle Myosin II and this interaction is required for Myosin II full activation during cytokinesis (Joo et al., 2007). Remarkably Sau protein localized to the cleavage furrow during early cytokinesis and Co-IP and GST-pull down analyses suggested that this protein might interact with both Septin 2 and Myosin II in male germ cells. Human GOLPH3 binds PtdIns(4)P and recruits MYO18A to the Golgi. GOLPH3 and MYO18A are required for tethering the Golgi to the actin cytoskeleton to stretch the Golgi and produce a tensile force that facilitates vesicle budding (Dippold et al, 2009). It is then possible that a module PtdIns(4)P-Sau-Myosin II at the cleavage furrow might be involved in producing a tensile force required to shape the actomyosin ring.

The cytokinetic phenotype of *sau* mutants might be also the consequence of malfunctioning of membrane trafficking pathways. Several studies have suggested an intimate connection between vesicle trafficking and actomyosin ring assembly and stability during cytokinesis. For example Syntaxin 1 is required for proper F-actin ring assembly in *Drosophila* S2 cells (Somma et al., 2002) and Albertson and coauthors (2008) have reported that F-actin are targeted on endosomal vesicles to the cleavage furrow of *Drosophila* postcellularized embryonic cells. In *Dyctiostelium* most clathrin null cells fail to undergo furrow ingression (Niswonger and O'Halloren, 1997; Gerald et al., 2001); in these

cells Myosin II is frequently associated with patches instead of forming a ring, a phenotype that is similar to that described for *sau*. Remarkably my results indicated that Sau protein is required for proper localisation of Clathrin light chain in dividing spermatocytes and that Sau protein might be a molecular partner of both Rab 5 and clathrin in *Drosophila* male meiotic cells. A potential molecular interaction between Clathrin and Sau is further suggested by the presence in Sau/GOLPH3 amino acid sequence of a putative clathrin binding motif (LLDLD indicated by purple triangles in **Figure 2**). However further investigations will be required to verify whether Sau directly binds Clathrin chains.
Because Sau not only binds PtdIns(4)P but also PtdIns(3)P, PtdIns(5)P in lipid binding assays it is likely that this protein is also involved in other membrane trafficking pathways that depend on these phosphoinositides during cytokinesis. Indeed several studies have indicated a role for PtdIns(3)P in cytokinesis (reviewed in Brill et al., 2011; Echard, 2012). PtdIns(3)P positive endosomes localize to the midzone of both fungal and mammalian cells (Sagona et al., 2010 and Schink and Bolker, 2009) and inhibition of PtdIns(3)P production results in cytokinesis failures in HeLa cells (Montagnac et al., 2008). Strikingly, I have found that Sau protein also binds the glycerophospholipid phosphatidic acid in lipid binding assays. One intriguing hypothesis would involve this lipid and Sau during cytokinesis . It has been shown that phosphatidic acid (PA) is an important lipid for plasma membrane curvature (Kooljmanet et al., 2003) and it is also an activator of PtdIns(4)P 5-kinase (Jarquin-Pardo et al., 2007). Thus we can speculate that Sau not only recruits PtdIns(4)P to plasma membrane that is phosphorylated by PtdIns(4)P 5-kinase to generate PtdIns(4, 5)P2 but it also contributes to PtdIns(4)P 5-kinase activation and membrane remodeling during cytokinesis through PA (**Figure 25**).

Fig. 25, Diagram illustrating the possible role of Sau during cytokinesis of telophase spermatocytes. Read the text for explanations.

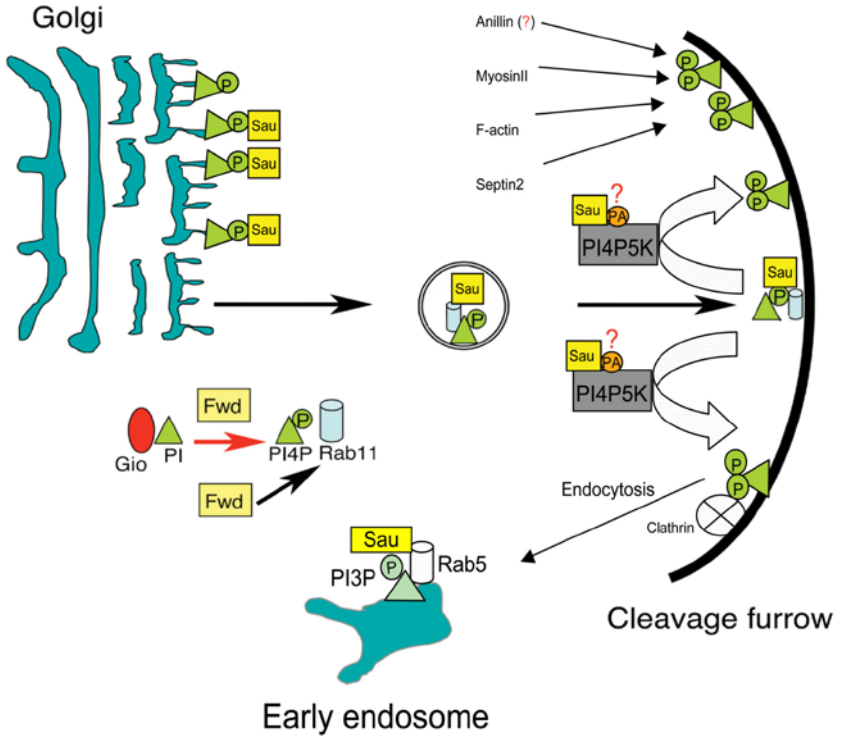

4 The role of *Drosophila Cog7* during male meiotic cytokinesis

Introduction

The conserved oligomeric Golgi (COG) Complex plays essential roles for Golgi function, vesicle trafficking and glycosylation. Mutations in the genes encoding human *COG1, COG4-COG8* have been associated with congenital disorders of glycosylation (CDG) (Folquier et al., 2006, 2007; Kranz et al., 2007; Lübbehusen et al, 2010; Ng et al., 2007; Paesold-Burda et al., 2009; Reynders et al., 2009; Spaapen et al., 2005; Steet and Kornfeld, 2006; Wu et al., 2004) indicating a role for COG in the transport and/or stability of Golgi glycosylation enzymes. Indeed studies in both yeast and mammalian cells have suggested that COG complex might function as a vesicle-tethering factor in intra-Golgi retrograde COPI transport (Ungar et al., 2002), thus regulating the distribution and the stability of Golgi resident proteins (Oka et al, 2004; Shestakova et al., 2006; Suvorova et al., 2001; Suvorova et al., 2002; Walter et al., 1998).
Drosophila spermatocytes are quite large cells (more than 20μm in diameter), that complete two meiotic divisions in less than two hours (Fuller, 1993; Giansanti et al., 2001). For these reasons, as explained in the Introduction, cytokinesis of these cells proved to be sensitive to mutations affecting vesicle traffic components (Brill et al., 2000; Farkas et al., 2003; Dyer et al., 2007; Gatt and Glover; 2006; Giansanti et al., 2006; Giansanti et al., 2007; Polevoy et al., 2009; Robinett et al., 2009; Xu et al., 2002). Among the COG subunits, the *Drosophila* Cog5 homologue Four way stop (Fws) has been implicated in both male meiotic cytokinesis and spermatid elongation (Farkas et al., 2003). As a part of my PhD project I contributed to the characterization of the *Drosophila* orthologue of human Cog7 (Belloni et al., 2012). Deletions of human *COG7* are associated with a rare multisystemic congenital disorder of glycosylation causing mortality within the first year of life (Morava et al., 2007; Ng et

al., 2007; Wu et al., 2004). Similar to Fws, Cog7 also controls furrow ingression during cytokinesis. Importantly, *Cog7* is required to localize the small GTPase Rab11 and the phosphatidylinositol transfer protein (PITP) Giotto (Gio) to the cleavage site of spermatocytes. In addition Gio coimmunoprecipitates with both Cog7 and Rab11 in *Drosophila* testes suggesting that these proteins may interact in male germ cells.

5 RESULTS.

5.1 Cog*7* is required for contractile ring constriction during spermatocyte cytokinesis.

Mutations in *fws* caused defects in F-actin ring constriction of telophase spermatocytes (Farkas et al., 2003). Staining of *Cog7* spermatocytes carrying null Cog7 alleles for tubulin and F-actin revealed a cytokinetic phenotype similar to *fws* (**Fig. 1A**). In 80% of mid-late telophases I from $Cog7^{z3\text{-}4495}/Df(3R)BSC861$ (*Cog7)* mutants, the F-actin rings failed to constrict to completion and the central spindles appeared less dense than in wild type (N=25 for wild type; N=30 for *Cog7;* **Fig. 1A**).

To determine the localization of Cog7 in testes I generated transgenic flies expressing a GFP-Cog7 fusion protein. The *GFP-Cog7* transgene rescued both male sterility and the phenotypic defects associated with *Cog7* null mutations indicating that the encoded protein is fully functional. In prophase I, GFP-Cog7 was enriched at multiple round structures that colocalized with the Golgi marker Lava Lamp (Lva, Sisson et al., 2000) indicating that Cog7 localizes to the Golgi stacks (**Fig. 2A**). During metaphase and anaphase of meiosis I, GFP-Cog7 was associated with Golgi organelles in the polar regions of the cell (**Fig. 2B, 2C**). In telophase cells, Cog7 signals appeared excluded from the cell equator just like Lva-Golgi organelles (**Fig. 2C, 2D**). In onion-stage spermatids, Cog7 localized to Golgi derived acroblasts (**Fig. 2E**).

The subcellular localization of Cog7 in spermatocytes is in accordance with the localization of the Fws/Cog5 protein (Farkas et al., 2003 and **Fig. 2F**). To determine the functional dependence between Fws/Cog5 and Cog7, *Cog7* mutants expressing GFP-Fws and *fws* mutants expressing GFP-Cog7 were examined. *Cog7* mutations completely abolished the localization of Fws at the Golgi and Cog7 was diffuse in the cytoplasm in the absence of Fws (**Fig. 2F**).

Since Cog7 and Fws/Cog5 are believed to reside in the same COG subcomplex (Ungar et al., 2002), we assessed whether the stability of either protein was affected in the reciprocal mutant (**Fig. 2G, H**). Western blots showed that GFP-Cog5 protein was decreased by 56% in testes from *Cog7* mutants relative to wild type (**Fig. 2G**) and GFP-Cog7 protein was decreased by 20% in testes from *fws* mutants relative to wild type (**Fig. 2H**).

5.2 Wild-type function of Cog7 is required to recruit Giotto and Rab11 at the cleavage site.

Previous data showed that the phosphatidylinositol transfer protein (PITP) Giotto/Vib (Gio/Vib) and the small GTPase Rab11 accumulate at the cleavage site and are both required for spermatocyte cytokinesis (Gatt and Glover, 2006; Giansanti et al., 2006, 2007; Polevoy et al., 2009). It was suggested that Rab11, Gio and the Phosphatidylinositol 4-kinase β (PI4Kb) Fwd function in the same pathway during cytokinesis, with Gio and Fwd acting upstream of Rab11 (Giansanti et al., 2007; Polevoy et al., 2009). Immunofluorescence analysis revealed that loss of Cog7 impaired the recruitment of Gio at the cell equator in 89% of telophase spermatocytes (Fig. 3A; N=32 for wild type; N=36 for *Cog7*). *Cog7* mutations also disrupted the localization of Rab11 in dividing spermatocytes. In both wild-type and *Cog7* prophase spermatocytes expressing Rab11-GFP, Rab11 was enriched at round structures corresponding to Lva-enriched Golgi stacks (not shown). Rab11-GFP colocalized with Lva in both wild type and *Cog7* prophase cells. However Cog7 mutant spermatocytes displayed few Golgi organelles relative to wild type control cells. In addition, Rab11 did not accumulate at the cell midzone in 90% of mutant telophases (**Fig. 3B, C**; N= 26 for wild type; N=30 for *DCog7*). Since localization of Rab11 to the cleavage site is dependent on both Gio (Giansanti et al., 2007) and Cog7 (this study) I performed Co-IP experiments using *Drosophila* testis protein extracts aimed at verifying interactions among these proteins. Protein extracts from testes expressing either GFP-Cog7 or Rab11-GFP were immunoprecipitated using the GFP-Trap (see

material and methods). I found that Gio co-immunoprecipitated with both Cog7 and Rab11 in *Drosophila* testes (**Fig. 3D**). Gio/Cog7 and Gio/Rab11 interactions were confirmed by a second experiment in which extracts from testes expressing Gio-RFP and either Rab11-GFP or GFP-DCog7 were immunoprecipitated using the RFP-Trap (**Fig. 3E, F**).

Because Gio co-immunoprecipitated with Cog7 in testis extracts, I asked whether the two proteins colocalized in dividing spermatocytes. To test this, I imaged spermatocytes expressing both GFP-Cog7 and Gio-RFP. Our analysis revealed that Gio partially colocalized with Cog7 at the Golgi membranes (**Fig. 3G**). Gio also localized to parafusorial and astral membranes where Cog7 was not detectable. In fixed dividing spermatocytes coexpressing Gio-RFP with Rab11-GFP, Gio colocalized with Rab11, consistent with previous results with anti-Gio and anti-Rab11 antibodies (Giansanti et al., 2007 and data not shown). During telophase Gio and Rab11 concentrated at the cleavage furrow (**Fig. 3A, B**), while Cog7 was excluded from the cell equator (**Fig. 2**).

Fig. 1, Contractile ring constriction fails in *Cog7* null mutant spermatocytes.

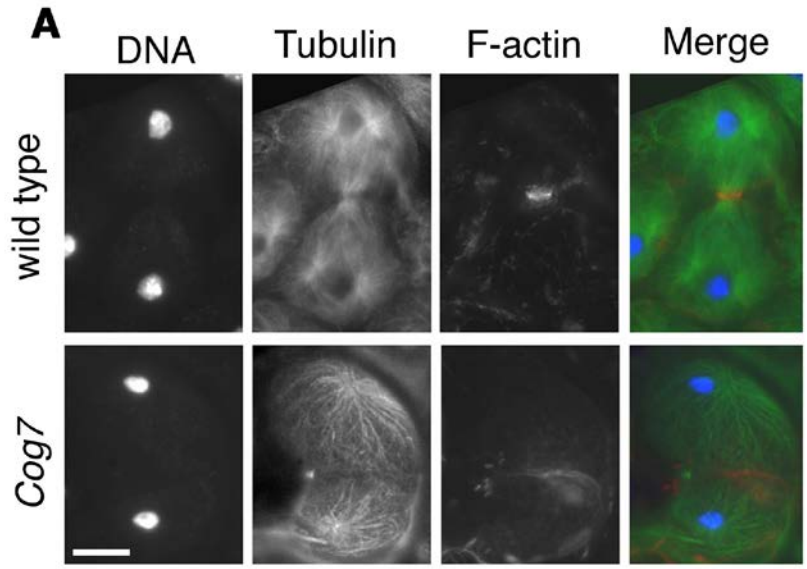

Late telophase I stained for Tubulin (green) F-actin (red) and DNA (blue).
Bar, 10 μm.

Fig. 2, Cog7 localizes to Golgi in wild type spermatocytes and spermatids.

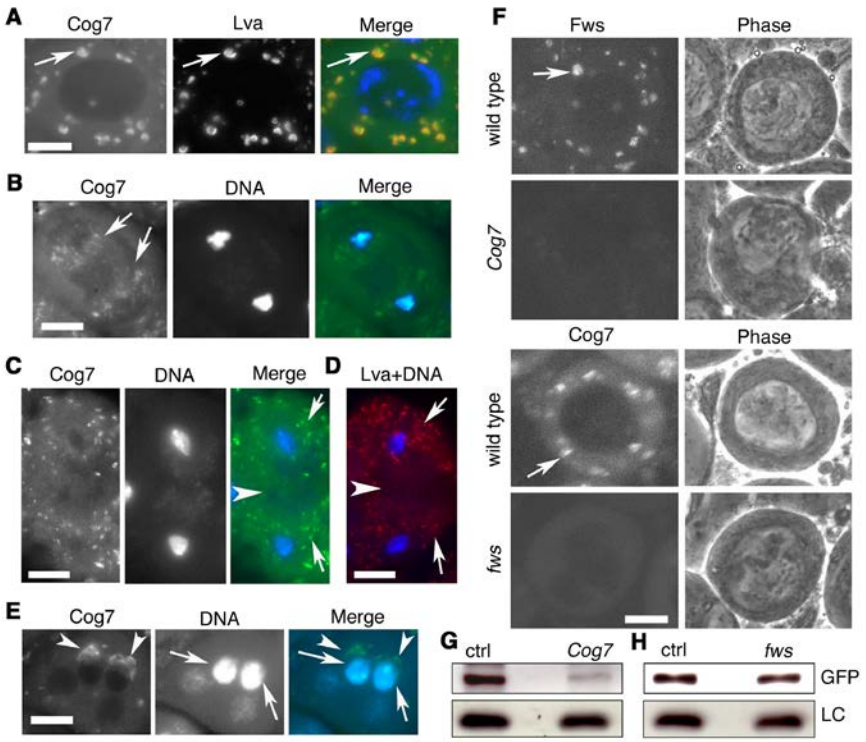

(**A**) Fixed Prophase I spermatocyte expressing GFP-Cog7 (green) stained for Lva (red) and DNA (blue) Arrows point to Golgi stacks. (**B, C**) Fixed anaphase (B) and telophase (C) spermatocytes expressing GFP-Cog7 (green) stained for DNA (blue). Arrows point to Golgi membranes enriched in Cog7. (**D**) Fixed telophase spermatocytes stained for Lva (red) and DNA (blue). Arrows point to Golgi membranes enriched in Lva. Arrowheads in C and D indiate the cell midzones. (**E**) Spermatids expressing GFP-Cog7 (green) fixed and stained for DNA (blue). Arrows indicate nuclei, arrowheads indicate acroblasts.
(**F**) Live wild type and mutant spermatocytes expressing either GFP-Fws or GFP-Cog7 were imaged at the same exposure time. Arrows point to Golgi stacks.

(**G**) Immunoblotting analysis of GFP-Fws in wild type, GFP-Fws; *Cog7*$^{z3\text{-}4495}$/+(ctrl) and *Cog7* (GFP-Fws; *Cog7*$^{z\text{-}5797}$/*Cog7*$^{z\text{-}4495}$) mutant testes. Anti-Gio was used as a loading control.
(**H**) Immunoblotting analysis of GFP-Cog7 in wild type, *fws*$^{z\text{-}0161}$/+; GFP-Cog7 (ctrl) and *fws* (*fws*$^{z\text{-}0161}$/*fws*$^{z\text{-}1201}$; GFP-Cog7) mutant testes. Anti-Gio was used as a loading control.
Bar, 10 μm

Fig. 3, Relationship between Cog7, Gio and Rab11 in dividing spermatocytes.

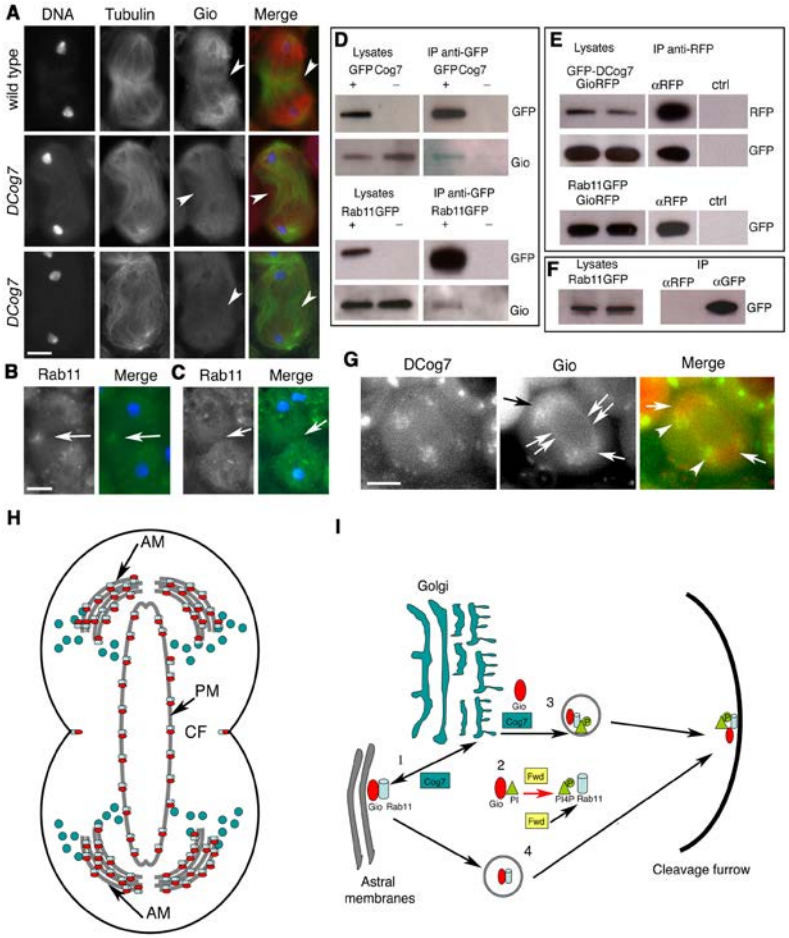

(**A**) Gio fails to concentrate at the cell equator in *Cog7* telophase spermatocytes. Spermatocytes were stained with anti-tubulin (Green), anti-Gio (Red) and with DAPI (Blue). Arrows indicate the cell midzones.
(**B, C**) Rab11 fails to localize at the cell midzone of *Cog7* telophase spermatocytes. Spermatocytes expressing Rab11-GFP (green) from wild

type (B) and Cog7 males (C) were fixed and stained for DNA (Blue). Arrowheads indicate the cell midzones.
(**D**) Co-IP of Gio with Cog7 and Rab11. GFP-Cog7 and Rab11-GFP were immunoprecipitated from either GFP-Cog7 or Rab11-GFP transgenic testes with anti-GFP (GFP trap) and blotted with anti-Gio. Negative control was a wild type, no transgenic stock. Left panels show expression controls. (**E**) Gio-RFP was immunoprecipitated with anti-RFP (RFP trap) from transgenic testes expressing Gio-RFP and either GFP-Cog7 or Rab11-GFP. Equal fractions of testis extracts were incubated with either RFP-trap beads (aRFP) or with control beads (ctrl). Left panels show expression controls for the two fractions. (**F**) Equal fractions from Rab11-GFP testis extracts were used to test the specificity of the anti-RFP-beads used in E. Rab11-GFP could be immunoprecipitated with with anti-GFP beads (GFP trap, aGFP) but could not be immunoprecipitated with anti-RFP beads (RFP trap, aRFP). (**G**) Live dividing spermatocytes expressing both GFP-Cog7 (Green) and Gio-RFP (Red) were imaged for GFP and RFP. Gio partially colocalizes with Cog7 in a fraction of the Golgi membranes, at the polar regions of dividing spermatocytes (arrowhead). Gio-RFP is also enriched at the astral membranes (arrows) and the parafusorial membranes (double arrows) that do not contain Cog7.
(**H, I**) Diagrams illustrating localization of Gio (red), Rab11 (light blue) and Cog7 (green) in telophase spermatocytes (H) and possible functions for the Cog7-Rab11-Gio network during cytokinesis (I). Astral membranes (AM) and parafusorial membranes (PM) in grey; CF, cleavage furrow. Cog7 might regulate retrograde/anterograde vesicle traffic between Golgi and ER astral/parafusorial membranes thus contributing to target Gio and Rab11 to membrane compartments (1). Gio provides the PI precursor for the synthesis of PI4P by Fwd on Golgi membranes (2). Fwd recruits Rab11 to Golgi where it becomes associated with organelles containing PI4P (2). Cog7 might also partecipate with Gio in the formation of secretory organelles that enrich the cleavage site (3). Rab11 and Gio might also reach the cleavage site through vesicle traffic from ER membranes to the CF (4).
Bar, 10 μm.

6 DISCUSSION.

Mutations in the gene encoding human Cog7 are associated with a lethal congenital disorder of glycosylation (CDG), causing multisystemic deficiencies including neurological, metabolic and anatomical abnormalities (Morava et al., 2007; Ng et al., 2007; Wu et al., 2004). Thus it was surprising that flies homozygous for null alleles of *Cog7* were viable, although males were sterile and displayed various defects during spermatogenesis,

Drosophila Cog7, along with the Cog5 homologue Fws, localized to Golgi throughout spermatogenesis. In addition Cog7 and Fws were interdependent for localization to Golgi membranes. Function of Cog7, like the Cog5 homologue Fws (Farkas et al., 2003), is essential for successful cytokinesis in *Drosophila* spermatocytes. Previous studies showed that the phosphatidylinositol transfer protein (PITP) Giotto/Vib (Gio/Vib) and the small GTPase Rab11 concentrate to the cleavage furrow and are both required for spermatocyte cytokinesis (Gatt and Glover, 2006; Giansanti et al., 2006, 2007; Polevoy et al., 2009). Rab11, Gio and the Phosphatidylinositol 4-kinase b (PI4Kb) Fwd might function in the same pathway controlling membrane addition to the spermatocyte cleavage site, with Gio and Fwd acting upstream of Rab11 (Giansanti et al., 2007). Fwd is required for the synthesis of PI4P on Golgi membranes and for the formation of Rab11-and PI4P containing organelles at the cell equator (Polevoy et al., 2009). Because PITPs can stimulate vesicle budding from the trans-Golgi network and also provide vesiculating activity for scission of coatomer-coated vesicles *in vitro* (Jones et al., 1998; Ohashi et al., 1995; Simon et al, 1998) Gio might be involved in vesicle formation. I have shown that localization of Gio and Rab11 to the cleavage furrow in dividing spermatocytes requires the wild-type function of Cog7, indicating that Cog7 might be an upstream component in a *gio-Rab11* pathway during cytokinesis (**Figure 3I**). Gio coimmunoprecipitates with both Rab11 and Cog7 in testes,

suggesting that these proteins may form a complex in male germ cells. Based on our results, Cog7 might be implicated in the Gio-mediated formation of Rab11 associated secretory organelles which become enriched in the cleavage site during spermatocytes (**Figure 3H, 3I**). However, I cannot exclude a role for Cog7 and the Cog complex in the regulation of a retrograde/anterograde traffic between Golgi membranes and ER during cytokinesis (**Figure 3I**).

7 MATERIALS AND METHODS.

The fly strain carrying *sau*^{z2217} allele was isolated in the course of a screen of a large collection of male sterile mutants for those affecting male meiotic cytokinesis and is described in Giansanti et al., 2004.
Chromosomal deficiencies *Df(2L)Exel6007, Df(2L)Exel7010* and the P element *l(2)s5379* were obtained from the Bloomington Drosophila Stock Center at Indiana University (www.flybase.org).
Flies carrying the *four way stop* (*fws*), *giotto* (*gio*), *four wheel drive (fwd)* and *Rab11* mutations
fws^{Z0161}, *fws*^{Z1201}, *gio*$^{RM1\text{-}r7}$, *gio*^{z3934}, *gio*^{EP513} , *Rab11* $^{e(To)3}$ and *Rab11*^{93Bi} and flies expressing GFP-Fws have been described in Farkas et al., 2003 and Giansanti et al., 2006. *UAS::Sau-RNAi* flies were from the Vienna Drosophila RNAi Collection (VDRC). Flies expressing Bam-GAL4 (Chen and McKearin, 2003) were a gift of J. Wakefield (University of Exeter, UK). Flies expressing Rab11-GFP (Dollar et al., 2002) were a gift from R. S. Cohen (University of Kansas); strains expressing the transgenes Rab5-GFP, Clc-GFP, Chc-RFP (Zhou et al., 2011) were a gift of H.C. Chang (Pardue University).

Molecular Biology and rescue experiments.

To generate either the GFP-Sau or the GFP-Cog7 constructs, the EGFP CDS was fused in frame to the aminoterminus of the full length cDNAs corrisponding to *CG7085* and *CG31040* genes and cloned into the transformation vector pJZ4 (provided by G.D. Raffa, Raffa et al., 2010) under the control of a tubulin promoter. To generate Vps35 -mRFP or Vps35-Flag flies we amplified either Vps35-mRFP or Vps35 cDNA from plasmids obtained by Viktor Korolchuk and described in Korolchuk et al. 2007. Germline transformation was performed by Bestgene, Inc. (Chino Hills, CA).
GFP-Sau and GFP-Cog7 were crossed respectively into the *sau* or *Cog7* mutant background to test for phenotypic rescue of male sterility and meiotic cytokinesis failures associated with *sau* and *Cog7* mutations

Microscopy and immunofluorescence.

Cytological preparations were made with testes from third instar larvae. *sau*^{z2217}*/Df(2L)Exel7010* mutants were used in all the immunofluorescence experiments involving *sau* mutations.
To visualize tubulin with either Rab11-GFP or Sqh-GFP or to stain F-actin with Rhodamine phalloidin (Molecular Probes) larval testes were fixed in 4% formaldehyde as described in Giansanti et. al. (2006).

Phalloidin staining was performed using the protocol described in Szafer-Glusman et al., 2008. For other immunostaining with testes, preparations were fixed using 3.7% formaldehyde in PBS and then squashed in 60% acetic acid according to Giansanti et al. (1999). Monoclonal antibodies were used to stain tubulin (T6199, Sigma-Aldrich, diluted 1:200). Polyclonal antibodies were as follows: anti-Myosin II (Royou et al., 2002), gift from R.E. Karess, diluted 1:400; rabbit anti-Lava Lamp (anti-Lva, Sisson et al., 2000) gift from O. Papoulas (University of Texas) diluted 1:500; rabbit anti-Gio (Giansanti et al., 2006) diluted 1:3000, rat anti-Rab11, gift of S. Cohen (Dollar et al., 2002). Secondary antibodies Alexa 555-conjugated anti rabbit IgG (Molecular Probes) and rhodamine/FITC-conjugated anti-mouse IgG (Jackson Immunoresearch, West Grove, PA), were used at 1:250 and 1:20 respectively. In all cases slides were mounted in Vectashield medium with DAPI. Images were captured with a charged-coupled device (CCD camera, Photometrics Coolsnap HQ), connected to a Zeiss Axioplan, epifluorescence microscope, equipped with an HBO 100-W mercury lamp, and 40 X or 100 X objectives as described in Giansanti et al., 2006.

Live imaging.

Larval testes were prepared for time lapse as per Inoue et al. (2004) and imaged as described in Giansanti et al. (2006). Spermatocytes were examined with a Zeiss Axiovert 20 microscope equipped with a 100X, 1. 25 NA and a 63X, 1.4 NA objectives and a filter wheel combination (Chroma Technology Corp.). Images were collected at one-minute intervals with a CoolSnap HQ camera (Photometrics) controlled through a Metamorph software (Universal imaging); eleven fluorescente optical sections were captured at 1-μm z steps. Movies were created using the Metamorph software and each frame shows the maximum-intensity projection of all the sections.

Mutagenesis.

For mutagenesis *sauron* cDNA (used to obtain K167A/ R170L and E273K mutations) I used the QuikChange® Site-Directed Mutagenesis Kit. The DNA constructs obtained after mutagenesis were verified by DNA sequencing by Bio-Fab research service.

Protein expression and purification.

To obtain GST fusion proteins, full-length wild type Sau-GST, K167A/ R170L Sau-GST and E273K Sau-GST, cDNAs were cloned in pGEX-6p2 (GE Healthcare) in frame with the GST sequence. GST-fusion

proteins were expressed in *Escherichia coli* BL21-CodonPlus (DE3) cells (Invitrogen), grown in LB medium with addition of Ampicillin and Chloramphenicol. Protein expression was induced when cell cultures reached an OD_{600} of 0.6 by the addition of 0.3 mM IPTG and incubation at 37°C for 3 h. Following protein induction, bacterial cultures were harvested and resuspended in Lysis Buffer (10 mM Tris-Cl, 1 mM EDTA, 150 mM NaCl, 0,2 % Triton X-100 and protease inhibitor cocktail). The cells were lysed using Microson Ultrasonic Cell Disruptor XL.

Generation of Anti GST-Sauron Antibody.

Polyclonal antisera were raised against the entire protein. The protein GST-Sau were eluted with glutathione (Sigma). One rabbit and one mouse were injected at Agro-Bio (www.agro-bio.com) Services using standard procedures. Both antibodies were tested for specificity by immunoblotting and immunofluorescence. Mouse antibody S11047 and Rabbit antibody L11047 were used at 1:2500 and 1:1000 for immunoblotting and immunofluorescence, respectively.

DNA Transfection in S2 cells.

The DMEL strain of S2 cells was grown in Shield and Sang M3 insect medium (Sigma) with the addition of 10% Fetal Bovine Serum (Sigma). Cellfectin® II Reagent (Invitrogen) was used for efficient transfection of S2 cells. 3 mg of plasmidic DNA was used in each transfection experiments. The following plasmids were transfected: pJZ4-GFP-Sau, pJZ4-Flag-Vps35 and pJZ4-GFP.

Immunoprecipitation and Western Blotting.

For immunoblotting analysis of Sau protein or GFP-tagged proteins, 40 adult testes from males of each genotype, were homogenized in 100ml of Lysis buffer (10mM Tris-HCl pH7.5, 150mM NaCl, 0.5 mM EDTA, 0.5%NP40, 1mM PMSF, 1xProtease inhibitor Cocktail) at 4°C.

Immunoprecipitation experiments from adult testes expressing GFP and/or RFP-tagged proteins, were performed using the GFP/RFP trap-A kits and control beads purchased from ChromoTek (Planegg-Martinsried). At least 200 adult testes were homogenized in 500ml of Lysis buffer at 4°C. Lysates were cleared by centrifugation and protein concentration was quantified using the Bradford protein assay(Bio-Rad, Hercules, 94547 CA). 4% of each sample was retained as the" input", the remainder was incubated with 20ml of either GFP trap-A/RFP trap-A or control beads for two hours at 4°C. In all cases beads were washed three times and bound proteins were eluted by boiling in SDS sample

buffer. For immunoblots, samples were separated on 4%-20% SDS polyacrilammide precast gels (Bio-Rad) and blotted to PVDF membranes. Blocking and antibody incubation were in Tris-buffered saline (Sigma-Aldrich) with 0,05 % Tween-20 (TBST) containing 4% nonfat dry milk (Bio-Rad; Blotting GradeBlocker).
Immunoprecipitation experiments for Sauron from wild type adult testes were performed using the Mouse anti-Sauron antibody S11047 using the same protocol described to immunoprecipitate GFP-tagged proteins, Sauron was revealed in immunoblots using the Rabbit anti Sauron, L11047. Primary antibodies were as follows: anti-Giotto (Giansanti et al., 2006) diluted 1:8000; rat monoclonal anti-RFP (Chromotek, 5F8) diluted 1:1000, mouse anti Sau (S11047) and rabbit anti Sau (L11047) diluited 1:2500 and 1:1000 respectively , anti-GFP HRP (Vector-Lab, MB-0712) diluited 1:1000, anti Flag M2 (Sigma, F-1804) diluited 1:1000. HRP-linked secondary antibodies (GE Healthcare) were used at 1:5000. After incubation with the antibodies, blots were washed in TBST and imaged using ECL detection kit (GE Healthcare).
Bacterial lysate were cleared by centrifugation at 400x g for 10 minutes at 4°C. Cleared bacterial lysates were incubated with glutatione sepharose 4B beads (QIAGEN, HiCap Matrix R10) pre-equilibrated with Lysis Buffer a 4°C for 2 hours with continuous gentle rotation. The beads were than washed three times a 4°C with Lysis Buffer.

Lipid binding assay.

The PIP Strips (Catalog No.: P-6001) were obtained by the company Echelon (Echelon Biosciences Incorporated, EBI) and used following the protocol described on the website www.echelon-inc.com. These strips consist of 2 x 6 cm hydrophobic membranes that have been spotted with 15 different biologically active lipids at 100 pmol per spot.
The wild type and mutant Sau proteins, expressed following the protocol described above, were incubated together PIP Strips at the concentration suggested by Echelon. Control reagents (for testing specific lipid binding) G0302, G0402 and G4501 were purchased from Echelon and and used at the recommended concentration. To detect the bound protein to PIP Strips I used anti-GST antibodies conjugated with Horseradish peroxidase purchased from Abcam (ab3416) diluited 1:1000 and the ECL prime western blotting detection reagent (RPN2232) from GE Healthcare. Images were acquired using a ChemiDoc XRS with Image Lab software, Eight-bit images were exported, and figures were prepared using Adobe Photoshop CS4.

8 REFERENCES.

Adam JC, Pringle JR, Peifer M. 2000. Evidence for functional differentiation among Drosophila septins in cytokinesis and cellularization. Mol Biol Cell 11:3123-3135.

Adams RR, Maiato H, Earnshaw WC, Carmena M. 2001. Essential roles of Drosophila inner centromere protein (INCENP) and aurora B in histone H3 phosphorylation, metaphase chromosome alignment, kinetochore disjunction, and chromosome segregation. J Cell Biol 153:865-880.

Albertson R, Riggs B, Sullivan W. 2005. Membrane traffic: a driving force in cytokinesis. Trends Cell Biol 15:92-101.

Barr FA, Gruneberg E. 2007. Cytokinesis: placing the final cut. Cell 131:847-860.

Barr FA, Sillje HH, Nigg EA. 2004. Polo-like kinases and the orchestration of cell division. Nat Rev Mol Cell Biol 5: 429-440

Beise N, Trimble W. 2011. Septins at a glance. J Cell Sci. 124:4141-4146.

Bell AW, Bergeron JJ and other 15. 2001. Proteomics characterization of abundant Golgi membrane proteins. J. Biol. Chem. 276, 5112-5165.

Belloni G, Sechi S, Riparbelli MG, Callaini G, Giansanti MG. 2012. Mutations in *Cog7* affect Golgi structure, meiotic cytokinesis and sperm development during *Drosophila* spermatogenesis. JCS. In press.

Bertin A, McMurray MA, Thai L, Garcia G 3rd, Votin V, Grob P, Allyn T, Thorner J, Nogales E. 2010. Phosphatidylinositol-4,5-bisphosphate promotes budding yeast septin filament assembly and organization. J Mol Biol. 404:711-731.

Bonaccorsi S, Giansanti MG, Gatti M. 1998. Spindle self-organization and cytokinesis during male meiosis in asterless mutants of Drosophila melanogaster. J Cell Biol 142:51-61.

Bonifacino JS, Hurley JH. 2008. Retromer. Curr Opin Cell Biol. 20:427-436.

Brennan IM, Peters U, Kapoor TM, Straight AF. 2007. Polo-Like Kinase Controls Vertebrate Spindle Elongation and Cytokinesis. PLoS One. 2: e409.

Bringmann H, Hyman AA. 2005. A cytokinesis furrow is positioned by two consecutive signals. Nature. 436:731-734.

Brill JA, Hime GR, Scharer-Schuksz M, Fuller MT. 2000. A phospholipid kinase regulates actin organization and intercellular bridge formation during germline cytokinesis. Development. 127:3855-3864.

Brill JA, Wong R, Wilde A. 2011. Phosphoinositide function in cytokinesis. Curr Biol 21:R930-934.

Bucciarelli E, Giansanti MG, Bonaccorsi S, Gatti M. 2003. Spindle assembly and cytokinesis in the absence of chromosomes during Drosophila male meiosis. J Cell Biol 160:993-999.

Burkard ME, Maciejowski J, Rodriguez-Bravo V, Repka M, Lowery DM, Clauser KR, Zhang C, Shokat KM, Carr SA, Yaffe MB, Jallepalli PV. 2009. Plk1 self-organization and priming phosphorylation of HsCYK-4 at the spindle midzone regulate the onset of division in human cells. PloS Biol 7:e1000111.

Caldwell CM, Green RA, Kaplan KB. 2007. APC mutations lead to cytokinetic failures in vitro and tetraploid genotypes in Min mice. J Cell Biol 178:1109-1120.

Carmena M, Riparbelli MG, Minestrini G, Tavares AM, Adams R, Callaini G and Glover DM. 1998. Drosophila polo kinase is required for cytokinesis. J Cell Biol 143:659-671.

Carvalho A, Desai A, Oegema K. 2009. Structural memory in the contractile ring makes the duration of cytokinesis independent of cell size. Cell.137:926-37.

Carvalho A., Carmena M., Sambade. C., Earnshaw WC, Wheatley SP. 2003. Survivin is required for stable checkpoint activation in taxol-treated HeLa cells. J Cell Sci 116:2987-2998.

Castrillon DH, Wasserman SA. 1994. Diaphanous is required for cytokinesis in Drosophila and shares domains of similarity with the products of the limb deformity gene. Development 120:3367–3377.

Chalamalasetty RB, Hümmer S, Nigg EA, Silljé HH. 2006. Influence of human Ect2 depletion and overexpression on cleavage furrow formation and abscission. J Cell Sci 119:3008-19.

Chang HC, Newmyer SL, Hull MJ, Ebersold M, Schmid SL, Mellman I. 2002. Hsc70 is required for endocytosis and clathrin function in Drosophila. J Cell Biol. 159:477-87.

Church K, Lin HP. 1982. Meiosis in Drosophila melanogaster. II. The prometaphase-I kinetochore microtubule bundle and kinetochore orientation in males. J Cell Biol 93:365-373.

D'Avino PP. 2009. How to scaffold the contractile ring for a safe cytokinesis - lessons from Anillin-related proteins. J Cell Sci 122:1071-1079.

D'Avino PP, Takeda T, Capalbo L, Zhang W, Lilley KS, Laue E, Glover DM. 2008. Interaction between Anillin and RacGAP50C connects the actomyosin contractile ring with spindle microtubules at the cell division site. J Cell Sci. 121:1151-1158.

D'Avino PP, Archambault V, Przewloka MR, Zhang W, Lilley KS, Laue E, Glover DM. 2007. Recruitment of Polo kinase to the spindle midzone during cytokinesis requires the Feo/Klp3A complex. PLoS One; 2::e572.

D'Avino PP, Savoian MS, and Glover DM. 2005. Cleavage furrow formation and ingression during animal cytokinesis: a microtubule legacy. J. Cell Sci; 118:1549-1558.

Dechant R, Glotzer M. 2003. Centrosome separation and central spindle assembly act in redundant pathways that regulate microtubule density and trigger cleavage furrow formation. Dev Cell. 4:333-344.

Dippold HC, Field SJ and other 13. 2009. GOLPH3 bridges phosphatidylinositol-4- phosphate and actomyosin to stretch and shape the Golgi to promote budding. Cell. 139, 337-351.

Douglas ME, Davies T, Joseph N, Mishima M. 2010. Aurora B and 14-3-3 Coordinately Regulate Clustering of Centralspindlin during Cytokinesis. Curr Biol 20:927-933.

Douglas ME, Mishima M. 2010. Still entangled:assembly of the central spindle by multiple microtubule modulators. Sem in Cell Dev Biol 21:899-908.

Dyer N, Rebollo E, Domínguez P, Elkhatib N, Chavrier P, Daviet L, González C, González-Gaitán M. 2007. Spermatocyte cytokinesis requires rapid membrane addition mediated by ARF6 on central spindle recycling endosomes. Development 134:4437-4447.

Eggert US, Mitchison TJ, Field CM. 2006. Animal cytokinesis: from parts list to mechanisms. Annu Rev Biochem 75:543-566.

Farkas RM, Giansanti MG, Gatti M, Fuller MT. 2003. The Drosophila Cog5 homologue is required for cytokinesis, cell elongation, and assembly of specialized Golgi architecture during spermatogenesis. Mol Biol Cell. 14:190–200.

Fujiwara T, Bandi M, Nitta M, Ivanova EV, Bronson RT, Pellman D. 2005. Cytokinesis failure generating tetraploids promotes tumorigenesis in p53-null cells. Nature 437:1043-1047.

Foulquier F, Vasile E, Schollen E, Callewaert N, Raemaekers T, Quelhas D, Jaeken J, Mills P, Winchester B, Krieger M, Annaert W and Matthijs, G. 2006. Conserved oligomeric Golgi complex subunit 1 deficiency reveals a previously uncharacterized congenital disorder of glycosylation type II. Proc Natl Acad Sci USA. 103:3764-3769.

Foulquier F, Ungar D, Reynders E, Zeevaert R, Mills P, García-Silva MT, Briones P, Winchester B, Morelle W, Krieger M, Annaert W and Matthijs G. 2007. A new in born error of glycosylation due to a Cog8 deficiency reveals a critical role for the Cog1-Cog8 interaction in COG complex formation. Hum. Mol. Genet. 16:717-730.

Fuller MT. 1993. Spermatogenesis. In Bate M and Martinez-Arias A, eds. The Development of Drosophila melanogaster. Cold Spring Harbor, NY: Cold Spring Harbor Press:71-147.

Gandhi R, Bonaccorsi S, Wentworth D, Doxsey S, Gatti M, Pereira A. 2003. The Drosophila Kinesin-like Protein KLP67A is essential for mitotic and male meiotic spindle assembly. Mol Biol Cell 15:121-31.

Gao S, Giansanti MG, Buttrick GJ, Ramasubramanyan S, Auton A, Gatti M, Wakefield JG. 2008. Australin: a chromosomal passenger protein required specifically for Drosophila melanogaster male meiosis. J Cell Biol 180: 521-535.

Gassmann R, Carvalho A, Henzing A.J., Ruchaud S, Hudson DF, Honda R, Nigg EA., Gerloff DL, Earnshaw WC. 2004. Borealin: a novel chromosomal passenger required for stability of the bipolar mitotic spindle. J Cell Biol 166: 179-191.

Gatt, MK and Glover, DM . 2006. The Drosophila phosphatidylinositol transfer protein encoded by vibrator is essential to maintain cleavage-furrow ingression in cytokinesis. J Cell Sci 119:2225-2235.

Gatt MK, Savoian MS, Riparbelli MG, Massarelli C, Callaini G, Glover DM. 2005. Klp67A destabilises pre-anaphase microtubules but subsequently is required to stabilise the central spindle. J Cell Sci 118:2671-2682.

Gerald NJ, Damer CK, O'Halloran TJ, De Lozanne A. 2001. Cytokinesis failure in clathrin-minus cells is caused by cleavage furrow instability. Cell Motil Cytoskeleton. 48:213-223.

Giansanti MG, Belloni G, Gatti M. 2007. Rab11 is required for membrane trafficking and actomyosin ring constriction in meiotic cytokinesis of Drosophila males. Mol Biol Cell 18:5034-5047.

Giansanti MG, Bonaccorsi S, Bucciarelli E, Gatti M. 2001. Drosophila male meiosis as a model system for the study of cytokinesis in animal cells. Cell Struct Funct 26:609-617.

Giansanti MG, Bonaccorsi S, Gatti M. 1999. The role of anillin in meiotic cytokinesis of Drosophila males. J Cell Sci 112:2323-2334.

Giansanti MG, Bonaccorsi S, Kurek R, Farkas RM, Dimitri P, Fuller MT, Gatti M. 2006. The class I PITP giotto is required for Drosophila cytokinesis. Curr Biol 16:195-201.

Giansanti MG, Bonaccorsi S, Williams B, Williams EV, Santolamazza C, Goldberg ML, Gatti M. 1998. Cooperative interactions between the central spindle and the contractile ring during Drosophila cytokinesis. Genes and Dev 12:396-410.

Giansanti MG, Bucciarelli E, Bonaccorsi S, Gatti M. 2008. Drosophila SPD-2 is an essential centriole component required for PCM recruitment and astral-microtubule nucleation. Curr Biol 18:303-309.

Giansanti MG, Farkas RM, Bonaccorsi S, Lindsley DL, Wakimoto BT, Fuller MT, Gatti M. 2004. Genetic Dissection of Meiotic Cytokinesis in Drosophila Mol Biol Cell 15:2509-2522.

Giansanti MG, Fuller MT. 2012. What Drosophila spermatocytes tell us about the mechanisms underlying cytokinesis. Cytoskeleton (Hoboken) 69:869-881.

Giansanti MG, Sechi S, Frappaolo A, Belloni G, Piergentili R. 2012. Cytokinesis in Drosophila male meiosis. Spermatogenesis 2:185-196.

Glotzer M. 2005. The molecular requirements for cytokinesis. Science 307:1735-1739.

Glotzer M. 2009. The 3Ms of central spindle assembly: microtubules, motors and MAPs. Nat Rev Mol Cell Biol. 10(1):9-20.

Goldbach P, Wong R, Beise N, Sarpal R, Trimble WS, Brill JA. 2010. Stabilization of the actomyosin ring enables spermatocyte cytokinesis in Drosophila. Mol Biol Cell 21:1482-1493.

Goode BL, Eck MJ. 2007. Mechanism and function of formins in the control of actin assembly. Anu Rev Biochem. 76:593-627.

Green RA, Paluch E, Oegema K. 2012. Cytokinesis in animal cells. Annu Rev Cell Dev Biol 28:29-58.

Gregory SL, Ebrahimi S, Milverton J, Jones WM, Bejsovec A, Saint R. 2008. Cell division requires a direct link between microtubule-bound RacGAP and Anillin in the contractile ring. Curr Biol. 18:25-9.

Guertin DA., Sabatini DM. 2007. Defining the role of mTOR in cancer. Cancer Cell. 12, 9-22.

Gunsalus KC, Bonaccorsi S, Williams E, Verni F, Gatti M, Goldberg ML. 1995. Mutations in twinstar, a Drosophila gene encoding a cofilin/ADF homologue, result in defects in centrosome migration and cytokinesis. J Cell Biol 131:1243-1259.

Guse A, Mishima M, Glotzer M. 2005. Phosphorylation of ZEN-4/MKLP1 by aurora B regulates completion of cytokinesis. Curr Biol 15:778-786.

Herrmann S, Amorim I, Sunkel CE. 1998. The POLO kinase is required at multiple stages during spermatogenesis in Drosophila melanogaster. Chromosoma. 107:440-451.

Hime GR,, Brill JA, Fuller MT. 1996. Assembly of ring canals in the male germ line from structural components of the contractile ring. J. Cell Sci; 109:2779-2788.

Honda R, Körner R, Nigg EA. 2003. Exploring the functional interactions between Aurora B, INCENP, and survivin in mitosis. Mol. Biol. Cell. 14, 3325-3341.

Hu BS, Hu H, Zhu CY, Gu YL, Li JP. 2012. Overexpression of GOLPH3 is associated with poor clinical outcome in gastric cancer. Tumour Biol. DOI: 10.1007/s13277-012-0576-z.

Hua X, Yu L, Pan W, Huang X, Liao Z, Xian Q, Fang L, Shen H. 2012. Increased expression of Golgi phosphoprotein-3 is associated with tumor aggressiveness and poor prognosis of prostate cancer. Diagn Pathol. doi: 10.1186/1746-1596-7-127.

Inoue YH, Savoian MS, Suzuki T, Máthé E, Yamamoto MT, Glover DM. 2004. Mutations in orbit/mast reveal that the central spindle is comprised of two microtubule populations, those that initiate cleavage and those that propagate furrow ingression. J Cell Biol 166:49-60.

Jarquin-Pardo M, Fitzpatrick A, Galiano FJ, First EA, Davis JN. 2007. Phosphatidic acid regulates the affinity of the murine phosphatidylinositol 4-phosphate 5-Kinase-lbeta for phosphatidylinositol-4-phosphate. J Cell Biochem 100:112-28.

Jones, SM, Alb JG Jr, Phillips SE, Bankaitis VA and Howell KE. 1998. A phosphatidylinositol 3-kinase and phosphatidylinositol transfer protein act synergistically in formation of constitutive transport vesicles from the trans-Golgi network. J. Biol. Chem. 273, 10349-10354.

Joo E, Surka MC, Trimble WS. 2007. Mammalian SEPT2 is required for scaffolding nonmuscle myosin II and its kinases. Dev Cell 13:677-690.

Jordan P, Karess R. 1997. Myosin light chain-activating phosphorylation sites are required for oogenesis in Drosophila. J Cell Biol. 139: 1805-1819.

Kamijo K, Ohara N, Abe M, Uchimura T, Hosoya H, Lee JS, Miki T. 2006. Dissecting the role of Rho-mediated signaling in contractile ring formation. Mol Biol Cell 17:43-55.

Kee YS, Ren Y, Dorfman D, Iijima M, Firtel R, Iglesias PA, Robinson DN. 2012. A mechanosensory system governs myosin II accumulation in dividing cells. Mol Biol Cell. 2:1510-1523.

Kinoshita M, Field CM, Coughlin ML, Straight AF, Mitchison TJ. 2002. Self- and actin-templated assembly of Mammalian septins. Dev Cell. 3:791-802.

Kitazawa D, Yamaguchi M, Mori, H, Inoue YH. 2012. COPI-mediated membrane trafficking is required for cytokinesis in Drosophila male meiotic divisions. J Cell Sci jcs.103317; doi:10.1242/jcs.103317.

Kranz C, Ng BG, Sun L, Sharma V, Eklund EA, Miura Y, Ungar D, Lupashin V, Winkel RD, Cipollo JF, Costello CE, Loh E, Hong W, Freeze HH. 2007. COG8 deficiency causes new congenital disorder of glycosylation type IIh. Hum Mol Genet. 16:731-741.

Kunigou O, Nagao H, Kawabata N, Ishidou Y, Nagano S, Maeda S, Komiya S, Setoguchi T. 2012. Role of GOLPH3 and GOLPH3L in the proliferation of human rhabdomyosarcoma. Oncol Rep. 26:1337-1342.

Kurasawa Y, Earnshaw WC, Mochizuki Y, Dohmae N, Todokoro K. 2004. Essential roles of KIF4 and its binding partner PRC1 in organized central spindle midzone formation. EMBO J 23:3237-3248.

Lange BM, Rebollo E, Herold A, González C. 2002. Cdc37 is essential for chromosome segregation and cytokinesis in higher eukaryotes. EMBO J.21:5364–5374.

Lens SM., Rodriguez JA, Vader G, Span SW, Giaccone G, Medema RH. 2006. Uncoupling the central spindle-associated function of the chromosomal passenger complex from its role at centromeres. Mol Biol Cell 17: 1897-1909.

Lewellyn L, Dumont J, Desai A, Oegema K. 2010. Analyzing the effects of delaying aster separation on furrow formation during cytokinesis in the Caenorhabditis elegans embryo.
Mol Biol Cell. 21(1): 50-62.

Li H, Guo L, Chen SW, Zhao XH, Zhuang SM, Wang LP, Song LB, Song M. 2012. GOLPH3 overexpression correlates with tumor progression and poor prognosis in patients with clinically N0 oral tongue cancer. J Transl Med. doi: 10.1186/1479-5876-10-168.

Lindsley DL, Tokuyasu KT. Spermatogenesis. In: Ashburner M, Wright TRF, eds. Genetics and Biology of *Drosophila* New York: Academic Press, 1980: 225-94.

Liu J, Fairn GD, Ceccarelli DF, Sicheri F, Wilde A. 2012. Cleavage furrow organization requires PIP(2)-mediated recruitment of anillin. Curr Biol. 22:64-69.

Lübbehusen J, Thiel C, Rind N, Ungar D, Prinsen BH, de Koning TJ, van Hasselt PM and Körner C. 2010. Fatal outcome due to deficiency of subunit 6 of the conserved oligomeric Golgi complex leading to a new type of congenital disorders of glycosylation. Hum Mol Genet 19:3623-3633.

Ma X, Kovács M, Conti MA, Wang A, Zhang Y, Sellers JR, Adelstein RS. 2012. Nonmuscle myosin II exerts tension but does not translocate actin in vertebrate cytokinesis. Proc Natl Acad Sci U S A. 109:4509-4514.

Morava E, Zeevaert R, Korsch E, Huijben K, Wopereis S, Matthijs G, Keymolen K, Lefeber DJ, De Meirleir L and Wevers RA. (2007). A common mutation in the COG7 gene with a consistent phenotype including microcephaly, adducted thumbs, growth retardation, VSD and episodes of hyperthermia. *Eur J Hum Genet* 156, 638-45.

McKay HF, Burgess DR. 2011. 'Life is a highway': membrane trafficking during cytokinesis. Traffic 12:247-251.

Miller AL. 2011. The contractile ring. Curr Biol 21:R976-978.

Miller KG, Field CM, Alberts BM. 1989. Actin-binding proteins from Drosophila embryos: a complex network of interacting proteins detected by F-actin affinity chromatography. J Cell Biol 109:2963-2975.

Montagnac G, Chavrier P. 2008. Endosome positioning during cytokinesis. Biochem Soc Trans. 36:442-443.

Montembault E, Zhang W, Przewloka MR, Archambault V, Sevin EW, Laue ED, Glover DM, D'Avino PP. 2010. Nessun Dorma, a

novel centralspindlin partner, is required for cytokinesis in Drosophila spermatocytes. J Cell Biol. 191:1351-1365.

Mostowy S, Cossart P. 2012. Septins: the fourth component of the cytoskeleton. Nat Rev Mol Cell Biol. 13(3):183-94.

Musacchio A and Salmon, ED. 2007. The spindle-assembly checkpoint in space and time. Nat Rev Mol Cell Biol 8: 379-393.

Naim V, Imarisio S, Di Cunto F, Gatti M, Bonaccorsi S. 2004. *Drosophila* citron kinase is required for the final steps of cytokinesis. Mol Biol Cell. 15:5053–5063.

Neef R, Klein UR, Kopajtich R, Barr FA. 2006. Cooperation between mitotic kinesins controls the late stages of cytokinesis. Curr Biol 16:301-307.

Neto H, Collins LL, Gould GW. 2011. Vesicle trafficking and membrane remodelling in cytokinesis. Biochem J 437:13-24.

Ng BG, Kranz C, Hagebeuk EE, Duran M, Abeling NG, Wuyts, B, Ungar D, Lupashin V, Hartdorff CM, Poll-The BT and Freeze HH 2007. Molecular and clinical characterization of a Moroccan Cog7 deficient patient. Mol Genet Metab 91, 201-04.

Nigg EA. 2002. Centrosome aberrations: cause or consequence of cancer progression? Nat Rev Cancer 11:815-25.

Nishimura Y, Yonemura S. 2006. Centralspindlin regulates ECT2 and RhoA accumulation at the equatorial cortex during cytokinesis. J Cell Sci 119:104-114.

Nislow C, Lombillo VA, Kuriyama R, McIntosh JR. 1992. A plus-end-directed motor enzyme that moves antiparallel microtubules in vitro localizes to the interzone of mitotic spindles. Nature 359:543-547.

Niswonger ML, O'Halloran TJ. 1997. A novel role for clathrin in cytokinesis. Proc Natl Acad Sci U S A. 94:8575-8578.

Oh Y, Bi E. Septin structure and function in yeast and beyond. 2011. Trends Cell Biol. 21:141-148.

Ohashi M, Jan de Vries K, Frank R, Snoek G, Bankaitis V, Wirtz K and Huttner WB. 1995. A role for phosphatidylinositol transfer protein in secretory vesicle formation. Nature 377, 544-547.

Oka T, Ungar D, Hughson FM and Krieger M. 2004. The COG and COPI complexes interact to control the abundance of GEARs, a subset of Golgi integral membrane proteins. Mol. Biol. Cell 155:2423-2435.

Paesold-Burda P, Maag C, Troxler H, Foulquier F, Kleinert P, Schnabel S, Baumgartner M and Hennet T. 2009. Deficiency in COG5

causes a moderate form of congenital disorders of glycosylation. Hum. Mol. Genet. 18:4350-4356.

Piekny A, Werner M, Glotzer M. 2005. Cytokinesis: welcome to the Rho zone. Trends Cell Biol 15:651-658.

Polevoy G, Wei HC, Wong R, Szentpetery Z, Kim YJ, Goldbach P, Steinbach SK, Balla T, Brill JA. 2009. Dual roles for the Drosophila PI 4-kinase four wheel drive in localizing Rab11 during cytokinesis. J. Cell Biol 187:847-858.

Pollard TD. 2010. Mechanics of cytokinesis in eukaryotes. Curr Opin Cell Biol. 22: 50-56.

Prekeris R, Gould GW. 2008. Breaking up is hard to do - membrane traffic in cytokinesis. J Cell Sci 121:1569-1576.

Rappaport R. 1961. Experiments concerning the cleavage stimulus in sand dollar eggs. J Exp Zool 148:81-89.

Rebollo E, Gonzalez C. 2000. Visualizing the spindle checkpoint in Drosophila spermatocytes. EMBO Rep 1:65-70.

Resnick TD, Satinover DL, MacIsaac F, Stukenberg PT, Earnshaw WC, Orr-Weaver TL, Carmena M. 2006. INCENP and Aurora B promote meiotic sister chromatid cohesion through localization of the Shugoshin MEI-S332 in Drosophila. Dev Cell 11:57-68.

Reynders E, Foulquier F, Leão Teles E, Quelhas D, Morelle W, Rabouille C, Annaert W and Matthijs G. 2009. Golgi function and dysfunction in the first COG4-deficient CDG type II patient. Hum. Mol. Genet. 1:3244-3256.

Riggs B, Rothwell W, Mische S, Hickson GR, Matheson J, Hays TS, Gould GW, Sullivan W. 2003. Actin cytoskeleton remodeling during early Drosophila furrow formation requires recycling endosomal components Nuclear-fallout and Rab11. J Cell Biol.163:143-154.

Riparbelli MG, Callaini G, Glover DM, Avides Mdo C. 2002. A requirement for the Abnormal Spindle protein to organise microtubules of the central spindle for cytokinesis in Drosophila. J Cell Sci 115:913-922.

Robinett CC, Giansanti MG, Gatti M, Fuller MT. 2009. TRAPPII is required for cleavage furrow ingression and localization of Rab11 in dividing male meiotic cells of Drosophila. J Cell Sci 122:4526-4534.

Ruchaud S, Carmena M, Earnshaw WC. 2007. Chromosomal passengers: conducting cell division. Nat Rev Mol Cell Biol 8:798-812.

Sampaio P, Rebollo E, Varmark H, Sunkel CE, Gonzalez C. 2001. Organized microtubule arrays in gamma-tubulin-depleted Drosophila spermatocytes. Curr Biol 11:1788-1793.

Santamaria A, Neef R, Eberspächer U, Eis K, Husemann M, Mumberg D, Prechtl S, Schulze V, Siemeister G, Wortmann L, Barr FA, Nigg EA. 2007. Use of the novel Plk1 inhibitor ZK-thiazolidinone to elucidate functions of Plk1 in early and late stages of mitosis. Mol Biol Cell 18:4024-4036.

Satterwhite LL, Pollard TD. 1992. Cytokinesis. Curr Opin Cell Biol 4:43-52.

Schmitz KR, Liu J, Li S, Setty TG, Wood CS, Burd CG, Ferguson KM. 2008. Golgi localization of glycosyltransferases requires a Vps74p oligomer. Dev Cell. 14:523-534.

Schoeder TE. 1990. The contractile ring and furrow in dividing cells. Ann N Y Acad Sci. 582:78-87.

Schweitzer JK, D'Souza-Schorey C. 2004. Finishing the job: cytoskeletal and membrane events bring cytokinesis to an end. Exp Cell Res 295:1-8.

Scott KL, Chin L and other 17. 2009. GOLPH3 modulates mTOR signalling and rapamycin sensitivity in cancer. Nature 459, 1085-1090.

Seaman MN. 2005. Recycle your receptors with retromer. Trends Cell Biol 15:68-75.

Shestakova A, Zolov S, and Lupashin VV. 2006. COG complex-mediade recycling of Golgi glycosyltransferases is essential for normal protein glicosylation. Traffic 7:191-204.

Simon JP, Morimoto T, Bankaitis VA, Gottlieb TA, Ivanov IE, Adesnik M and Sabatini DD. 1998. An essential role for the phosphatidylinositol transfer protein in the scission of coatomer-coated vesicles from the trans-Golgi network. Proc Natl Acad Sci U S A 95:11181-11186.

Sisson JC., Field C., Ventura R., Royou A., Sullivan W. 2000. Lava lamp, a novel peripheral golgi protein, is required for Drosophila melanogaster cellularization. J. Cell Biol. 151:905-918.

Skop AR, Liu H, Yates J 3rd, Meyer BJ, Heald R. 2004. Dissection of the mammalian midbody proteome reveals conserved cytokinesis mechanisms. Science 305:61-66;

Snyder CM., Mardones GA, Ladinsky MS, Howell KE. 2006. GMx33 associates with the trans-Golgi matrix in a dynamic manner and sorts within tubules exiting the Golgi. Mol Biol Cell. 17, 511-524.

Somers WG, Saint R.. 2003. A RhoGEF and Rho Family GTPase-Activating Protein Complex Links the Contractile Ring to Cortical Microtubules at the Onset of Cytokinesis. Dev Cell 4:29-39.

Somma MP, Fasulo B, Cenci G, Cundari E, Gatti M. 2002. Molecular dissection of cytokinesis by RNA interference in Drosophila cultured cells. Mol Biol Cell. 13:2448-2460.

Spaapen LJ, Bakker JA, van der Meer SB, Sijstermans HJ, Steet RA, Wevers RA and Jaeken J. 2005. Clinical and biochemical presentation of siblings with COG-7 deficiency, a lethal multiple O- and N-glycosylation disorder. J. Inherit. Metab. Dis. 28:707-714.

Steet R and Kornfeld S. 2006. COG-7-deficient Human Fibroblasts Exhibit Altered Recycling of Golgi Proteins. Mol. Biol. Cell 175:2312-2321.

Straight AF, Field CM, Mitchison TJ. 2005. Anillin binds nonmuscle myosin II and regulates the contractile ring. Mol Biol Cell. 16:193-201.

Suvorova ES, Kurten RC and Lupashin VV. 2001. Identification of a human orthologue of Sec34p as a component of the cis-Golgi vesicle tethering machinery. J. Biol. Chem. 276:22810-22818.

Suvorova ES, Duden R and Lupashin VV. 2002. The Sec34/Sec35p complex, a Ypt1p effector required for retrograde intra-Golgi trafficking, interacts with Golgi SNAREs and COPI vesicle coat proteins. J. Cell Biol. 157:631-643.

Szafer-Glusman E, Fuller MT, Giansanti MG. 2011. Role of Survivin in cytokinesis revealed by a separation-of-function allele. Mol Biol Cell 22:3779-3790.

Tanaka-Takiguchi Y, Kinoshita M, Takiguchi K. 2009. Septin-mediated uniform bracing of phospholipid membranes. Curr Biol.19:140-145.

Tates AD. 1971. Cytodifferentiation durng spermatogenesis in Drosophila melanogaster: an electron microscope study. Ph.D Thesis Leiden, Netherlands: Rijksuniversiteit de leiden.

Tong AH., Boone C. and other 48. 2004. Global mapping of the yeast genetic interaction network. Science 303, 808-813

Tu L, Tai WC, Chen L, Banfield DK. 2008. Signal-mediated dynamic retention of glycosyltransferases in the Golgi. Science. 321:404-407.

Ungar D, Oka T, Brittle EE, Vasile E, Lupashin VV, Chatterton, JE, Heuser JE, Krieger M and Waters MG. 2002. Characterization of a mammalian Golgi-localized protein complex, COG, that is required for normal Golgi morphology and function. J Cell Biol 29:405-415.

Vagnarelli P, Earnshav WC. 2004. Chromosomal passengers: the four-dimensional regulation of mitotic events. Chromosoma 113:211-222.

Vader G, Medema RH, Lens SM. 2006. The chromosomal passenger complex: guiding Aurora-B through mitosis. J Cell Biol 19:833-837.

Van der Waal MS, Hengeveld RC, van der Horst A, Lens SM. 2012. Cell division control by the Chromosomal Passenger Complex. Exp Cell Res. 318:1407-2140.

Vernì F, Somma MP, Gunsalus KC, Bonaccorsi S, Belloni G, Goldberg ML, Gatti M. 2004. Feo, the Drosophila homolog of PRC1, is required for central-spindle formation and cytokinesis. Curr Biol 14:1569-1575.

Wainman A, Giansanti MG, Goldberg ML, Gatti M. 2012. The Drosophila RZZ complex: roles in membrane traffic and cytokinesis. J Cell Sci jcs.099820; Advance Online Publication June 8, 2012, doi:10.1242/jcs.099820

Wakefield JG, Bonaccorsi S, Gatti M. 2001. The Drosophila Protein Asp Is Involved in Microtubule Organization during Spindle Formation and Cytokinesis. J Cell Biol 153:637-648.

Wakefield JG, Huang JY, Raff JW. 2000. Centrosomes have a role in regulating the destruction of cyclin B in early Drosophila embryos. Curr Biol 10:1367-1370.

Walter DM, Paul KS and Waters MG. 1998. Purification and characterization of a novel 13 S hetero-oligomeric protein complex that stimulates in vitro Golgi transport. J. Biol. Chem. 273:29565-29576.

Wang JH, Chen XT, Wen ZS, Zheng M, Deng JM, Wang MZ, Lin HX, Chen K, Li J, Yun JP, Luo RZ, Song LB. 2012. High expression of GOLPH3 in esophageal squamous cell carcinoma correlates with poor prognosis. PLos One 7: e45622.

Williams BC, Riedy MF, Williams EV, Gatti M, Goldberg ML. 1995. The Drosophila kinesin-like protein KLP3A is a midbody

component required for central spindle assembly and initiation of cytokinesis. J Cell Biol 129:709–723.

Wilson GM, Fielding AB, Simon GC, Yu X, Andrews PD, Hames RS, Frey AM, Peden AA, Gould GW, Prekeris R. 2005. The FIP3-Rab11 protein complex regulates recycling endosome targeting to the cleavage furrow during late cytokinesis. Mol Biol Cell. 16:849-860.

Wolfe BA, Takaki T, Petronczki M, Glotzer M. 2009. Polo-like kinase 1 directs assembly of the HsCyk-4 RhoGAP/Ect2 RhoGEF complex to initiate cleavage furrow formation. PLoS Biol. 7:e1000110.

Wong R, Hadjiyanni I, Wei HC, Polevoy G, McBride R, Sem KP, Brill JA. 2005. PIP2 hydrolysis and calcium release are required for cytokinesis in Drosophila spermatocytes. Curr Biol 15:1401-1406.

Wood CS, Schmitz KR, Bessman NJ, Setty TG, Ferguson KM, Burd CG. 2009. PtdIns4P recognition by Vps74/GOLPH3 links PtdIns 4-kinase signaling to retrograde Golgi trafficking. J Cell Biol. 87:967-975.

Wu X, Steet RA, Bohorov O, Bakker J, Newell J, Krieger M, Spaapen L, Kornfeld S and Freeze HH. 2004. Mutation of the COG complex subunit gene COG7 causes a lethal congenital disorder. Nat Med 10:518-523.

Xu H, Brill JA, Hsien J, McBride R, Boulianne GL, Trimble WS. 2002. Syntaxin 5 is required for cytokinesis and spermatid differentiation in Drosophila. Dev Biol 251:294-296.

Yin HL, Janmey PA. 2003. Phosphoinositide regulation of the actin cytoskeleton. Annu Rev Physiol. 65:761-789.

Yüce O, Piekny A, Glotzer M. 2005. An ECT2-centralspindlin complex regulates the localization and function of RhoA. J Cell Biol 170:571-582.

Zeng Z, Lin H, Zhao X, Liu G, Wang X, Xu R, Chen K, Li J, Song L. 2012. Overexpression of GOLPH3 promotes proliferation and tumorigenicity in breast cancer via suppression of the FOXO1 transcription factor. Clin Cancer Res. 18:4059-4069.

Zerial M, McBride H. 2001. Rab proteins as membrane organizers. Nat Rev Mol Cell Biol. 2:107-117.

Zhao WM, Fang G. 2005. MgcRacGAP controls the assembly of the contractile ring and the initiation of cytokinesis. J Cell Biol 102:13158-13163.

Zhou J, Xu T, Qin R, Yan Y, Chen C, Chen Y, Yu H, Xia C, Lu Y, Ding X, Wang Y, Cai X, Chen J. 2012. Overexpression of Golgi

phosphoprotein-3 (GOLPH3) in glioblastoma multiforme is associated with worse prognosis. J Neurooncol. 110:195-203.